UNIVERSITA' DEGLI STUDI DI PADOVA

Sede Amministrativa: Università degli Studi di Padova

Dipartimento di Scienze Sperimentali Veterinarie

SCUOLA DI DOTTORATO DI RICERCA IN SCIENZE VETERINARIE

INDIRIZZO: SCIENZE BIOMEDICHE VETERINARIE E COMPARATE

CICLO XXI°

TESI DI DOTTORATO DI RICERCA:

HORSE HEART STUDY: LEFT VENTRICULAR CARDIOMYOCYTES ISOLATION, HISTIDINE-RICH Ca^{2+}- BINDING PROTEIN AND MYOSTATIN ESPRESSION

Direttore della Scuola : Ch.mo Prof. Massimo Morgante

Supervisore :Ch.mo Prof. Francesco Mascarello

Dottoranda : Evgeniya Sharova

2 Febbraio 2008

INTRODUCTION

MATERIALS AND METHODS

SOMMARIO

Il cavallo è da sempre considerato un "campione sportivo" nell'ambito del mondo animale. Le capacità atletiche di questo animale dipendono da molti fattori. I più significativi sono il suo sistema cardiovascolare e le caratteristiche fisiologiche del cuore equino. E' di notevole importanza il fatto che la frequenza cardiaca del cuore di cavallo a riposo è bassa (25-40 battiti al min) ma che può aumentare rapidamente durante l'esercizio fisico fino a raggiungere i 240 battiti al min e oltre. Inoltre il cuore di cavallo si caratterizza una maggiore durata del potenziale d'azione (0.6-1 s) se paragonato a quella degli altri mammiferi (0.2-0.35 s). Il cuore di equino presenta inoltre significative differenze per quel che riguarda la frequenza, l'ampiezza e la velocità dei transienti di calcio. Per spiegare queste caratteristiche peculiari del cuore di cavallo sono state fatte delle ipotesi. Una più elevata capacità di immagazzinamento del calcio da parte del reticolo sarcoplasmatico, o un'alterazione nella quantità o nella funzionalità di alcune proteine leganti calcio implicate nel processo di eccitamento/contrazione, sono state proposte come possibili cause di queste particolarità dei cardiomiociti equini /Loughrey et al. 2004). Queste caratteristiche hanno fatto ricadere la mia attenzione su due proteine: la "histidine-rich Ca2+-binding protein" (HRC) e la miostatina.

L' HRC è una proteina a cui è stato assegnato un ruolo nella regolazione dell'immagazzinamento del calcio da parte del reticolo sarcoplasmatico e nelle funzionamento cardiaco. La Miostatina invece è un componente della superfamiglia dei "transforming growth factor-β" che viene regolata in situazioni fisiologiche e patologiche che coinvolgono la massa muscolare cardiaca, tra cui la modulazione della crescita cardiaca (McKoy G et al. 2007), l'ipertrofia dovuta ad attività atletica (Matsakas A et al. 2006), i processi di rigenerativi post infartuali, l'infiammazione post infartuale (MacLellan et al., 1993, Sharma M et al. 1999), i processi fibrotici del miocardio e le disfunzioni cardiache (Hoenig MR, 2008).

L'HRC nel muscolo scheletrico, è risultata per struttura e funzione simile alla calsequestrina, ma sembra avere un ruolo importante e particolare anche nel cuore. L'HRC, una proteina che lega calcio a bassa affinità ma ad elevata capacità, presenta un ruolo nell'immagazzinamento del calcio nel reticolo sarcoplasmatico delle cellule cardiache durante il processo di accoppiamento eccitamento/contrazione (Gregory et al.

2006). Grazie al suo ruolo come regolatore del rilascio di calcio e della funzionalità cardiaca, recentemente all'HRC è stato assegnato un ruolo come ulteriore componente di un complesso molecolare costituito da quattro proteine(Lee H et al. 2001), che localizzato a livello della componente giunzionale del reticolo sarcoplasmatico: il recettore della Rianodina/canale di rilascio del calcio, la calsequestrina e la sue proteine di ancoraggio triadina e giuntina. L'HRC potrebbe rappresentare una proteina chiave in questo complesso, in grado di facilitare il rilascio del calcio dal reticolo sarcoplasmatico mediante l'interazione proteina-proteina.

In questo periodo di Dottorato, io ho ipotizzato che le particolari caratteristiche del cuore di cavallo tra cui la durata del potenziale d'azione, potessero trovare una spiegazione nelle caratteristiche e/o alterazione dell'HRC. Inoltre la maggior comprensione dei meccanismi regolativi della miostatina, potrebbero essere di utilità nella pratica di clinica veterinaria poiché l'ipertrofia cardiaca nei cavalli atleti è un fenomeno comune.

Per raggiungere gli obiettivi preposti in questo lavoro, ho usato tecniche di Real time PCR e standard PCR all scopo di studiare in dettaglio l'espressione della HRC e della miostatina nelle varie parti anatomiche del cuore equino. Inoltre l'espressione dell'HRC nel cuore equino è stata paragonata nel cuore di bovino. Per studiare invece l'espressione dell'HRC a livello proteico, dopo estrazione e purificazione do membrane del reticolo sarcoplasmatico, sono stati eseguiti esperimenti di Western blotting. Esperimenti di immunofluorescenza su sezioni longitudinali di ventricolo sinistro di cavallo hanno permesso di studiare la localizzazione dell'HRC.

I miei risultati mostrano che l'HRC a livello di mRNA è maggiormente espressa nei ventricoli. Inoltre, dal confronto con il bovino, un'altra specie animale di interesse veterinario, è emerso che la sovra espressione dell'HRC è ristretta alla specie equina. La diversa espressione di HRC in atri e ventricoli, potrebbe essere dovuta a caratteristiche intrinseche alle porzioni anatomiche che potrebbero in qualche modo essere evidenziate dalla particolare durata del potenziale d'azione di questa specie. A tal proposito, nell'insieme i miei dati che indicano una overespressione di HRC nei ventricoli, potrebbero rafforzare l'ipotesi che vede l'HRC un regolatore del calcio nel reticolo sarcoplasmatico durante il processo di eccitamento/contrazione.

I dati ottenuti riguardanti la espressione del gene della miostatina principalmente nel ventricolo sinistro, potrebbero invece rappresentare un ulteriore sostegno a favore di questa ipotesi, visto che il ventricolo sinistro ha un ruolo primario nel fenomeno di adattamento

all’aumento del volume di sangue *(stroke volume)* che viene pompato durante nelle varie fasi di esercizi fisici estremi, così da incrementare l’output cardiaco finale.

SUMMARY

The horse has always been considered as a sport champion in the animal world. Horse athletic ability depends of many factors. The most important are cardiovascular system and heart physiology. It is noteworthy that horse heart rate is slow at rest (25-40 bmp) but can elevate rapidly during exercise to over 240 beats per minutes. In addition, horse heart is characterized by an higher cardiac action potential duration (APD) (0.6-1s) compared to that of other mammals (0.2-0.35s). Significantly differences in frequency, amplitude and calcium wave velocity have also been observed. These extraordinary features of the horse heart could be explained by some hypothesis: it may be a result of high calcium loading capacity of sarcoplasmic reticulum of horse cardiomyocytes or altered quantity/function of calcium bindings proteins that participate in excitation contraction coupling cycle of cardiac cell (Loughrey et al. 2004). These special characteristics of horse heart put my attention to two proteins, histidine-rich Ca^{2+}-binding protein and myostatin. Histidine-rich Ca^{2+}-binding protein (HRC) is one of the best candidates to regulate reticulum calcium sequestration and cardiac function. While myostatin is member of the transforming growth factor-β superfamily, shown to be regulated during different physiological and pathological situations which affect cardiac muscle mass, including cardiac growth modulation (McKoy G et al. 2007), athletic hypertrophy (Matsakas A et al. 2006), postmyocardial infarction remodeling process, infarction-associated inflammation (MacLellan et al., 1993, Sharma M et al. 1999), fibrosis of the myocardium, and cardiac dysfunction (Hoenig MR, 2008).

HRC has a similar protein structure and function to calsequestrin in skeletal muscle and seems to play the particular role in the heart. This low affinity and high capacity Ca^{2+} binding protein has a Ca^{2+} storage role in cardiac SR during EC-coupling (Gregory et al. 2006). Due to its important role as regulator of Ca release and normal cardiac function, recently HRC has been suggested to be an additional component of SR protein quaternary molecular complex (Lee H et al. 2001), associating into a stable complex at the junctional membrane: the Ryanodine channel, calsequestrin and its putative “anchoring” proteins triadin and junctin. HRC could be a key protein that manipulates the facilitation of Ca^{2+} release from SR through protein-protein interaction.

In this work we hypothesed that the particular characteristic of the horse heart and long APD could be explained by HRC alteration in equine horse heart. On the other hand

understanding of the MSTN pathway could have an important approach into veterinary clinical practice used during horse training when athletic hypertrophy is a common phenomenon.

To achieve objective of this work we have used Real-time PCR and Standard PCR to investigate in details the expression of HRC and myostatin in various compartments of horse heart. We also compared the HRC mRNA expression of horse heart *vs* that of bovine. In order to gain insight protein level expression of HRC in horse heart, electrophoretic gel analysis were performed on membrane fractions extracted from horse cardiac muscle followed by Western blotting. Besides of immunofluorescence experiments on longitudinal cryosections from left ventricle have been carried out to study the cellular localization of HRC in horse heart.

Our findings showed that HRC mRNA is mainly expressed in ventricles. Moreover, by comparison with another species of veterinarian interest, such as cattle, Real Time PCR data showed that the enhanced expression of HRC seems restricted to equine species. The dissimilar HRC mRNA expression in atria and ventricles may be due to the intrinsic features of heart parts, that could be emphasize by the special equine action potential duration. On account of the special features exhibited by horse cardiac tissue, taken together my data showing the overexpression of HRC in ventricular chambers, could strengthen the hypothesis of HRC as a candidate regulator of SR Ca^{2+} cycling during ECC.

The interesting results revealed the upregulation of MSTN gene expression detected in left ventricular of horse heart could be an interesting data in favor to this hypothesis since the left ventricular chamber has a primary role in heart adaptation increased blood volume *(stroke volume)* to be injected during exhaustive sport exercise and therefore incrementing the final cardiac output.

INTRODUCTION

Horse, animal with an exceptional ability

The horse has always been considered a sport champion amongst mammals' world. What makes the horse such a good athlete? Horse athletic ability depends of many factors. The most important are the special adaptations of the equine cardiovascular system and heart physiology. The cardiovascular system of the Thoroughbred racehorse has evolved to allow it to consume more oxygen per kilogram than most other large mammals (Derman KD & Noakes TD, 1994). The superiority of the Thoroughbred cardiovascular system rests in a proportionately lager heart (Gunn HM, 1989) and spleen per unit body mass than other large mammals (Poole DC & Erikson HH, 2003). The equine cardiovascular system is hugely compliant with a *heart rate*, the number of times the heart beats per minute, range from 20 beats min^{-1} to 240, under strenuous exercise (Table.1) and a splenic red cell reserve able to double packed-cell volume and oxygen delivery during maximal exercise (McKeever KH et al. 1993).

Table 1. Affect of exercise on the horse cardiovascular system. The maximum heart rate was measured during peak exercise in the Thoroughbred horse. By Young L.E, Centre for Equine Studies, Animal Health Trust, Newmarket, UK.

Activity	**Heart rate (b.p.m)**
Rest	28-40
Low (walk)	60-120
Moderate (trot, canter 7m/s)	120-180
Intense (canter 8m/s-11m/s)	180+
Maximum (canter 12 m/s)	220-240

These adaptations are clearly of huge benefit in optimising oxygen transport in this species, as Qo_2 (oxygen delivery) is the product of cardiac output and arterial oxygen content. With each beat, a typical adult horse pumps approximately one litre of blood out of its heart, this is a *stroke volume* (volume of the blood pumped by the heart per beat). With a rest heart rate of

30-40 beats per minute, the horse's resting *cardiac output*, is 30-40 litres per minute in contrast this to man with an average output of 5 litres per minute. Although maximal *heart rate* is important in determining maximal *cardiac output*, the *stroke volume* will be determined principally by heart size (*Cardiac Output* = *Stroke Volume* x *Heart Rate*). The stroke volume in the resting horse is approximately 800-900 ml. When the heart beats, it does not empty completely, instead a proportion of blood remains in the left heart chamber. When exercise begins, circulating adrenaline makes the contraction of the heart muscle more forceful; so more blood is ejected from the ventricle with each beat. Additionally the huge muscles of locomotion contract and squeeze more blood back to the heart increasing the amount of the blood available in the circulation and further increasing stroke volume. In horses, the proportion of skeletal muscle exceeds 50% of body weight and the energetic capacity of equine muscle far exceeds the capacity of the cardiovascular system to deliver oxygen (Poole DC & Erikson HH, 2003). As a result, the stroke volume of equine heart is likely to be particularly important in determining aerobic capacity for individuals (Young LE, 2003). Also the huge range of heart rate is the most important mechanism for increasing cardiac output during insensitive exercises. Impressively is how horse's heart rate above 200 beats per minute ensure that cardiac output increases from 35 litres per minute at rest to above 200 litres per minute during maximal exercise. Summary in the major heart adaptation and in general cardiovascular plasticity under stress during exercise makes the horse such a good athlete.

Horse heart anatomy

The heart is an adaptive organ for pumping blood, responding to changing needs by modifying contractile strength and beating rate (Bers DM, 2001). The blood flow supplies all of the muscles and organs with oxygen and nutrients and carries away the waste products also sustained the thermoregulation of the animal. It does this under all conditions: when the horse is galloping after hounds, or when it's asleep, in a very rhythmical and predictable manner. To do this efficiently, the heart is divided into two sides: the left side consisting of left ventricle and left atrium, takes oxygenated blood from the lungs and supplies muscles and organs; and the right heart, whose right atrium pump chamber receives the de-oxygenated blood and pumping it via right ventricle chamber to the lungs, where it is replenished with oxygen to be returned in the left heart.

Depending on the breed and the amount of training, the weight of the heart relative to body weight ranges between 0.6% for a draft horse and 1% for a Thoroughbred. The organ structure and major vessels position of the horse heart is well known and not different from the other mammals (Fig.1) and species-specific features of the organ serve to distinguish it mainly from the bovine heart, which attains comparable size. The horse's heart is cone shaped, anatomically there are distinguished a base and a bland apex when it is relaxed (diastole), atrial and auricular face, right and left ventricular margins (Budras KD & Sack WO, 1994, Bortolami R, 2006). The heart along with a small amount of fluid, is contained in the thoracic cavity within a noncompliant fibrous sac called the *pericardium* whose inner surface, the parietal pericardium, is continuous with the *epicardium*, a layer of connective tissue that covers the outer surface of the heart and contact with the vast majority of the heart's muscular walls, *myocardium*, contains both cardiac myocytes and connective tissue (vascular smooth muscle, endothelial cells, and fibroblasts). The cavities of the atria e ventricles, along with the valves, are lined with another connective tissue layer called the *endocardium* (Brutsaert DL, 1989). *Atrioventricular valves* separate atria and ventricles cavities: the *tricuspid valve* on the right and the *mitral valve* on the left. *Semilunar valves*, named for their crescent-shaped cusps, separate each ventricle from its great artery: the *pulmonic valve* between the right ventricle and pulmonary artery and the *aortic valve* between the left ventricle and aorta. The presence of the thick nodes on the free margins of the cusps of these valves is the particular characteristic of the horse heart anatomy (Dyce KM et al. 2006). The semilunar aortic and pulmonary valve cusps are supported by thick tendinous margins.

Fig.1 Horse heart anatomical structure with major vessels. * The letters of the above legend in squares on the drawings of the heart. By Budras KD et al, 1994

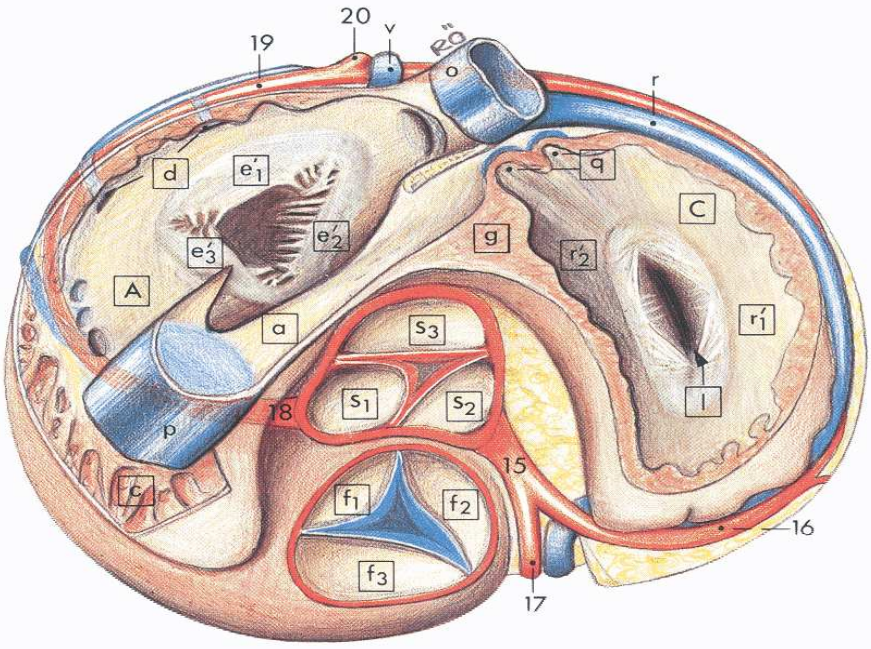

A* Right atrium

a Sinus venosus
b Coronary sinus
c Pectinate muscles
d Veins entering atrium

C Left atrium

q Entrance of pulmonary veins

g Interatrial septum
h Fossa ovalis
i Epicardium
j Myocardium
k Endocardium

B Right ventricle

e Right atrioventricular (AV) valve
e'_1 Parietal cusp
e'_2 Septal cusp
e'_3 Angular cusp
e''_1 Great papillary muscle
e''_2 Lesser papillary muscles
e''_3 Subarterial papillary muscle
f Pulmonary valve
f_1 Right semilunar valvule
f_2 Left semilunar valvule
f_3 Intermediate semilunar valvule

D Left ventricle

r Left atrioventricular (AV) valve
r'_1 Parietal cusp
r'_2 Septal cusp
r''_1 Subauricular papillary muscle
r''_2 Subatrial papillary muscle
s Aortic valve
s_1 Right semilunar valvule
s_2 Left semilunar valvule
s_3 Septal semilunar valvule

l Atrioventricular orifice
m Interventricular septum
n Trabeculae septomarginales
o Trabeculae carneae
p Chordae tendineae

Fig.1 continuous Base of the horse heart, sectioned in the dorsal (horizontal) plane. * The letters of the above legend in squares on the drawings of the heart. By Budras KD et al. 1994

The larger cusps of the mitral and tricuspid valves are tethered at their margins by fibrous *chordae tendinae* that attach to *papillary muscles*, which are "fingers" of myocardium that project into the right and left ventricular cavities and operate valves opening/closing. All four valves lie in a plane within a part of the connective tissue "skeleton" that separates the atria and ventricles within which the mitral, tricuspid, and aortic valves surround a big one fibrous triangle called the *right fibrous triangle* that could be calcified in a old horse.

Architecture of the heart walls is in the strict according of the blood flow applied pressure. The thin-walled atria, which develop relatively low pressures, contain ridges of myocardium called *pectinate muscles*. The ventricles develop much higher pressures than atria and therefore have thicker muscular walls. The muscular walls of the ventricles are made up of overlapping sheets, named spiral muscles, that follow spiral paths as they sweep from the fibrous skeleton at the base of the heart to its apex (Grant RP, 1965). The left ventricle, which has approximately three times the mass and twice the thickness of the right ventricle, can be viewed as a "pressure pump". The right ventricle, which pumps at lower pressure and operates as a "volume pump", is shaped like a crescent with inflow through the tricupsid valve at one and outflow through the pulmonic valve at the other.

The heart receives a rich supply of nerves, which play a role in increasing and decreasing the heart rate.

Cardiac muscle tissue organization

Several types of cardiac myocytes are found in myocardium. The most numerous are working atrial and ventricular myocytes. The cells of the myocardium are arranged in a branched network, where the intercalated discs, which are densely staining transverse bands that characteristically appear at right angles to the long axis of the cardiac myofibers, represent specialized cell-cell junctions that contain regions of low electrical resistance. So the heart function as if all of the myocytes are in free electrical communication.

The heart undergoes a cycle of events that cause blood to be propelled to the lungs and the body. These events can be divided into two stages: diastole and systole. During the diastolic stage, the atrial and ventricular myocytes are relaxed.

Systole refers to the period of contraction and consequent ejection of blood from the ventricles to the pulmonary artery or aorta. The cardiac cycle is initiated by the sinoatrial node – a group of specialized non-contractile cardiac myocytes positioned in the wall of the right atrium. All of the cells in the heart have an intrinsic ability to generate action potentials (electrical impulses). However, the sinoatrial node acts as the primary pacemaker because its cells naturally discharge at a high rate, and so override the other potential pacemaking sites. Hormonal modulation of the sinoatrial node is one of the principal mechanisms for altering the frequency of the heartbeat. From the sinoatrial node, the action potential spreads over the atria causing them to contract and push blood into the ventricles. As the wave of depolarization sweeps across the heart, it reaches the atrioventricular node, which filters and relays the signal to the ventricles via specialized conduction tissue including the Purkinje fibers. The atrial chambers contract and relax before the ventricular systole, and their activation is evident as separate electrical activity in an electrocardiogram. The time course of contraction is marginally shorter in atria compared to ventricles. Both cell types reach peak contraction within a few tens of millisecondi (Luss I et al. 1999).

The ventricles contract more forcefully than the atrial chambers and are predominantly responsible for forcing blood out of the heart. However, atria can play a significant role in altering the amount of blood that loads into the ventricles before to systole. When a person is at rest, the contribution of atria to the filling of ventricles with blood is relatively low. The majority (~90%) of ventricular refilling occurs as a consequence of the venous pressure of blood returning to the heart. However, if the heart rate increases, such as during exercise or stress, then atrial contraction can account for ~20-30% of the volume of blood in the ventricles. This contribution to ventricular refilling is known as ‘atrial kick’ (Lo HM et al. 1999).

Working cardiac myocytes structure

Working cardiac myocytes usually contain a single centrally located nucleus. The contractile proteins, actin and myosin, which make up almost one-half of the volume of working cardiac myocytes, are organized in regular array of cross-striated myofibrils. Most of the remaining cell volume is occupied by mitochondria, the energy generator of

contraction. Key membrane systems that regulate cardiac performance include the plasma membrane, called sarcolemma, which separates the cytosol from the surrounding extracellular space, and the intracellular membranes of the sarcoplasmic reticulum (Katz AM, 2006). Sarcolemma forms a deep invagination protruding into the centre of the cell, called T-tubules. These narrow (average diameter ~200 nm) inwardly directed projections of the sarcolemma running perpendicularly into the cells, arise at each of the Z-lines within cardiac muscle and have a regular spacing (~1.8 μm).

Ultrastructural studies have demonstrated that sarcoplasmic reticulum in mammalian cardiac myocytes contains at lest four distinct but continuous regions: the sarcotubular network SR; the junctional and peripheral SR; the corbular RS (*corbula* means 'little basket' in Latin) (Jorgensen AO et al. 1993) (Fig.2). The sarcotubular network, corresponding to the longitudinal SR of skeletal muscle fibers, consists of 25-60 nm diameter sarcotubules organized in an anastomosing network that surround the myofibrils fairly uniformly along the entire length of sarcomere. The junctional and corbular SR are structurally specialized domains extending from the network SR and contain electron-dense material in their lumen. They are most densely distributed in the interfibrillar spaces neighboring the central region of the I-band. The prominent structural difference between these two regions of cardiac SR is that junctional SR is physically connected to either T-tubules or to sarcolemma via 'feet' structures, whereas corbular SR is not. The association of a junctional SR domain with the transverse T-tubule invagination of the sarcolemma membrane or with the sarcolemmal surface is called dyad junction. The triad junction, comprising a pair of junctional SR cisternae and the T tubule, is a common feature of skeletal muscle fibers. It has been reported that electron dense structures similar to 'feet' structures project from the surface of corbular SR into the cytoplasm (Jorgensen AO at al. 1993). It has been demonstrated that the 'feet' structures of both junctional and corbular SR, correspond to the SR Ca^{2+} release channels known as ryanodine receptors (RyR2). Electron microprobe analysis studies showed that the lumen of junctional SR and corbular SR store calcium (Jorgensen AO et al. 1988). Immunoelectron microscopical studies demonstrated that the main protein components of network SR are the SR-Ca^{2+}-ATPase (Jorgensen AO et al. 1982) and its regulator phospholamban, that are uniformly distributed in the network SR. Calsequestrin, the high capacity low affinity Ca^{2+} binding protein, is present in the lumen of junctional SR and corbular SR (Jorgensen AO & Campbell KP, 1984; Jorgensen AO et al. 1984, 1985, 1988) and is responsible of the Ca^{2+} storage.

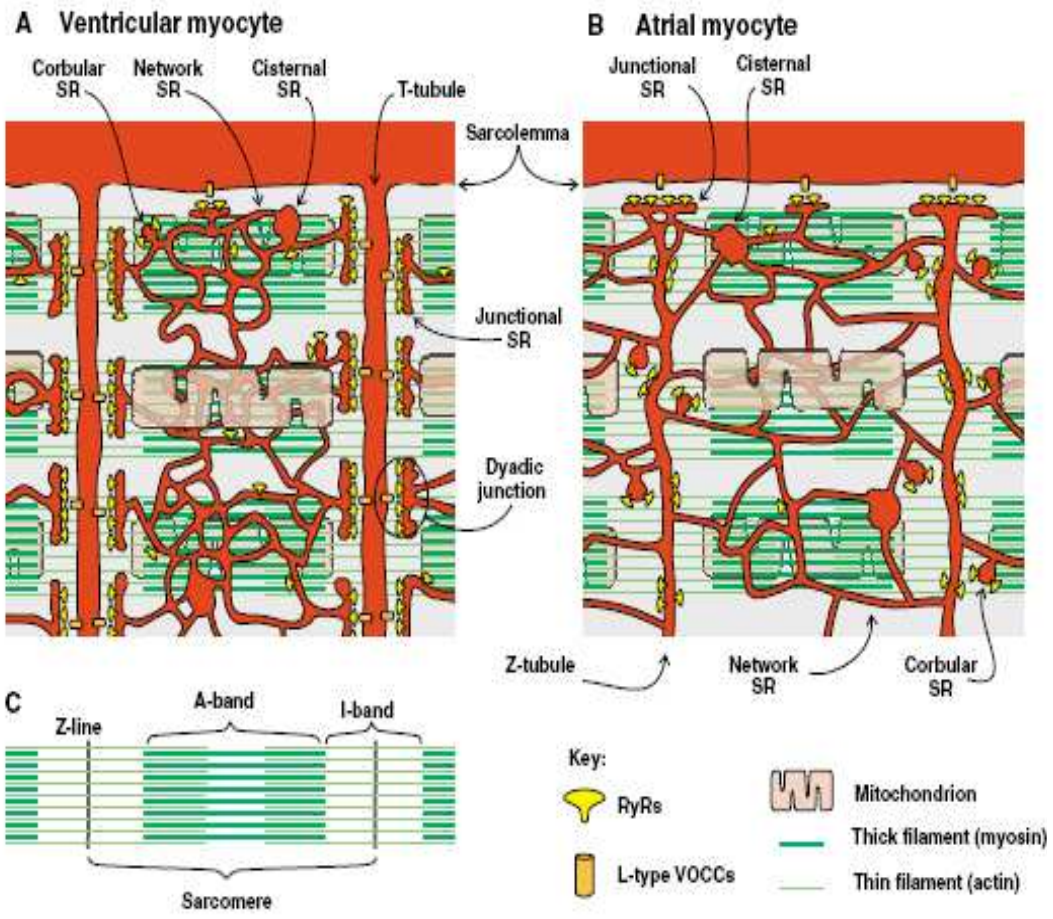

Fig.2 Structure of ventricular, atrial cardiac myocytes. Panels A and B illustrate the relative positioning of some of the key elements involved in EC coupling. The network SR elements wrap around both the myofibrils and mitochondria. By Bootman MD et al. (2006). Panel C shows the topology of a myofibril relative to the ventricular myocyte section above it in A.

Ca^{2+} is accumulated into the lumen of the SR across the entire surface of the network SR via the Ca^{2+}-ATPase. Ca^{2+} subsequently diffuses to the lumen of junctional and corbular SR where it is sequestered by calsequestrin and stored until it is released via the ryanodine receptor RyR2, in response to plasma membrane depolarization.

Cardiac excitation-contraction coupling machinery

Cardiac excitation-contraction (ECC) coupling is the process from electrical excitation of the myocytes to contraction of the heart (Bers DM, 2002).

During an action potential initiating at sinoatrial node, the consequent depolarization of cardiomyocytes membrane induces a Ca^{2+} influx through sarcolemmal voltage-gated L-type Ca^{2+} channels into the cytoplasm. Efficiency of excitation-contraction in the cardio myocytes is enhanced by structural features of this highly organized cells with its scalloped surface formed by periodic anchorage points at the Z-line. At those points the T-tubules bring the action potential into the centre of the cell. Initially, the wave of depolarization spreads rapidly along the myocardial sarcolemma membrane, opening the voltage dependent L-type Ca^{2+} channels in the T-tubule membrane to deliver a brief pulse of trigger Ca^{2+} from extracellular space (Berridge MJ, 2002). The small Ca^{2+} influx through sarcolemmal, triggers a much larger release of Ca^{2+} from the sarcoplasmic reticulum via Ca^{2+} release channels ryanodine receptors (RyR2). The process is called Ca^{2+}-induced Ca^{2+}-release (CIRC) (Meissner G, 2004) (Fig.3).

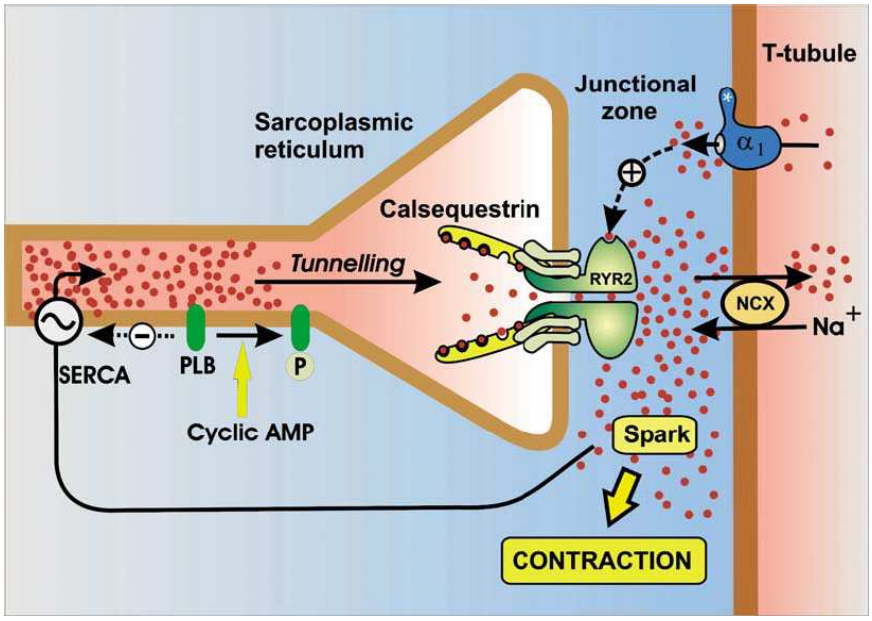

Fig.3 Excitation-contraction coupling in cardiac cell occurs through a mechanism where calcium induced calcium release. By Berrige MJ, 2002

At the dyads junction, T-tubules come into very close opposition with flattened cisternae of sarcoplasmic reticulum in these regions but don't fuse. So the RyR and L-type Ca^{2+} channels are located in a close functional association, thus allowing rapid CIRC to occur (Sham JSK et al. 1995), diffusing only across the narrow gap of the junctional zone. The cytosolic free Ca^{2+} is increased 10- to 100-fold during this period, named systolic. This Ca^{2+} influx occurs into a narrow (~10 nm) cleft, referred to as the "dyadic" or "tryadic"

cleft (Ayettey AS & Navaratnam V, 1978). The density of RyRs is particularly high at the clefts, where the SR and sarcolemma are in close apposition, and they are therefore located directly opposite voltage-gated L-type Ca^{2+} channels. When Ca^{2+} floods into the cytoplasm through voltage-gated L-type Ca^{2+} channels, it does not have far to diffuse before encountering RyRs.

The Ca^{2+} concentration within this small space cannot be measured at present, but using mathematical modeling it has been estimated that the Ca^{2+} rise may exceed several millimolar in the centre of the cleft (Peskoff A & Langer GA, 1998; Jones PP et al. 2006). Localized SR Ca^{2+} release originating from a single cluster of RyR2s is called a Ca^{2+} spark. The spontaneous production of these events is a function of both cytoplasmic and luminal Ca^{2+}. Ca^{2+} wave initiation is thought to be the result of both the "temporal and spatial summation of Ca^{2+} sparks" in a discreet area of the cell. The increase in cytosolic Ca^{2+} originated by Ca^{2+} wave, allows the actin and myosin contractile filaments to engage and slide past each other, thus leading to myocytes contraction and producing the force to propel blood.

After generating a Ca^{2+} spark, the RyR2 inactivates and the released Ca^{2+} is then removed during the diastole or relaxation period. Most of Ca^{2+} is pumped back from the cytoplasm to SR lumen via sarcoplasmic reticulum Ca^{2+}-ATPase (SERCA2 cardiac isotype). The SR coordinates the movement of cytosolic Ca^{2+} during each cycle of cardiac contraction and relaxation.

Calcium is extruded from the cytoplasm also via sarcolemmal Na^{+}/ Ca^{2+} exchanger (NCX), plasma-membrane pump (PMCA), and mitochondrial Ca^{2+} uniporter. Quantitatively, SERCA and NCX are most important (Bers DM, 2000). A proportion similar to that entering through the L-type channel is removed from cell by NCX while the remainder is taken back into the SR by the SERCA pumps distributed over the non-junctional regions of the SR. The activity of SR Ca^{2+}-ATPase is higher in rat ventricle than in rabbit ventricle (because of a greater concentration of pump molecules), and Ca^{2+} removal through NCX is lower, resulting in a balance of 92% for SR Ca^{2+}-ATPase, 7% for NCX and 1% for the slow systems. Analysis in mouse ventricle is quantitatively like rat, whereas the balance of Ca^{2+} fluxes in ferret, dog, cat, guinea pig and human ventricle are more like rabbit. Thus, mouse and rat ventricle (which also show very spike like action potentials) poorly mimic human with respect to the quantitative balance of cellular Ca^{2+} flux. Moreover, during heart failure in humans and rabbits, functional expression of SR Ca^{2+}-ATPase is reduced and

NCX is increased, such that these systems contribute more equally to the decline in intracellular Ca^{2+} concentration. These changes counterbalance each other with respect to twitch relaxation and intracellular Ca^{2+} concentration decline, leaving it unaltered. But both changes tend to reduce Ca^{2+} content in the SR, limiting SR Ca^{2+} release, and this may be a central cause of systolic contractile deficit in heart failure.

The Ca^{2+} entering these non-junctional regions is then transferred back to the junctional zone through a process of tunneling (Berridge MJ, 2002) to be used the next cycle of contraction/relaxation cycle.

Calcium cycling in the cardiac myocytes is a complex process, and further elucidation of the proteins involved in its uptake, storage, and release is necessary to better understand the basic physiology and pathophysiology of the heart (Fan G et al. 2004).

Ventricular myocyte EC-coupling

Cardiac Ca^{2+} signaling has been most extensively studied in myocytes isolated from the ventricles. It is well established that Ca^{2+} signals in mammalian ventricular myocytes take the form of homogenous whole-cell increases Such global Ca^{2+} responses reflect the spatial and temporal summation of signals from many Ca^{2+} spark sites, which are synchronously recruited during depolarization. The critical ultrastructural detail of mammalian ventricular myocytes that promotes homogenous global Ca^{2+} transients is the presence of an extensive 'transverse tubular' system (T-tubules. The typical striated distribution of ventricular myocyte T-tubules can be shown by immunofluorescence techniques using antibodies against sarcolemmal proteins involved in generating and reversing Ca^{2+} signals, that are concentrated at the T-tubules, such as Na^{+}/ Ca^{2+} exchanger. Moreover, T-tubules serve to bring voltage-gated L-type Ca^{2+} channels and RyRs into close proximity. Indeed, immunostaining ventricular myocytes for voltage-gated L-type Ca^{2+} channels and RyRs reveals that these proteins largely appear in discrete clusters within a 3-dimensional matrix throughout the cells (Chen-Izu Y et al. 2006). The clusters of voltage-gated L-type Ca^{2+} channels and RyRs have substantially overlapping distributions, indicating that they are in very close proximity. When ventricular myocytes are depolarized, the action potential is relayed to voltage-gated L-type Ca^{2+}channels within the T-tubule network. This means that even those Ca^{2+} spark sites deep within a ventricular cell are recruited during EC coupling,

thereby giving rise to a synchronized global Ca^{2+} signal. If ventricular myocytes are imaged at high speed during the onset of EC coupling, the Ca^{2+} signal can be seen to arise with a striated appearance. This reflects the initiation of Ca^{2+} release adjacent to the T-tubules before the Ca^{2+} signal has managed to diffuse from the dyadic junctions.

Atrial myocyte EC-coupling

Unlike ventricular myocytes, atrial cells do not possess an extensive T-tubule system: the Na^{+}/ Ca^{2+} exchanger immunostaining is around the outside of the cell only. Some atrial cells possess a more rudimentary transverse-axial tubular network. In place of the T-tubules, atrial cells have prominent sarcoplasmic reticulum elements, which have been described as 'Z-tubules' (Yamasaki Y et al. 1997). Just like T-tubules, these structures are perpendicular to the long axis of the cells. Atrial cells therefore contain a form of transversely oriented tubule, but it is formed from internal SR membrane and not the sarcolemma.

The sarcoplasmic reticulum in cardiac muscle has a highly convoluted organization that can be classified into four major structural elements: junctional, corbular, cisternal and network (Fig.2). Both ventricular and atrial cells possess all these SR forms, but their relative abundance is different (Yamasaki Y et al., 1997). For example, ventricular myocytes have a more extensive network SR running alongside the myofibrils and interweaving with the mitochondria. By contrast, atrial myocytes have a less complex network SR, but substantially more corbular compartments (Franzini-Armstrong C et al. 2005). The corbular SR possesses both RyRs and the Ca^{2+} storage protein calsequestrin (Jorgensen AO et al., 1993) and is therefore a potential source for amplification of Ca^{2+} responses by voltage-gated L-type Ca^{2+} channels. Owing to its abundance in atrial myocytes, the corbular SR may contribute significantly to the generation of Ca^{2+} signals. The pattern of RyR localisation in atrial myocytes has some similarity to that observed in ventricular cells, in that most RyRs lie within regularly spaced transverse striations corresponding to the positions of the Z-tubules. However, there is one crucial difference between atrial and ventricular myocytes: that is the expression of additional RyR clusters around the periphery of the atrial cells.

Atrial myocytes therefore possess two populations of RyRs. One minor group (junctional RyRs), sit just beneath the sarcolemma. The other channels (nonjunctional RyRs) are deeper inside the cell and constitute the bulk of the RyR population.

Although the junctional RyRs represent a small fraction of the total number of channels, they are crucially important in atrial EC-coupling. The localization of voltage-gated L-type Ca^{2+} channels is entirely different in ventricular and atrial myocytes. Because of the general lack of T-tubules, the sarcolemma does not regularly protrude into atrial cells, and voltage-gated L-type Ca^{2+} channels only function around the outside of the myocytes (Mackenzie L et al. 2001, 2004). As a consequence, the close apposition of RyRs and voltage-gated L-type Ca^{2+} channels that is necessary for triggering EC coupling occurs only at the cell periphery. These differences in ultrastructure have a significant effect on the spatial properties of the Ca^{2+} signals. As described above, ventricular myocytes display homogenous responses, which arise from the simultaneous recruitment of Ca^{2+} sparks throughout a cell. However, in atrial myocytes, EC coupling is initiated around the periphery of the cells, because this is the only place where the voltage-gated L-type Ca^{2+} channels and junctional RyRs come together.

Calcium uptake

Calcium uptake and thus the rate of relaxation of the heart during diastole are controlled by phospholamban (PLN) whereas Ca^{2+} release is modulated by alterations in the RyR activation state through protein-protein interaction of RyR accessory proteins in systolic period, and SR Ca^{2+}storage capacity, that depend on intraluminal accessory calcium buffering protein, one of which is calsequestrin.

Phospholamban, a small reversibly phosphorylated, transmembrane protein that is located in the cardiac SR. In its dephosphorylated form, PLN binds to and reversible inhibits SERCA's activity by lower its calcium binding affinity. The phosphorylation of PLN and Ca^{2+} binding to SERCA are driving forces for the dissociation of the PLN-SERCA complex, thereby activating SERCA. As a result, the rate of cardiac relaxation is increased, so the same contractility is increased in proportion to the elevation in the size of the SR Ca^{2+} store and the resulting increase in Ca^{2+} release from SR. So PLN is not only an inhibitor of Ca^{2+} pump but also allows the use of cardiac reserve where it is presented as a

crucial regulator of the kinetics of cardiac contractility (MacLennan DH & Kranias EG, 2003).

Calcium release and storage: RyR2 and its accessory proteins, components of quaternary complex

RyR2 that play a primary role as a cardiac Ca^{2+} release channel is a very large protein (MW 565 kDa) and it exists as a tetramer (MW 2.2 MDa). It also serves as a scaffold protein for an increasing number of other proteins (Marx SO et al. 2000, Zhang L et al. 1997, Fan G et al. 2004) making it a huge macromolecular complex that can be discerned as a junctional "feet" in electron micrographs (Franzini-Armstrong C et al. 1999). Zhang et al. (2004) suggest that the several key proteins that have been found to be localized to junctional SR may associate into a stable complex at the junctional membrane to facilitate the release of Ca^{2+}. Components of this protein complex identified to date include RyR or Ca^{2+} release channel; calsequestrin, a high capacity Ca^{2+}-binding protein located in the junctional SR lumen, which buffers the calcium that is released during muscle contraction; and triadin and junctin, putative "anchoring" proteins, which appear to stabilize calsequestrin at the inner face of the junctional SR membrane.

Calsequestrin

Calsequestrin is the major intra-SR Ca^{2+}-binding protein and it is localized entirely within the junctional SR lumen, where the protein appears to be physically connected to RyR by "anchoring strands" (Franzini-Armstrong C et al. 1987).

Cardiac CSQ (MW 45,269) (Scott BT et al. 1988) is highly acidic with 119 Glu and Asp residues (net 64 negative charge). It is capable of binding and releasing large quantities of Ca^{2+} rapidly: each molecule binds about 20 calcium ions with low affinity (K_d=~1mM) (Mitchell RD, 1988). CSQ forms a linear polymer at physiological luminal Ca^{2+} concentrations (Fryer MW & Stepherson DG, 1996). The model for Ca^{2+} -dependent conformational changes presented by Wang et al. predicts the formation of thioredoxin-like folds with a Ca^{2+} concentration of ~ 10μM which then condense into a compact monomer

as [Ca^{2+}] increase. The monomers dimerise by back-to-back and in following form polymer by front-to-front interactions (Wang S et al. 1998; Beard NA et al. 2004; Park H et al. 2003).

This protein undergoes a structural change upon Ca^{2+} binding (Ikemoto N at al. 1972) and also changes its structure during EC coupling, after t-tubule depolarization and before Ca^{2+} release from SR (Ikemoto N et al. 1991). These suggest that CSQ is the transmitter of the luminal Ca^{2+} content to the Ca^{2+} release channel (Györke at al. 2003; Beard NA et al. 2004) and actively participates in muscle contraction by regulating the amount of Ca^{2+} released by the ryanodine receptor (Terentyev D et al. 2003).

Junctin and triadin

Although junctin (MW 26 kDa)(Jones LR et al. 1995) and triadin (MW 32, 35, 75 kDa splice variants) (Guo et al. 1996), the integral membrane proteins "anchoring" CSQ, are the products of different genes, they exhibit intriguing similarities in structure and as it seems in their biological role. "KEKE" motifs, long runs of alternating positively and negatively charged residues enriched in lysine and glutamic acid, presented in their primary structures are thought to be involved in the promotion of several types of protein-protein interactions (Realini C et al. 1994, 1995). The association of junctin and triadin with CSQ is inhibited by increasing calcium concentrations whereas their binding to the RyR and to one another is Ca^{2+}-independent (Zhang L et al. 1997).

It is not known whether CSQ can bind directly to the RyR when triadin and junctin are present or whether the presence of triadin/junctin prevents it or in any case altered the effect of CSQ on RyR.

The dates on today clearly indicate that all of the components of quaternary complex have a primary importance for the cardiac EC-coupling function by means of RyR2 calcium release regulation by modulating its gate opening probability and calcium quantity outflow. Cardiac-specific overexpression of CSQ (on high levels 10- to 20-fold) resulted in increased SR Ca^{2+}storage capacity in transgenic cardiomyocytes decreased CICR RyR activity, but Ca^{2+}release induced by the RyR agonist caffeine is of 10-fold greater amplitude than in controls. This cardiac phenotype led to cardiac hypertrophy (Jones LR et al. 1998; Sato Y et al. 1998). More moderate levels of adenoviral CSQ overexpression (2-

to 4-fold) in adult ventricular myocytes resulted in enhanced Ca^{2+} transient and Ca^{2+} spark amplitude, increased SR Ca^{2+} load, with prolonged SR Ca^{2+}-release time (Terentyev D et al. 2003) which indicate that cardiac CSQ plays pivotal roles both in Ca^{2+} storage and in regulation of Ca^{2+} release via the type 2 RyR.

Based on RyR2 bilayer studies Györke et al. suggest that the open probability of RyR2 (with TRI and JN) is inhibited by CSQ at low luminal $[Ca^{2+}]_{sr}$, but that this inhibition is relieved with luminal $[Ca^{2+}]_{sr}$ increase due to weakness of CSQ-JN-TRI interaction and possible CSQ dissociation from a complex (Györke I et al. 2004).

Moreover, the cardiac CSQ (cCSQ) is interested in arrytmogenic disorders caused sudden cardiac death. A point mutation in a highly conserved region of cardiac CSQ, D306H, was found to be the cause of the autosomal recessive form of catecholamine-induced polymorphic ventricular tachycardia (CPVT). Additionally, three CSQ-related CPVT families were discovered (Lahat H et al. 2001, Postma A et al. 2002, Eldar M et al. 2003). The mechanism of exercise-induced arrhythmia (CPVT) caused by reduced capacity of mutated cCSQ in calcium and TRI-JN binding (Houle TD, 2004) was discussed: cCSQ influences the frequency of spontaneous Ca^{2+} waves by determining the rate recovery of luminal SR calcium concentration (Kubalova Z et al. 2004, Viatchenko-Karpinski S et al. 2004, Terentyev D et al. 2003).

About a physiological role of TRI and JN is little more known it is thought that they may play more direct roles in Ca^{2+} release beyond simply anchoring CSQ to the RyR.

The junctin or triadin overexpression was associated with an impaired relaxation in isolated cardiomyocytes and papillay muscles (JN) and lead to hypertrophy (Kirchhefer U et al. 2001, 2003, 2006). Importantly, no alterations in other Ca^{2+}-cycling protein levels were registered when junctin levels were decreased/increased in adenovirus transfected adult rat cardiomyocytes that resulted increase of the rate of contraction and relaxation and Ca^{2+} transient peak and accelerated Ca^{2+} decay in case of downregulation of junctin however, all these contractile parameters were depressed significantly in case of upregulation of junctin (Fan GC et al. 2007).

As well as CSQ also TRI and JN overexpression was found correlated with arrhythmia predisposition (Hong CS et al. 2002, Terentyev D et al. 2005). These findings suggest that both TRI and JN plays a prominent role in cardiomyocyte Ca^{2+}-cycling and contractility.

Histidine-rich Ca^{2+} binding protein (HRC)

Recently, another protein, named histidine-rich Ca^{2+} binding protein (HRC) has been suggested to be an additional component of the upper described SR quaternary structure involved in Ca^{2+} release (Lee H et al. 2001) especially in heart (Fig.4).

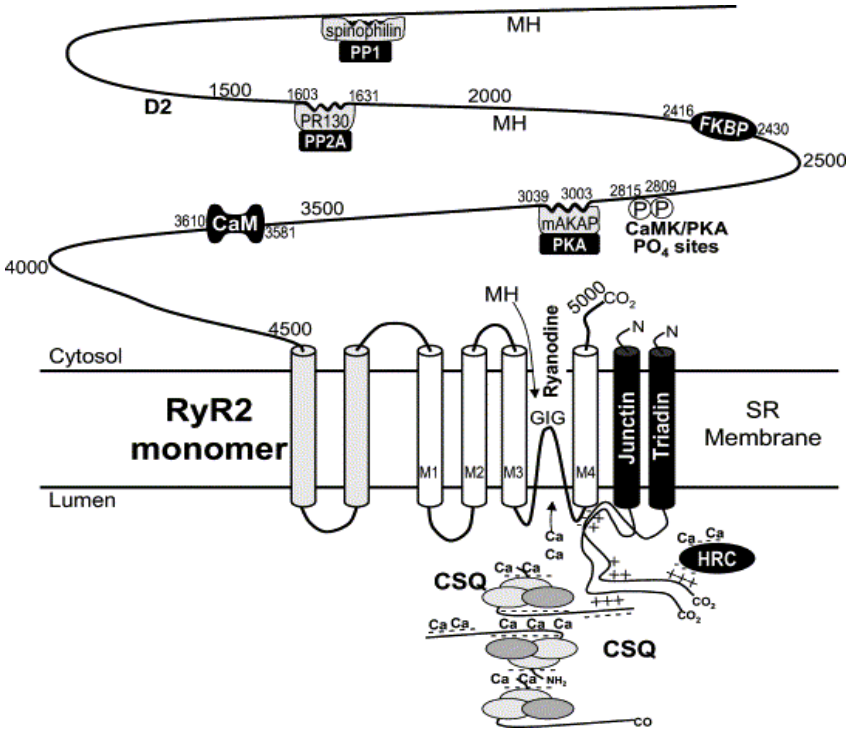

Fig.4 Cardiac RyR with interaction sites of some associated proteins M1-M4 indicate the four transmembrane domains described by Takeshima et al. (1989) with the putative pore region (GIG). Proteins that form a stable quaternary complex with RyR2 on junctional SR membrane are calsequestrin (CSQ), triadin and junctin, and HRC.

HRC was described for the first time in SR from rabbit skeletal and cardiac muscles by Hofmann and co-workers (1989). They identified it as a moderately abundant calcium binding protein, migrating with an apparent molecular weight of 165.000 on SDS polyacrilamide gels (Hofmann SL, 1989). The protein was found expressed only in cardiac and skeletal muscles, both red and white, and resulted to correspond to the 170 kDa protein previously described by Campbell and co-authors (Campbell KP et al. 1983). The apparent molecular weight of HRC was very similar to that of sarcalumenin, another calcium binding protein localized into the lumen of SR, but in contrast to sarcalumenin and also to calsequestrin, HRC did not contain carbohydrate. The two main features of HRC protein are: the 45 Ca^{2+} binding on nitrocellulose blot overlays, and the staining blue with the dye

Stains-All, a cationic dye that stains metachromatically blue the Ca^{2+}-binding proteins. In their first work, Hofmann and co-workers reported also that the HRC protein was identified because of its ability to bind 125I labeled plasma low-density lipoprotein (LDL). LDL is know to bind polyanions so that the ability of the HRC protein to bind LDL suggested that the protein may have extended sequences of acidic amino acids.

On the same year, Hofmann and co-workers reported the complete amino acid sequence of the rabbit HRC muscle protein, as deduced from a cDNA clone. The rabbit protein consists of 852 amino acids with a hydrophobic sequence at the NH_2-terminus (Fig.5). This sequence consists with the general properties of an endoplasmic reticulum signal sequence. The middle of the protein contains nine histidine-rich acidic repeats, which give the name to the protein. Every acidic repeat contain 29 residues and is made by: a histidine-rich NH2 terminus followed by a string of 10 to 11 negatively charged amino acids, a serine/threonine containing segment and a positively charged COOH terminus. The histidine content of HRC protein is near 13% and results much higher than the 3% content of most proteins. All of these repeats resulted also nearly identical at the nucleotide level. The COOH terminus of the protein contains a sequence of acidic repeats with 13 consecutive glutamic acid residues, followed by a cysteine rich region. The protein is quite acidic with 12% of aspartic and 19% glutamic acids. The calculated isoelectric point is 5.68.

The HRC cDNA have been cloned in many mammalian species as: rabbit, human, mouse, rat, monkey (Hofmann SL et al. 1989, 1991; Ridgeway AG et al. 1999) and recently in cow. The deduced amino acid sequences have revealed some differences between species: HRC protein is 699 and 852 amino acids long in human and rabbit respectively. Although the differences in length, the protein structural organization consistent in a signal sequence, histidine rich acidic repeat region and cysteine-rich region, is unique.

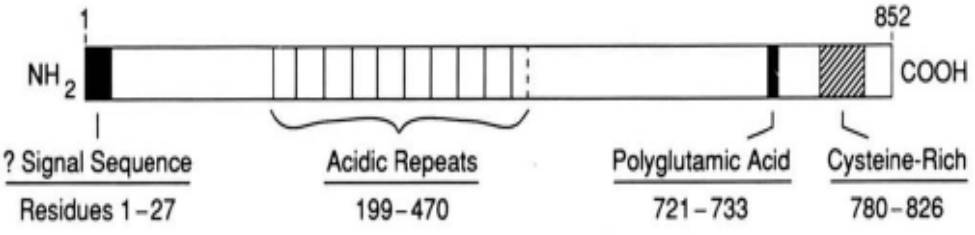

Fig.5 A major structural features of HCP protein deduced from rabbit cDNA sequence is rappresented by Hofmann SL et al. (1989)

The expression pattern of mammalian HRC genes in different tissues was also studied in the same mammalian species in which the HRC cDNA was cloned. Using a semi-quantitative PCR method, the HRC gene resulted expressed only in skeletal and cardiac tissues, being totally absent in all other tissues (lung, liver, brain and many others). Using RNA blot hybridization of HRC mRNA from rabbit tissues, it was shown that also in rabbit the HRC mRNA was expressed only in cardiac and skeletal muscle tissues and that no mRNA could be detected in ten other tissues. Although differences in methods, it was clear that in small size animals such as rat mouse and rabbit, HRC mRNA was expressed in an equal amount, while human and primate HRC gene was expressed more abundantly in the heart than in skeletal muscle. In addition, the human and mouse HRC genes were expressed in the aorta. By the analysis of HRC gene expression in cardiac mouse tissue during pre and post-natal development, it was found that HRC gene expression starts early during embryos development, at least at 12.5 embryonic days, and its level increases during development. In mouse heart, the early expression of HRC resembles that of calsequestrin cardiac isoform 2. To date there is no evidence that different HRC isoforms has been expressed in skeletal, both fast and slow twitch, and cardiac muscles.

The localization of this protein on SR is still controversial: it was demonstrated with different methods that HRC is located both on the cytoplasmic surface of SR or in the SR lumen. Hofmann and co-workers (1989), by immunolocalization studies using electron microscopy techniques, suggested that HRC is a lumenal protein, diffusely distributed within SR membrane system. This data were later supported by HRC fusion protein data (Lee HG et al. 2001). On the other hand another group found that the protein is localized on the cytoplasmic side of SR. They used phosphorylation assays with both PKA and CaM kinase II, which are known to reside in the cytoplasm of muscle fibres, and trypsin treatment of sealed SR membranes to demonstrate the cytoplasmic localization of HRC and also, almost in the skeletal muscle, the HRC protein localization is restricted only to the terminal cisternae portion of SR.

All authors agree with the idea that HRC may attach to SR membrane not directly but through binding to an intermediate protein. The intermediate protein has been identified in rabbit and human with triadin. (Sacchetto R et al. 1999, 2001; Lee HG et al. 2001; Arvanitis DA et al. 2007). However results regarding the HRC and triadin domains involved are contradictory. One group reported that histidine and acidic-rich repeats, including amino acids 199-470 of rabbit HRC, interact with the luminal domain triadin

(Lee HG et al. 2001), strengthening the hypothesis of a luminal localization of HRC. Other studies indicated that the COOH-terminal domain, including amino acids 569-852 of rabbit HRC, binds to the 47 cytoplasmic amino acid stretch of triadin, and that the 13 amino acid polyglutamic stretch is responsible for this interaction (Sacchetto R et al. 1999, 2001). These data obviously supported the idea that in rabbit muscles the HRC is located on the cytoplasmic side of SR. Using pull-down assays with human cardiac homogenates and recombinant human HRC peptides, resulted that also in human the COOH-terminal cysteine-rich domain, containing amino acids 600-699, binds to native human triadin (Arvanitis DA et al. 2007).

Protein functions:

It has been provided evidence that HRC is a regulator of SR calcium sequestration and cardiac function. Studies of HRC overexpression in adult cardiac myocytes, revealed an increased SR Ca^{2+} load; however, because of binding of this Ca^{2+} by the excess of HRC, the result is that the release of Ca^{2+} from SR is severely depressed. This is correlated with attenuation of cardiac contractility. The diminished cytosolic Ca^{2+} levels, during contraction would lead to an attenuation of SERCA Ca^{2+} transport rates and diminished rates of relaxation (Fan G et al. 2004). A quaternary structure composed by RyR, TRI, CS and JNT and involved in Ca^{2+} release has been described (Lee HG et al. 2001). Due to its important role as regulator of Ca^{2+} release and normal cardiac function, recently HRC has been suggested to be an additional component of SR quaternary molecular complex (Lee HG et al. 2001). Transgenic mice for HRC were used to study the effects of overexpression of HRC in vivo. Three lines of transgenic founders were created. Quantitative immunoblotting revealed approximately 1.7 fold and 3.2 fold cardiac overexpression of HRC in two lines in the one line respectively. In the last one phenotypic alterations were described. Moreover HRC mice exhibited congestive heart failure by 16-18 month of age and cannot tolerate the physiological stress of aging. On the contrary, lower HRC overexpression (two fold) exhibited by two of the three lines, elicited no phenotypic alterations even throughout the aging process. Taken together these data indicate that there may be a threshold level for HRC abundance in the cardiac SR. The main features of HRC overexpressing cardiomyocytes are:

- The time constant of twitch Ca^{2+} decay was prolonged by 41% in HRC overexpressing myocytes. This effect of in vivo HRC overexpression was different

than the pronounced effects of acute HRC overexpression in cardiomyocytes culture. This implies an impaired SR Ca^{2+} uptake and a delayed Ca^{2+} decline rates.

- The SR Ca^{2+} content was not altered in HRC myocytes (there was no differences in mean SR Ca^{2+} load between HRC myocytes and WT), unlike the increased SR Ca^{2+} content observed by HRC overexpression in myocytes.
- The activity of Na^{+}/Ca^{2+} exchanger was significantly (27%) depressed in HRC overexpressing myocytes; furthermore SR Ca^{2+}-ATPase function was significantly (25%) depressed. These data taken together suggested that the impaired Ca^{2+} removal by both SERCA and NCX contribute to the prolonged times of twitch Ca^{2+} decline elicited by chronic HRC overexpression
- The maximum rate of SR Ca^{2+} uptake was significantly (35%) reduced in HRC compared to WT hearts, although there was no differences in the apparent affinity of SERCA2 for Ca^{2+}
- The attenuation of Ca^{2+} signal decay, was not correlated to alterations in protein content (immunoblotting) of: SERCA2, PLN, P-PNL, CS, RyR, P-RyR and Junctin. However protein levels of cardiac isoform of triadin were upregulated, similar to previous findings in HRC cardiomyocytes culture. Furthermore the protein levels of the NCX were significantly increased.
- HRC overexpression is associated with more Ca^{2+} current entering through the L-type Ca channel; it may be an important compensatory mechanism to maintain SR Ca^{2+} load in the face of depressed SR Ca^{2+} transport activity
- Echocardiographic assessment indicated decreased heart rate (318 bpm against 541 bpm) in HRC overexpressing heart (equine cardiac muscle).

The most relevant effect of HRC overexpression seems to be the attenuation of twitch Ca^{2+} decline rates without any effects on both peak Ca^{2+} transient amplitude, or SR Ca^{2+} content. Both HRC overexpression in heart and in cultured cardiomyocytes was associated with compensatory alterations, indicating that HRC is an important regulatory protein in the heart and alteration in its expression levels trigger cardiac responses in attempt to maintain Ca^{2+} homeostasis. The cellular modifications induced by the overexpression of HRC in cardiac myocytes, were similar to the intrinsic features exhibited by cardiac cells of equine species.

It has been reported (Zhou X et al. 2007) that experimental heart mouse models overexpressing HRC have significantly less ischemia/reperfusion-induced injury. This

observed protection is possibly attributed to the attenuation of SR and cytosolic Ca^{2+} rise during ischemia/reperfusion, which alleviates ischemia/reperfusion induced apoptosis and necrosis.

Recently, a polymorphism in the human HRC has been indicated to be a powerful predictor for the occurrence of ventricular arrhythmias (Arvanitis DA et al. 2008).

Myostatin or growth differentiated factor 8

Myostatin (MSTN), a new member of the transforming growth factor-β superfamily, was described by McPherron et al. (1997). This secreted signaling molecule is expressed specifically in developing and adult skeletal muscle and it has been characterized as a negative regulator of skeletal muscle mass in rodents, cattle and other mammalians and fish (Patruno M, 2009). MSTN was noted to affect both hyperplastic (increase in the number of muscle fibers) and hypertrophic (thickness of the fibers) skeletal muscle growth in mammalians (McPherron AC et al. 1997). Its mechanism of action appears to be on resident muscle progenitor cells, satellite cells (Thomas M et al. 2000) which are activated to proliferate and differentiate in its absence.

Although the predominant MSTN expression was detected in skeletal muscles recently a low levels of MSTN mRNA and protein have been shown to be expressed in the myocardial tissues of sheep, mice, rat and cattle (Sharma M et al. 1999, Shyu KG et al. 2005, Matsakas et al. 2006, Morissette MR et al. 2006). It is known that putative receptor to myostatin, the activin receptor IIB is expressed in cardiac tissue (Lee SJ et al. 2005) but it is not clear whether the circulating MSTN secreted by skeletal muscle or endogenous heart MSTN play the precise functional role in the postnatal heart.

As other members of the TGF-β superfamily, myostatin is synthesized as a 376 amino acid precursor protein containing a signal sequence, an N-terminal propeptide domain and a C-terminal domain that consisting of the active ligand (McPherron AC et al. 1997) (Fig. 6). The predicted murine and ovine heart myostatin proteins are identical in the biologically active carboxy-terminal region, indicating that the myostatin gene is well conserved during evolution. Notably that Belgian Blue bull has the same deletion in heart myostatin cDNA sequences as that was observed for the skeletal muscle cDNA allele of the animal (Sharma

M et al. 1999). These facts suggest an important role of myostatin in mammalian heart as well as in skeletal muscle.

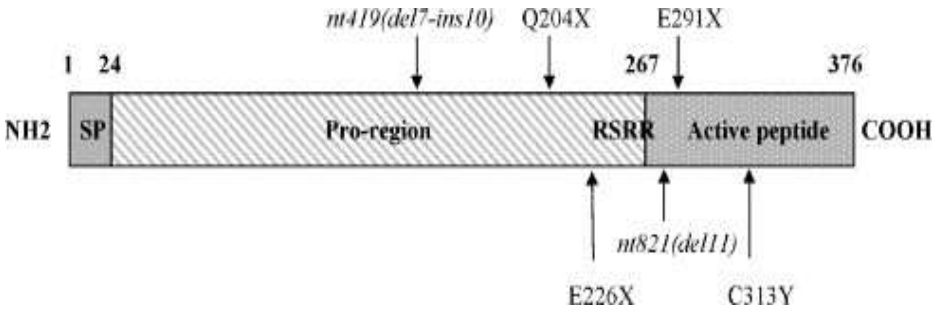

Fig.6 Structure of myostatin protein and natural mutations occurring in bovine myostatin gene and the position of inactivating mutations (arrows). The three domains represented in the scheme are the signal peptide (SP), the pro-region, which will be cleaved by proteasic digestion at the RSRR site during maturation, and the active peptide at the C-terminal part of the myostatin precursor.

The expression of myostatin has been detected in developing and in adult hearts in vitro and in vivo models (MacLellan et al. 1993, Sharma M et al. 1999, Shyu KG et al. 2005, McKoy G et al. 2007).

Myostatin transcript and/or protein expression have been shown to be regulated during different physiological and pathological situations which affect cardiac muscle mass, including cardiac growth modulation (McKoy G et al. 2007), athletic hypertrophy (Matsakas A et al. 2006), postmyocardial infarction remodeling process, infarction-associated inflammation (MacLellan et al., 1993, Sharma M et al. 1999), fibrosis of the myocardium, and cardiac dysfunction (Hoenig MR, 2008).

MSTN expression is regulated developmentally in rat cardiomyocytes: a 6-fold increase in myostatin expression is detected in foetal cardiomyocytes with high proliferation index compared of embryos proliferating cardiomyocytes and is maintained at a much lower level in adult cells. Knockout mice cardiomyocytes display exuberant cell enlargement in response to the hypertrophic agonist, phenylepherine (Morissette MR et al. 2006).

These dates revealed the same physiological role of myostatin in heart like in skeletal muscle as negative regulator of proliferation caused cell cycle arrest (McKoy G et al. 2007).

Nevertheless MSTN null mice do not display the profound alterations in cardiac muscle mass evident in skeletal muscle (McPerron AC et al. 1997) and neither loss of MSTN does not prevent the development of cardiac fibrosis in dystrophin-deficient *mdx* mice (Cohn RD et al. 2007) as it could be expected.

Besides being upregulated in cardiomyocytes bordering an infarct area after experimentally induced myocardial infarction (Sharma M et al. 1999) myostatin has been noted to be upregulated in hypertrophied hearts of transgenic mice with cardiac-specific expression of activated protein kinase Akt. The insulin-like IGF-1 pathway, in which Akt is involved, appears to be critical in determining the type of cardiac hypertrophy that occurs in athletes during physical training. This confirms the role of MSTN as a "chalone" of the insulin-like growth factor I pathway in the cardiac muscle (Gaussin V & Depre C, 2005). Finally myostatin is suspected to be another neurohumoral mediator of cardiac cachexia (Hoenig MR, 2008).

Taken together more then one possible physiological role of MSTN in cardiac muscle is discussed and remains to be elucidated.

MATERIALS AND METHODS

Animals and sampling

The total number of horses used in experiments was six (n = 6). Four adult horses used in experiments were commercial breeds killed in a slaughterhouses (Pantano Carni, Piove di Sacco and Fossò slaughterhouses), aged 3-10 years with heart weight 3.5-5 kg and have no cardiovascular system disorders. One heart was obtained from one-day-old colt died by unknown cause and another from career finished 25 old horse with right wall thinning and right ventricular dilatation heart probably caused by chronic pneumonia syndrome, heart weight was 3.4 kg. The horse was euthanized at the Veterinary University Clinics (Legnaro).

The hearts was dissected from horse's thorax after 30 min. The pieces of a left ventricular part was used for the cells isolation and frozen for an immunohistochemical analysis.

Tissue samples for RT-PCR and quantitative Real-time PCR were analyzed from heart muscle of six horses, including 1 day old and one 25 years old horse. There were collected six anatomical zones from horse heart and two types of skeletal muscles (Table. 1.) While skeletal muscle samples were taken from only three horses: the same one colt, 25 years old career finished horse and one adult horse without any health disorders.

Bovine cardiac tissue was collected for RT-PCR and Real-time PCR from six anatomical zone the same that from horse.

Table 1. Summary table of the heart tissue and skeletal muscle tissue sampled.

Animal	*Number*	**Origin information /slaughterhouse, age, particular characteristics/**	*Sampled muscle*
Horse	3	Piove di Sacco, Arre; 3-10 years old	Heart tissue left atrium right atrium left ventricle right ventricle intraventricular septum papillary muscle
Bos	1	Arre, adult 3-10 years old	
Horse	1	Fossò; 2 years old	Heart tissue left atrium right atrium left ventricle right ventricle intraventricular septum papillary muscle Skeletal muscle tissue longissimus toracicus head /Tricipite/
Horse	1	Legnaro; 1 day-old colt; died	
Horse	1	Legnaro; 25 years old, euthanized	

RNA extraction

Muscles collected from all horses (n=6) were cut to small single dimension (< 0.5 cm) and immediately immersed in RNA-later reagent (Ambion), than after storing at 4°C overnight frozen it at -20°C until required for RNA extraction, to protect it from degradation.

Total RNA was extracted from about 100 mg of various horse skeletal (Head of Tricipite and Longissimus toracicus) and cardiac muscles (atria, ventricles, intraventricular septum and papillary muscle of left ventricular part) muscles following a single-step acid guanidium phenol-chloroform extraction procedure employing OMNIzol™ reagent (EuroClone, Wetherby, UK) according to the manufacturer's protocol and then quantified by a spectrophotometer (Pharmacia). OMNIzol® reagent is a ready-to-use reagent for the isolation of total RNA from cells and tissue. During sample homogenization or lysis, OMNIzol® reagent maintains the integrity of the RNA, while disrupting cells and dissolving cell components. Generally muscle tissue needs an additional step before adding the reagent because it is rich in protein and connective tissue. To this end, the previously minced tissue pieces were immersed in liquid nitrogen was finely mechanically disrupted using a mortex and subsequently homogenized in a potter with with OMNIzol reagent to

release the RNA content. Following homogenization it is recommended to remove insoluble material by centrifugation at 12.000g, at 2-8°C, for 10 min. Next ice-cold chloroform (100 μl for each ml of OMNIzol used) was added to separate the RNA from nucleoprotein complexes, the solution was shaked carefully by hand and incubated for 5 minutes in wet ice. Then it was centrifuged at 12.000g 2- for 15 min at 2-8°C to obtain three different phases. Colorless upper aqueous phase containing RNA was collected and transferred into a new tube, where equal amount of cold isopropanol was added. The sample was stored in wet ice for 15 minutes and RNA was finally precipitated as gel-like pellet on the bottom of the tube by following centrifugation at 12.000g at 2-8°C for 15 min. The pellet was washed with 1 ml of 75 % ethanol for each sample and centrifuged at 8.000g at 2-8°C for 15 minutes to remove ethanol entirely. The pellet was briefly dried and redissolved in DEPC (diethyl pyrocarbonate-treated) water in volume from 20 to 50 μl. To increase the RNA solubility the purified samples were incubated for 10 minutes at 55°C.

Before reverse-transcription of the RNA into cDNA, to assess the integrity and the amount of the RNA extracted, 1.8% ethidium bromide stained agarose gel electrophoresis and spectrophotometric $A_{260/280}$ readings were performed. The optimal range value is 1.8-2. Briefly, 1 μl of RNA and 2 μl of RNA Loading Dye denaturating buffer containing formamide also stained with bromophenol blue (Sigma) were put at 65°C for 10 minutes, chilled on ice and were loaded into the 1.5-2 % agarose gel together with 100 bp DNA ladder. The gel was run with TAE buffer at 80 mV for 20 minutes and visualised under UV light. The RNA concentration (μg/μl) was misured by spectrophotometer measuring absorbance (A) at 260 nm (water was used as blank). RNA samples were stored at -80°C until required or retrotranscribed.

In a next step, RNA samples were treated with Deoxyribonucleose I, Amplification Grade (Invitrogen, Life technologies, UK) which digests single-end double-stranded DNA to oligodeoxy-ribonucleotides containing a 5'-phosphate. It is suitable to eliminate contaminating genomic DNA during critical RNA purification procedures prior to use it for retrotranscription and so Real time gene analysis.

2 μg of total RNA was reverse-transcribed with the SuperScript™ II RT kit (Invitrogen, Life technologies, UK). To the final solution 1 μl of random hexamers and 1 μl of dNTP mix of oligo nucleotides were added in DEPC water and incubated at 65°C for 5 minutes and chilled on ice. Subsequently at the mixture were added the other reagents: 4 μl of 5x

First Strand buffer, 2 µl of DTT, 1 µl of RNAse out and after 2 minutes 1 µl of SuperScript II RT. The mixture were agitated gently and centrifuged to collect the content of the tube, incubated at room temperature for 10 minutes and then at 42°C. Finished the incubation time the reaction was inactivated by heating at 70°C for 15 minutes. The obtained from the various samples complementary DNAs after the extraction and retrotranscription were used as templates for PCR expression analysis.

Primers design and Standard polymerase chain reaction RT-PCR

PCR reactions were carried out under the conditions reported in Table. 2, using specific primers designed based on the published database sequence of mRNA. There were used the following target gene sequences Genebank: MSTN (NM_001081817, Equus caballus; NM_001001525 Bos taurus) and HRC (EF555593, Equus caballus; NM_001102313, Bos taurus).

A two series of primers were designed for quantitative RT-PCR analysis and standard PCR for HRC gene separately (Table. 2). Primers for standard semiquantitative RT-PCR were designed using primer designer software Oligo (National Bioscience) and that for quantitative RT-PCR were designed with Primer Express 3.0 software to span introns in the genomic DNA in order to minimize non-specific fluorescence signals due to contaminating genomic DNA. Briefly, primers for each gene target were selected containing minimal internal structure (i.e., hairpins and primer–dimer formation as determined by the software) and havingcompatible T_m's (i.e., each within 1°C of the other). To obtain equine HRC specific sequence unknown before (EF 555593), mammalian sequences (rat, mouse, rabbit, human and dog) from Genbank/EMBL were included in the alignment: NM_181369, Rattus norvegicus; NM_010473, Mus musculus; NM_001082234, Oryctolagus cuniculus; NM_001102313, Bos taurus; EF555593, Equus caballus; NM_002152, Homo sapiens; XM_541501, Canis lupus familiaris (Fig.1). Alignments of the deduced amino acid sequences of the fragments were generated with ClustalW (http://www.ebi.ac.uk/Tools/clustalw2/) to identify the regions of homology and chose the most highly conserved area and the primers were designed around that area. So one degenerated forward primer and two degenerated reverse primers were designed to amplify a fragment corresponded to bases 305 and 444 of equine histidine-rich calcium binding protein. All PCR were performed in 20 µl of PCR mix: 1x PCR buffer

(Invitrogen), 1.8 mM $MgCl_2$, 0.1 mM of each dNTPs, 0.5 µM of each primer, 0.5 U Taq DNA Polymerase and 2 µl of cDNA. PCR products (5 µl) were electrophoresed on 1.5 % agarose gel, stained with ethidium bromide, and visualised under UV light to confirm the adequate amplification. To confirm the identity of the DNA fragments the rest volume of amplified PCR products were sequenced by the CRIBI (University of Padua) sequencing service where it was used ABI PRISM® 3730XL (Perkin-Elmer, Applied Biosystems) sequencer with help of the ABI PRISM dye-terminator cycle sequencing ready reaction kit. The nucleotide and putative amino acid sequences obtained were used to perform BLASTN and the BLASTP analysys (http://www.ncbi.nlm.nih.gov.gov/blast) on the complete non-redundant GenBank database sequences, using default settings.

Subsequently, HRC specific oligonucletides were designed to amplify a 60 bases product in a qualitative RT-PCR. Both forward and reverse HRC primers were designed into the third exon.

Another gene that was investigated was myostatin (MSTN) named also GDF8, using a couple of specific primers designed into the second exon on the known horse sequence (GenBank, NM_001081817). The product of amplification corresponded to bases 135 of growth differentiation factor 8 protein. Cause of very conserved MSTN gene sequence primers were used also for a Real-time PCR analysis of three different species of mammalians including horse.

Specific primers were also chosen to amplify a fragment of one of the "housekeeping" gene β-actin as an internal control for the quality and quantity of the DNA samples to verify the efficiency of the reverse transcription and to exclude genomic DNA contamination. It was designed to span an intron basing on published sequence (GeneBank, AF035774).

At the beginning all couple of primers were tested in qualitative PCRs reactions with specific cDNA templates in order to check their specificity and control of the amplified product size for then to be used it in the gene analysis by quantitative real-time PCR.

Reverse Transcription Polymerase Chain Reaction (PCR) is a technique that results in exponential amplification of a target DNA sequence. By cycling through various temperatures, PCR results in the extension of a sequence–specific primer by a DNA polymerase such as DNA polymerase isolated from *Thermus aquaticus* (Taq). The DNA polymerase reads the template and incorporates a complimentary nucleotide yielding a

newly assembled complimentary strand. RT-PCR is a very sensitive, qualitative and semiquantitative method consists of three steps denaturation, annealing and extension.

The cDNA of the samples was amplified using a Taq DNA Polymerase (Invitrogen), the final concentration of enzymes was 2.5 units and the RT-PCR conditions were: 3 minutes at 94°C, 32 cycles with 45 seconds at 94°C, 45 seconds at annealing temperature, specific for each primer pairs (reported on Table. 2), and an extension step of 45 seconds at 72°C, followed, a final step of 5 minutes at 72°C before cooling to 4°C. Samples (5µl) were size-fractionated on 1.5% agarose gels, contaning ethidium bromide at 80mV for about 20 minutes, by comparison with a HighRanger Plus100 bp DNA ladder (Norgen, Biotek Corporation).

Table 2. Primers used in the real time-PCR and Standard RT-PCR reactions. Ta, anealling temperature; MSTN, myostatin; GAPDH, glyceraldehyde-3-phosphatase dehydrogenase.

Gene symbol and primers number	Function	Forward primer (5'-3'), Reverse primer (5'-3')	Product size (bp)	PCR condition, Ta
β-actin	Cytoskeletal structural protein	CCATCTACGAGGGGTACGCCC TGCTCGAAGTCCAGGGCGACGTA	180	58°C
GAPDH	Glycolytic enzyme	AGGACTCATGACCACAGTCCATG TGTTCTGGAGAGCCCCTC	112	60°C
MSTN	Growth differentiated factor family protein	CCAGAGAGATGACAGCAGTGATG AATGCTCTGCCAAATACCAGC	135	58°C
HRC, degenerated primers	Cardiac contraction regulatory calcium binding protein	TTCACCAT(CT)ATCCC(AC)AACCC(AG)CT CGGGGAGCACGTTTATTC(AG)GAGA GA(GC)GAGGAGAA(AG)TAGTC(AG)ACGTAGCTTCC	305 444	58°C 58°C
SYBR-green HRC		GGTGCACGGAATGTGAGAACT GGTCACAGTGCTCTCCCATGT	60	58°C

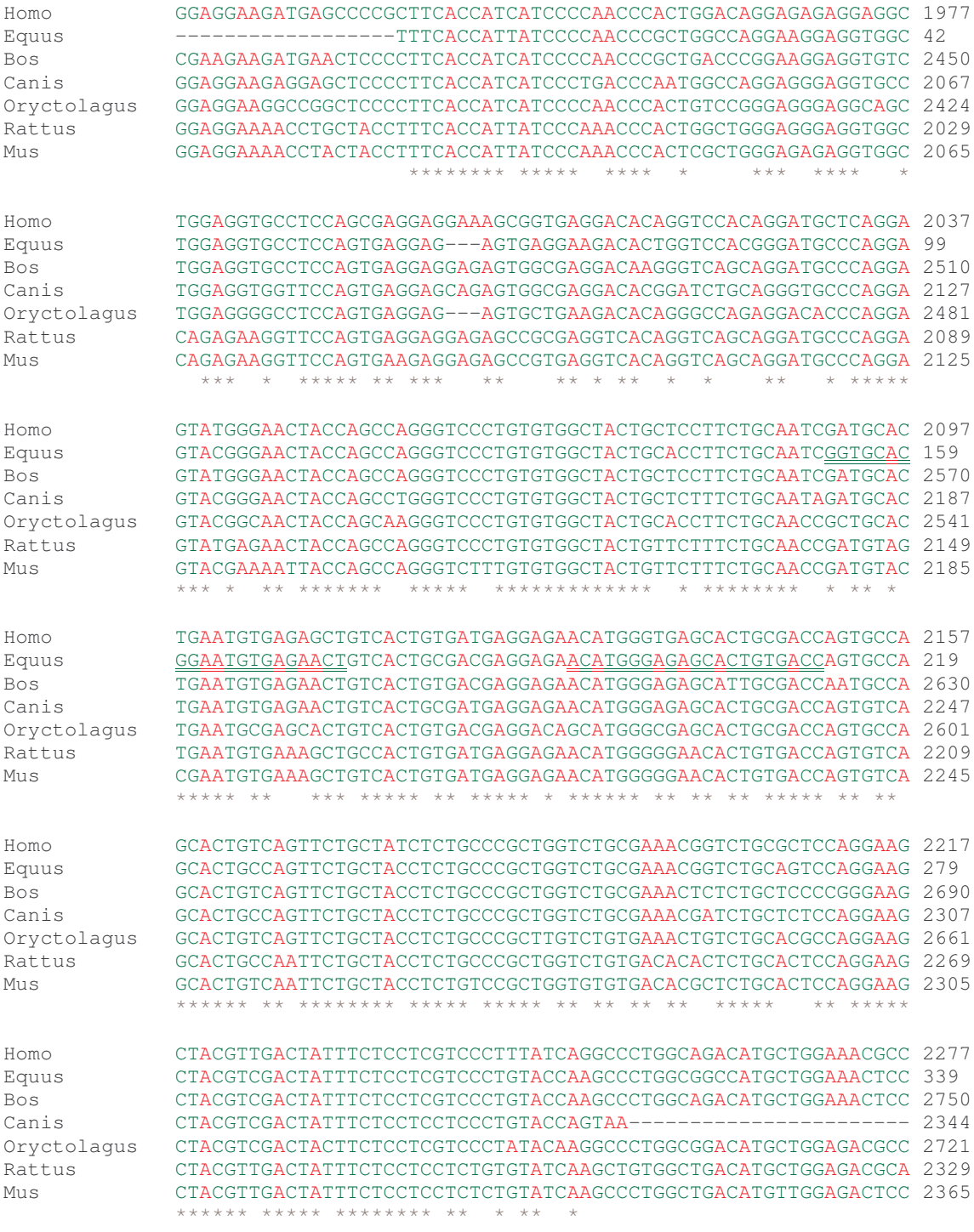

Fig. 1 A multiple alignment of seven histidine rich calcium binding domain nucleotide sequences by ClustalIW2. Residues are coloured according to the following criteria: Small (small+ hydrophobic (incl.aromatic -Y)) are shown in red, Hydroxyl + Amine + Basic - Q are green and all other residues are grey. The residue range for each sequence is shown after the sequence name. The colouring of residues takes place according to physicochemical criteria highlighting conserved positions in the sequences. A consensus line is also displayed below the alignment with the '*' symbol denoting the degree of conservation observed in each column, here are identical residues in all sequences.

Quantitative Real-time PCR

The real-time, fluorescence-based reverse transcription polymerise chain reaction (RT-PCR) is one of the enabling technologies of the genomic age and has become the method of choice for the detection of mRNA (Bustin SA, 2000). It is a perfect method to determine the expression of a particular mRNA in an organ. The HRC and miostatin gene expression in heart and sckeletal muscle tissue were analysed here by ABI 7500 Real-Time PCR System using SYBR Green I dye chemistry detection (Applied Biosystems, Foster City, CA) as described by our group elsewhere (Patruno M et al. 2006, 2007). Real-time conditions were the same for all primers pairs: 2 min at 50°C, 10 min at 95°C followed by 40 cycles of denaturation at 95°C for 15 s and annealing/extension at 60°C for 1 min. For this essay system 96 well plates were used. Each well was contained 30 µl of PCR mixture (SYBR Green PCR Master Mix, Applied Biosystem), including 3 µl of cDNA at a dilution of 1:20 for cardiac and skeletal muscles samples. Each reaction was run in triplicate with appropriate negative controls, a sample without cDNA template used to verify that the master mix was free from contaminants.

The relative mRNA expression of target genes was calculated with the comparative cycle threshold (Ct) method, which calculates changes in gene expression as a relative fold difference between an experimental and calibrator sample.

To perform the ΔΔCt method for relative quantification (comparative method), a validation experiment was required in order to demonstrate that the efficiency of the target amplification and that of the reference amplification were almost equal. Additionally, the reference gene represents the basis of normalisation, need to be constitutionally expressed at high level in the heart and skeletal muscle tissue and has no inter-individual variability.

For the first standard curves for both targets and the endogenous reference gene, created on the basis of the linear relationship between the Ct value and the logarithm of the starting amount of cDNA, showed acceptable slope values (included between –3.8 and –3.3). Standard curves were obtained by using serial dilutions of sample cDNA (1:8, 1:16, 1:32, 1:64, 1:128). There were validated two traditionally used housekeeping genes: glyceraldehydes-3-phosphate dehydrogenase (GAPDH) and β-actin. Common PCR efficiencies were measured. Based on the adequate absolute value of the slope (slope<0.1) an endogenous control gene β-actin was accepted as an active reference to normalize quantification of an mRNA target (Fig. 2).

The β-actin gene was amplified in separate tubes. Three replicates of endogenous control were amplified. Real-time PCRs for genes of interest and reference genes were run in the same RT reaction. Data from SYBR Green I PCR amplicons were collected with ABI 7500 System SDS Software. The fluorescence signal baseline and threshold were set manually for each detector (MSTN, HRC, β-actin), generating a threshold cycle (Ct, the time at which fluorescence intensity is greater than background fluorescence) for each sample. An amplification plot graphically displayed the fluorescence detected over the number of cycles that were performed.

The difference between Ct values was calculated for each mRNA by taking the mean Ct of triplicate reactions and subtracting the mean Ct of triplicate reactions for the reference RNA measured on an aliquot from the same RT reaction ($\Delta Ct = Ct_{target\ gene} - Ct_{reference\ gene}$). All samples were then normalized to the ΔCt value of a calibrator sample to obtain a ΔΔCt value ($\Delta Ct_{target} - \Delta Ct_{calibrator}$). The calibrator, defined as the sample used as the basis for comparative results, could represent an untreated control or has the lowest expression level of the target (see Chemistry Guide, Applied Biosystem, 2003). So left atrium was chosen as the calibrator here. For the comparative method, relative quantifications were calculated in relation to the concentrations of the calibrator sample (2^{-DDCt}), expressed in arbitrary units and normalized to the endogenous reference gene (i.e., β-actin). Therefore, by using the $2^{-\Delta\Delta Ct}$ method, data were recorded as the fold-change in gene expression normalized with the endogenous reference gene and relative to the calibrator sample (Livak KJ & Schmittgen TD, 2001). Dissociation melting curves confirmed the specific amplification of the cDNA target and the absence of nonspecific products.

The obtained dates were collected in Excel worksheet, visualized with Chart Wizard graphics and processed with statistical analysis.

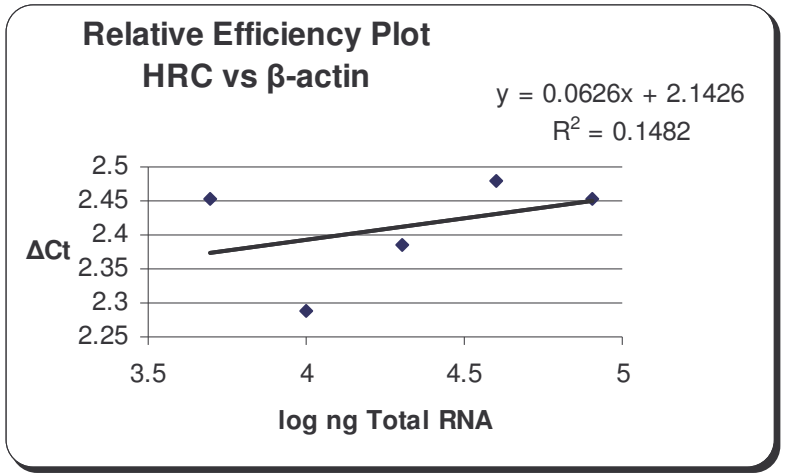

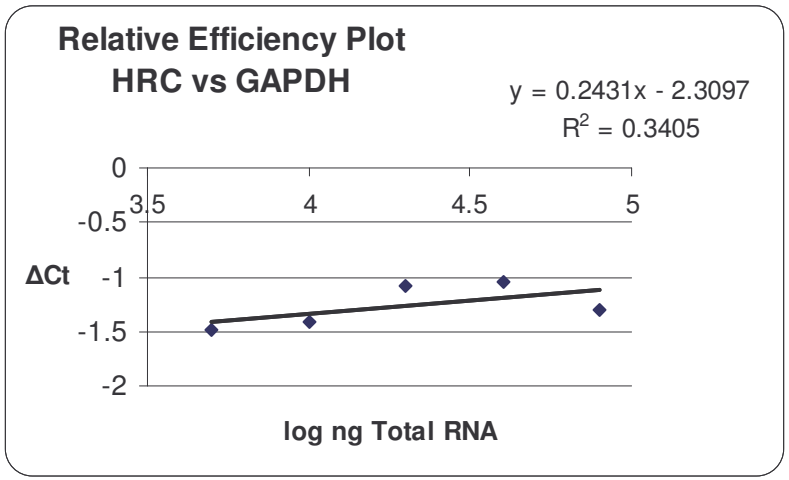

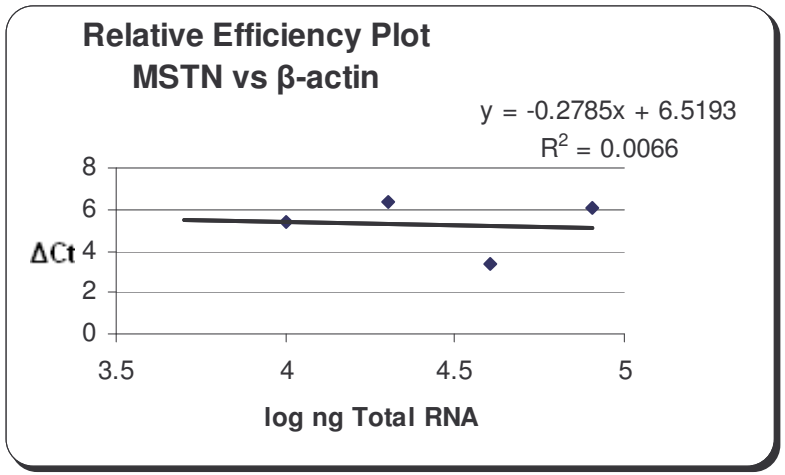

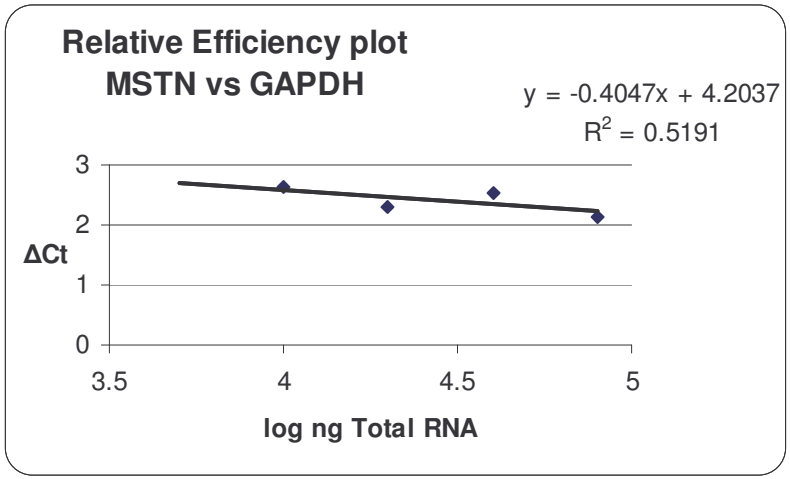

Fig. 2 Validation of the 2^{-DDCt} method. The efficiency of amplification of the target gene (A. HRC, B. MSTN) and internal control (C. GAPDH, D. β-actin) was examined using real-time PCR and SYBR Green I dye chemistry detection. The ΔCt was calculated for each cDNA dilution. The data were fit using to construct least-squares linear regression line, the slopes were found.

Statistical analysis

Data are expressed as the mean ± standard error. Normality of the data was checked with a Kruskal–Wallis test (a 95%). Statistical differences in HRC mRNA levels, between the calibrator sample (left atria tissue) and horse heart various sections and skeletal muscles were detected by one-way analysis of variance (ANOVA) using the GraphPad Prism software. The Tukey honestly post-hoc test was used to further characterize statistical differences among the tissue examined. The level of statistical significance was set at $p<0.05$ and $p<0.01$.

Immunohistochemistry on frozen cardiac left ventricular muscle tissue

Immunohistochemistry is a technique for marking cellular or tissue constituents (antigen) by means of antigen-antibody interactions. The antibody-binding site is identified either by direct labelling of the antibody, or by using a secondary labelling method.

Part of left ventricular cardiac muscle tissue from horse heart was dissected, combined into composite blocks and frozen in isopentane cooled with fluid nitrogen. The block containing the tissue was sectioned using a cooled (-20°C) cryostat (Microm Cryo-Star HM 560, Kalamazoo MI) at 12 µm thicknesses. Tissue sections were collected and mounted on gelatine-coated slides stored at –80°C until use.

To proceed with immunohistochemistry the slides with tissue section was left to warm on the room temperature for some minutes. The condensate was dried and the sections were rehydrated for 5 minutes with a Phosphate Buffered Saline (PBS) 1x solution composed by (in mM): 7mM Na_2HPO_4, 3mM NaH_2PO_4, 147mM NaCl, pH 7.4. To facilitate the access of antigen to antibody the tissue sections was permeabilize for 5 minutes with 0.3 % Triton X-100 diluted in PBS, then after three additional washes with PBS 1x were blocked with 1% bovine serum albumin for 1 hour for saturation of non-specific binding sites. The primary antibodies were diluted in PBS 1x and added (100µl) to cover the tissue cryosections. The staining protocol was carried out in a moist chamber to avoid dehydration. Cryosections from horse heart left ventricle were incubated with primary polyclonal antibodies to HRC (1:100 dilution; a generous gift from Prof. Damiani) or commercial monoclonal antibody to RyR2 (1:100 dilution; Affinity Bioreagents) and PLB

(1:100 dilution; Affinity Bioreagents) for 2 hours, followed by three serial washing for 10 minutes each with PBS 1x and final incubation for 1 hour in the dark chamber with the appropriate secondary antibody conjugated with TRITC (1:100 dilution) or FITC (1:100 dilution) respectively. After the last three PBS 1x washing for 10 minutes each the cryosections were included with 70% glycerol.

To assess the good quality of the reaction and avoid undesirable autofluorescence effect the appropriate negative control was performed for each type of secondary antibody.

All images were acquired with Leica TCS-SP2 confocal laser scanning microscope (CLSM; Leica, Heidelberg, Germany) equipped with a 63x1.32, 40x1.25, 16x0.5 numerical aperture oil immersion objective.

Horse single ventricular cardiomyocyte isolation

Equine hearts obtained from slaughtered horses without any cardiovascular system disorders only were used for cardiomyocytes isolation. Single ventricle myocytes from left ventricular heart portion through enzymatic dissociation of tissue pieces, known as "chunks method" (Workman AJ et al. 2001)

Briefly, a 3g tissue section of midmyocardium from the left ventricle was minced into 1-3 mm^3 pieces, washed more times and transported in ice-cold following solution (in mM) to the laboratory: *20 mM* Glucose, *20 mM* Na-Hepes, *16 mM* MgCl2, *15 mM* KCl, *90 mM* NaCl, *1 mM* Mannitol, *1 mM* Adenosine, *5 mM* Taurine, *5 mM* Na-pyruvate, *0.6 mM* $CaCl_2$, pH 7,4 (9°C). In safety condition high potassium solution was substitute by washing 3 times for calcium free Krebs-Henseleit solution (KHS), composed of (in mM): *11.1 mM* Glucose, *20 mM* Na-Hepes, *1.2 mM* $MgCl_2$, *5.4 mM* KCl, *120 mM* NaCl, *10 mM* Creatine, *5 mM* Taurine, *10 mM* Na-pyruvate, pH 7,42 (28°C). The tissue pieces were then distributed for three or more $25cm^2$ flasks and digested with 100U/ml of Collagenase I (GIBCO) for 15 min in KHS with 0.075 mM calcium slightly shaken at 37°C. The cells containing solution was collected and replaced with the same fresh enzyme free KHS for a second time 10 min digestion at 37°C. To divide the single cells from undigested tissue the supernatant collected from two-step digestion was filtered through gauze of mesh size 255 um and centrifuged for 2 min 50g. to let the cells go down. Pellet was resuspended in the fresh KHS with addition of 0.1% BSA and 0.125 mM calcium at room temperature. After 15 min the concentration of Ca^{2+} was gradually adjusted to 0.5 mM to reach to 1.8 mM

calcium finally by changing KHS each time. The last KHS was also supplemented with 100 U/ml penicillin and 0.1 mg/ml streptomycin. Glass coverslips were prepared: washed with distillate water, then treated with 1% Triton (Sigma) solution for 30 minutes, rinsed and etched in HCl 1 N (Sigma) for 30 minutes to create, rinsed thoroughly and used after sterilization on the fire. The laminin (Invitrogen) was applied overnight at 37°C the day before cells plating. It was aspirate and coverslips was rinsed 2 times with PBS 1x before adding cell suspension. Ones isolated, myocytes yield was assessed microscopically, the density was diluted and the cells were plated onto laminin-coated (50 g/cm^2) 24 mm culture glass coverslips at approximately 1× 10^4 cells/cm^2 and incubated overnight in at 37°C 5% CO_2-incubator up to allow attaching or loaded immediately with Di-4-ANEPPS for confocal imaging.

Cells were considered viable if they demonstrated a clear striation, characteristic rod shape without blebbing. To explore the physiological viability the cells were contracted after electrical pacing at frequencies of 0.25-1 Hz using a 5 ms duration pulse with a pair of platinum field-stimulation electrodes mounted in a plastic chamber (Elettrofor) inserted on Olympus IX 51 microscope plate shown on the Fig.3.

Electrical stimulation triggers a cascade of events in cardiac muscle that results in a cytoplasmic calcium transient and, eventually, contraction. The events that occur in electrically stimulated cardiac myocytes mimic the normal physiological events in vivo (Sathish V et al. 2006).

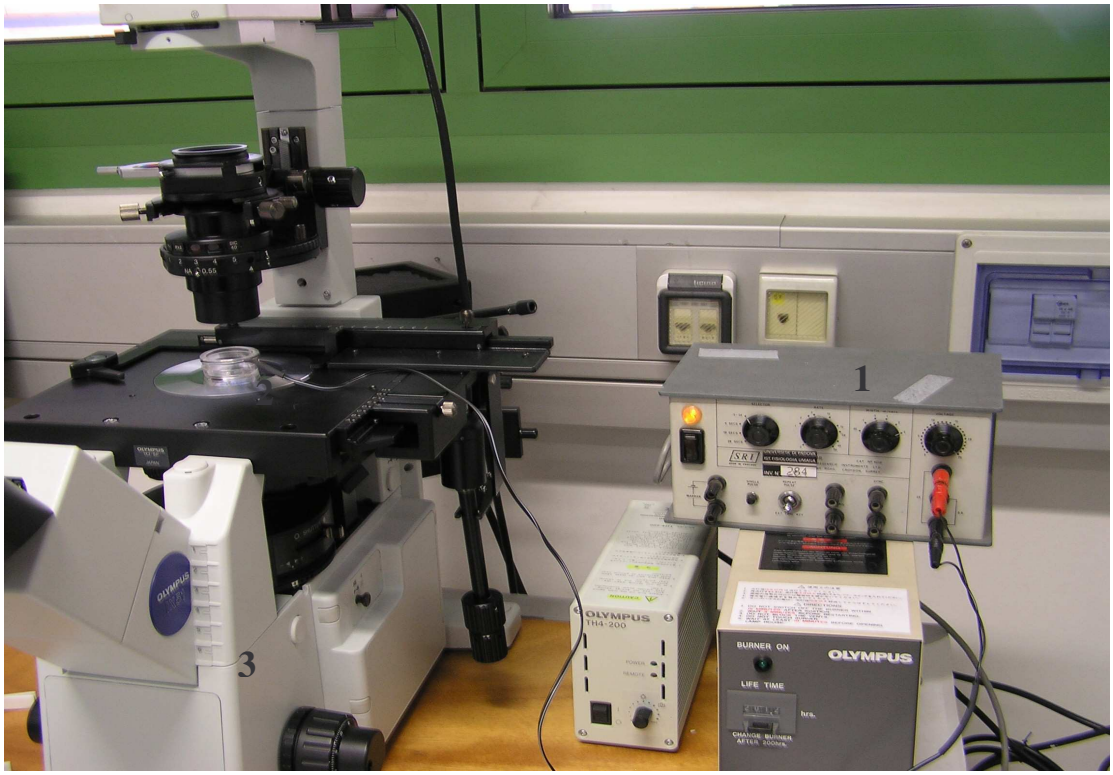

Fig. 3. Muscle contractile system consistent of Cell STIMULATOR indicated **1**(Scientific Research Instruments, Ingland), cells chamber (**2**) with incorporated platinum electrode and posed on Olympus IX 51 microscope (**3**).

Immunohistochemical examination of myocytes cultures

To examine the structural integrity and organization of the myofibrillar apparatus contractile elements and cytoskeletal protein and Na^{+}/Ca^{2+} exchanger, we rinsed out detrite and non settled cells with warm KHS w/t bovine serum albumin and fixed cardiac myocytes attached to a laminin-coated coverslip with room temperature 4% paraformaldehyde diluted in PBS 1x for 10-15 min, washed three times with PBS and permeabilized in 0.3 % Triton X-100 (Sigma) in PBS for 5 minutes, then after three additional washes blocked with 1% bovine serum albumin for 1 hour. Subsequently the cells were incubated with anti-plectin (1:100 dilution; Sigma), anti-α-actinin sarcomeric (1:100 dilution; Sigma), anti-vinculin (1:50 dilution; Sigma) and anti-NCX (1:100 dilution; Santa Cruz Biotecnology) antibody for 2 hour at room temperature in the wet chamber, followed by FITC-conjugated polyclonal horse anti-mouse or TEXAS RED goat anti-rabbit (Vector Lab.; 1:100 dilution) antibody for 1 hour at room temperature in the dark. All antibodies (Table 4) were diluted with PBS 1x. The cells were rinsed three times for 10 minutes after each incubation. Finally, glass coverslips with cells were mounted on the

glass slides with mounting medium (Vectashield, Vector Laboratories, Burlingame, Calif., USA), a photobleaching inhibitor.

The prepared slides were imaged identically as described before for a frozen cardiac section.

Table 4. Antibodies used for cardiomyocyte immunofluorescence and left ventricular criosection histochemistry. The dilution of each type antibody was 1:100 excepted of the vinculin where it raised to 1:50. SR, sarcoplamic reticulum.

Cardiac muscle protein markers	**Antibody name and clone number**	*Subcellular localization*
Cytoskeleton markers: α-actinin sarcomeric	Mouse monoclonal EA-53	Z-lines
Vinculin sigma	Mouse monoclonal VIN-11-5	Costameric pattern at sarcolemma, intercalared disks staining
Plectin sigma	Mouse monoclonal 7A8	Cytoskeletal architecture/functional integrity of cardiac cell
SR markers: RyR2	Mouse monoclonal 34C	Junctional sarcoplasmic reticulum
SERCA2	Mouse monoclonal IID8	Longitudinal tubules of sarcoplasmic reticulum
HRC	Guinea pig polyclonal, clone 3	Junctional sarcoplasmic reticulum
PLB	Mouse monoclonal 2D12	Longitudinal tubules of sarcoplasmic reticulum
Sarcolemma marker: NCX	Rabbit Polyclonal H-300	Z-lines, T-tubule

Transverse tubular system labelling

To characterize the integrity of the transverse tubules, fresh isolated adult horse cardiomyocytes were loaded with Di-4-ANEPPS (a generous gift from Prof. Smith). Di-4-ANEPPS is a hydrophobic membrane-potential sensitive fluorescent dye that is commonly used for the detecting the action potential across all, or portions of, the membranes of cardiac muscle living cells. A stock solution of Di-4-ANEPPS (Molecular Probes, Inc., Eugene, OR) was made up as 1 mg/ml in absolute ethanol. For a loading the dye was diluted to rich a final concentration of 1 μM in Krebs Krebs-Henseleit buffer and the cells were loaded for 3 min at room temperature. Once the dye loading was complete, the dye-containing saline solution was removed and replaced with plain saline solution for fluorescence imaging. The sarcolemmal membrane system was visualized with confocal

optical section images obtained under 488-nm excitation. Fluorescence was collected simultaneously in green (510–570 nm) wavelength bands.

Preparation of membrane fraction from horse cardiac muscle

Cardiac muscle SR and plasmatic membranes fraction were prepared from defrozen left ventricular sample of horse heart. The piece of cardiac muscle about 40 g were minced and homogenized in potter where it were added 200 ml (five volumes of the muscle mass) of the following components of buffer: 0.3M sucrose, 5mM imidazole, 1mM EGTA, pH 7.4 supplemented with 1µg/ml leupeptin and 100 µM PMSF as antiproteolytic factors. These and the following operations were occurred at 4°C. Myofibrillar pellet was sedimented by centrifugation of the samples for 10 min at 7.700 x g at 4°C. Postmyofibrillar supernatant SP1 composed of major by longitudinal reticulum that was obtained in this step was filtered through gauze treated with 0.1 mM EGTA and kept for following processing. On the second step after new homogenisation in the buffer indicated above for 1 min the myofibrillar pellet was centrifuged for 20 min at 15.000 x g. Pellet that is composed of nuclei, mitochondria and myofibrillar components was not used, while postmitochondrial supernatant SP2 enriched in junctional sarcoplasmic reticulum was unite with SP1. After that unique supernatant was ultra centrifuged at 150.000 x g for 90 min. The pellet contained microcomal fractions obtained from this centrifugation was collected, resuspended in the same homogenisation buffer and stratified on a isopycnic sucrose-density gradient formed by four increasing sucrose interfaces as 27%, 32%, 38% and 45% (weight/weight) in 5 mM imidazole (pH 7.4 at 44°C) initiating from the top of the tube respectively. Gradients were centrifuged at 70.000 x g for 16-28 hours at 4°C. Termed the centrifugation each of the four membrane layers stratified between sucrose-density gradients were collected in a separate tubes and diluted in 4mM imidazole solution. The tubes were subsequently ultra centrifuged at 150.000 for 90 min to precipitate the membrane fraction. All fractions (R1, R2, R3, R4) were resuspended in 0.3 mM sucrose and 5 mM imidazole solution with addition of antiproteolytic factors on ice and stored at –80°C until used.

Finally four membrane fraction were obtained from cardiac horse tissue are R1, prevalently enriched of T-tubule membranes, R2, consist of vesicles derivated from

longitudinal sarcoplasmatic reticulum, R3, contained two components of R3 and R4 fractions, R4, is formed by junctional terminal cisternae vesicles.

Protein concentration dosage

Protein concentration was determinated by the method of Lowry OH et al. (1951), as modified by Campball and Sargent (1967), using bovine serum albumin (Bochringer, Mannheim, Germany) as a standard. In general 5 µl of the sample were diluted in 5 % of 100 µl of DOC solution and ported to 1ml with distillated water. After mix it 4 ml of the fresh solution consist of 100 volumes of $NaOH/Na_2CO_3$, 1 volume of 2% Na^+-K^+ tartrate and 1 volume of 1% $CuSO_4$. After 10 min of incubation 0.5 ml of fresh water diluted Folin-Ciocalteus (1:1.36) reactive were added to each sample. After incubation time for 30 min absorbance of each sample was measured at 660 nm. Protein concentration was extrapolated using a standard curve of bovine serum albumin.

Sodium Dodecyl Sulfate-Polyacrylamide Gel Electrophoresis (SDS-PAGE)

Porosity of the gel acts as a gauze filter and thus separating in a difference manner the proteins of a different molecular mass. One-dimentional SDS-PAGE was conducted according to Laemmli (1970) with 4% stacking gel and 5-10% (1.5 M Tris-HCl, pH 8.8, 0.4% SDS, 29.2% acrilamide, 0.8% bis-acrilamide, 50% glycerol, TEMED and ammonium persulfate) lineal gradient running gel in the presence of β-mercaptoethanol. Horse cardiac membrane fractions R1, R2, R3 and R4 in 100 µg, 50 µg and 100 µg of rabbit skeletal and cardiac muscle respectively, 60 µg of rat skeletal muscle, 1.5 µg of purified HRC protein from rabbit cardiac muscle were loaded in SDS-PAGE to be stained with Stains-All after electrophoresis._ Samples were prepared by solubilization of membrane aliquote in a following solution: 62.5 mM Tris-HCl, pH 6.8, 10% glycerol (w/w), 5% β-mercaptoethanol for separating on polyacrilamide slab gels after denaturation in SDS. The running solution was contained of 25 mM Tris, 192 mM glicine, 0.1% SDS, pH 8.3. Electrophoresis was carried out at room temperature for 3-4 hours at a constant voltage of 140 V (Fig. 4).

Slab gel was stained with Coomassie blue and subsequently with Stains-All. Coomassie Blue (CB) is an anionic dye that colour all proteins in the aspecific manner. CB staining

allows having the complete picture of all separated proteins but do not give us any information about its identity.

The staining procedure was performed for 30 min shaking gel slab in the solution containing 2.5g of CB diluted in 454 ml of methanol, 92 ml of acetic acid adjusted to a one litre with distillated water.

After CB coloration gels were partially decolorated with 50% methanol and 10% acetic acid, washed with distillated water and subsequently stained with Stains-All (0.0025%) containing also 7.5% formamide, 25% isopropanol and 3% sodium carbonate adjusted to pH 9 with a formic acid and sodium carbonate. Gels were left in this solution for up to 18 hours until to be photographed.

Stains-All is a methacromatic cationic dye, which molecules bound to negative charges aminoacids of the protein in a manner to absorb a light about 600 nm. Thus calcium-binding proteins like calsequestrin or HRC appears strongly evidenced in blue after Stains-All staining while other protein is stained in red.

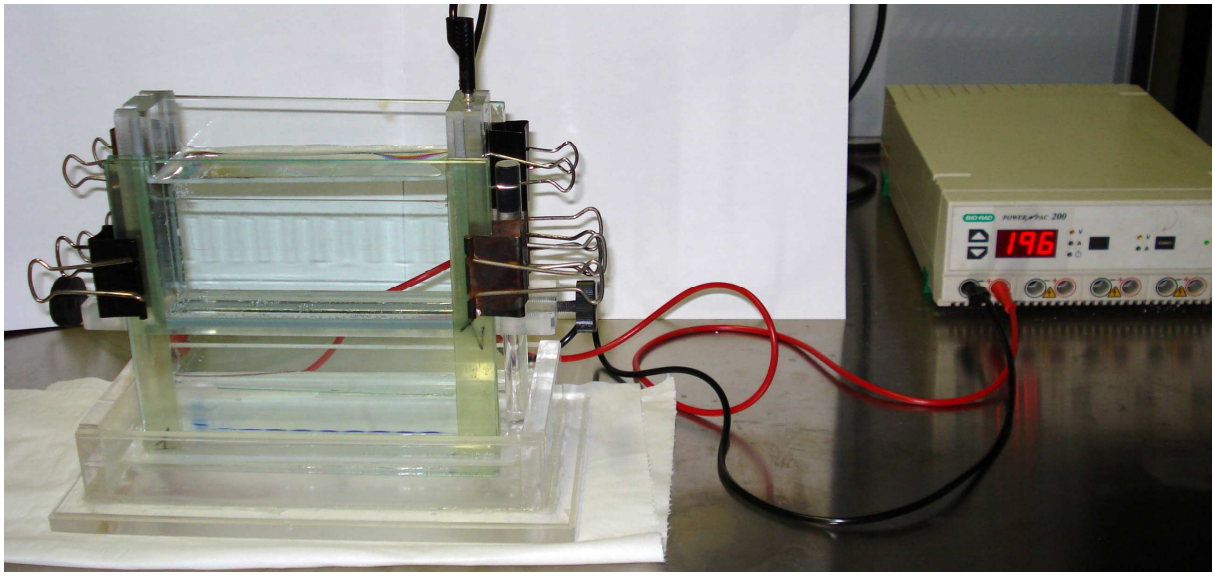

Fig.4. Gradient SDS-PAGE in the finish of the running. The voltage was slowly increased just in the end of electrophoretic running.

Electrophoretic protein transfer to nitrocellulose (Western blot)

Western blot technique is based on the feature of the nitrocellulose to have porosity and a charge, which immobilize the proteins. Proteins transfer to nitrocellulose was carried out,

as described by Towbin (1979). In order to have approximately equal amounts of HRC protein on blot, 120, 100 μg of microsomal fractions were loaded for horse and rabbit cardiac muscles, respectively, 50 μg of the rabbit skeletal muscle membrane fraction and 0.5 μg of purified rabbit cardiac HRC protein. Untreated with any dye, gels slab were transferred onto the nitrocellulose sheet and closed between two sponges which formed so named "sandwich" to be positioned into blotting camera filling with the solution containing 25 mM Tris, 192 mM glicine pH 8.3 and 20% methanol. The proteins were transferred from polyacrilamide slab gel to nitrocellulose during 16-20 hours at 130 mA at room temperature.

To verify the quality of a transfer of the separated proteins the blot was stained with Ponceau Red. This staining is reversible and ones decoloured with 50% methanol/ 10% acetic acid, the blot were used for immunoblotting.

Immunoblotting with antibody for HRC

In order to detect the specific protein named histidine-rich calcium-binding protein in a total protein extract. Nitrocellulose blots were probed with guinea pig polyclonal antibody to rabbit HRC. Primary membrane was blocked for 1 hour with 1% BSA diluted in PBS/0.05% Tween 20 solution and then was incubated with the specific primary antibody for guinea pig polyclonal rabbit-anti-HRC (fraction 3, 5.1 μg/μl, generous gift of prof. Damiani lab.) appropriately diluted to final concentration 5 μg/ml in solution composed in PBS, 0.05% Tween 20. After three washing for 5 min each in NaCl 0.9%/ 0.1% Tween 20 solution, the membranes were incubated with alkaline phosphatase-conjugated anti-guinea pig antibody diluted 1:2000 in PBS/0.05% Tween 20 for 1 hour. After three washing for 5 min in NaCl 0.9%/ 0.1% Tween 20 solution, the membrane was immersed in the next additional solution composed of Tris/ 0.1 M HCl, 0.1 M NaCl, 5 mM $MgCl_2$ (AP buffer) to be adjusted to pH 9.5, that is an ideal condition for the alkaline phosphatase reaction. Antibody binding was detected by immunoenzymatic staining. For it the mixture of two salts 5 mg of bromochloroindolilphosphate in 100 μl of N, N-dimethylformamide and 1 mg of nitroblueditetrazolium (NBT/BCIP) was added to the blot as a substrate of for the alkaline phosphatase. Enzyme reacts with a substrate and the insoluble salt as a product of this reaction is formed to determinate the coloration of the immunoreactive protein band.

RESULTS

HRC is expressed in horse heart and its sequence shows high homology with previously reported mammalian sequences of this gene

To gain insight into HRC gene expression and distribution in different parts of equine heart, RT-PCR experiments and agarose gel analysis have been employed. To the best of our knowledge, HRC expression in horse heart has never been described. The HRC gene has been cloned and sequenced in many small laboratory mammalian species as rabbit, mouse and rat and also in human species. cDNA sequences have been deposit in GenBank. Among large mammals of veterinarian interest, HRC has been cloned only in cow. The deduced amino acid sequences obtained from all these species, revealed a variability in protein length, although the structural organization of the protein is unique: a conserved N-terminal signal sequence (amino acids 1-28); an acidic repeat region (amino acids 213-481); a cysteine repeat region (amino acids 654-700); and a stretch of 13 glutamic acid residues (amino acids 590-602). In order to evaluate HRC expression in horse, another mammalian species of veterinarian interest, I first designed specific primers. Being not available the HRC horse cDNA sequence, I based primers design principally on HRC nucleotide sequence of rabbit, human and cow. The structural domain used to design primers was restricted to the HRC COOH-terminal region, within cysteine repeat region. Two couples of primers have been designed, amplifying a cDNA fragment of 444 and 305 bp respectively. Various anatomical parts of horse heart (wall of right and left atria and ventricles) were collected from adult animals killed at slaughterhouse. After being extracted, total mRNA was retro-transcribed into complementary cDNA. DNA was amplified by RT-PCR using HRC primers and PCR products were resolved onto agarose gel. A band of the expected dimension resulted amplified by primers in both atria and ventricles of adult horse heart. In Figure 1, only the bands of the highest dimension (444 bp) are shown. The PCR products were excised from agarose gel and were sequenced at the BMR Genomics (University of Padova). The novel horse cardiac HRC sequence, although partial has been deposit with GenBank with the accession number EF555593. The structural region amplified by primers, correspond to the cysteine-rich region localized at the carboxyl-terminal domain. By BLAST sequence comparison of the predicted nucleotide sequences from other mammalians species, including human species with new

horse heart partial HRC sequence has emerged a high homology. The carboxyl-terminal nucleotide sequence of horse HRC shows up to 90% identity with the same region of HRC of other mammals and human (Table.1). The highest similarity was found with HRC bovine sequence, whereas many differences were found with rodents sequence. This indicates that the carboxyl-terminal domain HRC is very well conserved during evolution. The polyglutamic stretch near the carboxyl-terminus has been identified as the Ca^{2+} binding site and the carboxyl-terminal region of HRC protein, has been indicated to be responsible for protein-protein interaction with triadin (Sacchetto et al 2001, Avarantis DA et al. 2007). This could explain the high conservative homology of this portion among mammals.

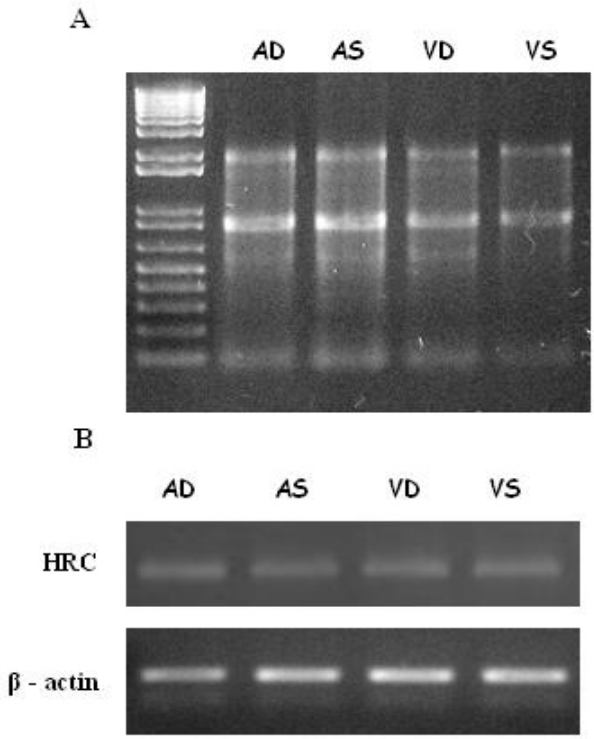

Fig.1 Qualitative analysis of HRC gene expression (B) in horse heart anatomical parts: right atrium (AD), left atrium (AS), right ventricle (VD) and left ventricle (VS). (A) The total RNA was isolated from samples of various anatomical parts of the horse heart and retrotranscribed into cDNA. (B) Equivalent amounts of cDNA templates from all heart portions were amplified by RT-PCR. The 444 bp PCR product bands are found in all investigated heart samples. The size standard used was the 1Kb Plus DNA Ladder (Invitrogen). β-actin (180 bp product) was used as internal control.

Table 1. Residues homology (%) between some of the reported HRC sequences of the mammalians and horse. The comparison is restricted to the COOH-terminus within cysteine repeat region.

Seq Name	Len(nt)	Seq Name	Len(nt)	Score(%)
Rattus	2367	Equus	444	67
Mus	2443	Equus	444	67
Oryctolagus	2810	Equus	444	79
Canis	2344	Equus	444	63
Homo	2430	Equus	444	87
Bos	2986	Equus	444	90

The basic level of HRC is found in atria and skeletal muscle of adult horse while overexpression of this gene is found in ventricular part of the horse heart

To further study the relative expression of HRC in horse heart and, by comparison in horse skeletal muscles, I based experiments on the obtained horse HRC nucleotide partial sequence. Real-Time PCR experiments were used to study the HRC transcriptional activity. Specific primers used in Real Time experiments were designed within sequenced carboxyl-terminal region of horse cardiac HRC. HRC mRNA expression levels were studied in the anatomical parts of adult horse heart already sampled for RT-PCR: wall of the right and left ventricles and wall of the right and left atria. In addition the analysis of HRC mRNA expression, was extended to subatrial papillary muscles of left ventricle and interventricular septum.

The histogram represented on the Fig.2 shows HRC transcriptional activity in various portions of horse heart and in two representative skeletal muscles of the horse.

Quantitative analysis of HRC mRNA levels shows that this gene seems upregulated in ventricular part of the horse heart (wall of the right and left ventricles), including papillary muscles and interventricular septum. No significant differences were observed between skeletal muscle and both heart atria, being the HRC transcriptional activity almost equal in all these samples (Fig.2). As far as we know, there are no data in literature about the distribution of endogenous HRC level in the heart anatomical parts. Unless our findings are consistent with those of Anderson (2004), suggesting that the human HRC promoter directs strong expression to the ventricles in transgenic mice and weak or no expression to the atria. It was described that total contraction time is consistently shorter in atria than in ventricles of many studied species (including man) (Braunwald E, 1997; Tanaami T et al.

2005). The basis for this regional difference could lie within the altered regional expression of triadin, junctin, HRC proteins (junctional SR area proteins). Here we report that high HRC expression level in the ventricular region (about three times) *vs* atria may account for the contractile difference in these regions, especially with regard to relaxation and time of contraction.

It must be noted also that the HRC transcriptional activity in various portions of horse heart seems to be the same in two extreme cases: 25 years old and the 1-day old horses (data not shown).

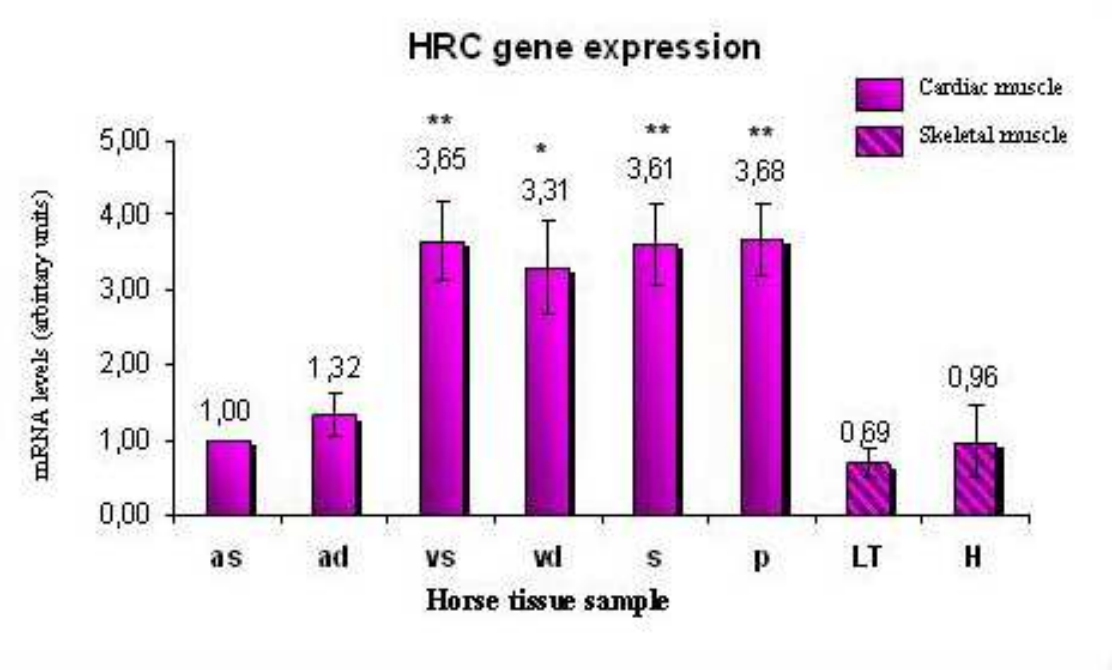

Fig.2 HRC expression in horse heart and skeletal muscle tissues. HRC gene expression is upregulated in right ventricle (vd), left ventricle (vs), interventricular septum (s) and papillary muscle (p), while HRC mRNA level in right (ad) and left atrium (as) is not different from that of skeletal muscle *Longissimus toracicus* (LT) and *Triceps-long heard* (H). Values are shown as arbitrary units ± standard error obtained from six separate experiments and three experiments in case of skeletal muscle. (**P< 0.01, *P<0.05 *vs* left atrium (as)).

HRC mRNA level is significantly less in bovine heart than in horse heart in all studied anatomical part

In order to study if the up-regulation of HRC mRNA in ventricular parts of the horse heart could be a special feature of this species, HRC mRNA expression levels were investigated in cattle heart, another large size animal of veterinarian interest. Real Time experiments

were used to study HRC transcriptional activity in various parts of cattle heart (right atrium, wall of the right and left ventricles, subatrial papillary muscles of left ventricle and interventricular septum). The primers used for Real Time experiments with cattle heart were the same used in horse heart experiments, being the homology of HRC carboxyl-terminus sequence high between these mammalian species. Figure (Fig.3) shows the histogram obtained by Real Time PCR experiments. Any difference was noticed between anatomical parts of bovine heart but HRC transcriptional activity in bovine samples resulted lower than in left atrium of the horse heart. Therefore the HRC is homogenously distributed in bovine heart in contrast to horse heart however expressed in lower level than it is expressed in the horse heart. *Equus caballus* and *Bos Taurus* have evolutionary close relationship: moreover they have similar body weight, heart mass and cardiovascular system.

Whereas the resting heart rate of cattle is twice of that of the horse while maximal heart rate. The maximal cattle heart rate is variable and difficultly counted but it was noted that heart rate of the cow could increased consistently from around 60 (resting heart rate) to over 160 beats per minute during repeated agonistic encounters between animals or under the stress condition during transportation. On the other hand the horse heart could increase from 25/30 (resting heart rate) to 240 beats under the daily sport exercise. It is the first data about HRC mRNA distribution in cattle, as we know. Comparison of to similar species that have different sport capacities could be a key to understanding and improving of that reserve backup cardiac plasticity of the horse.

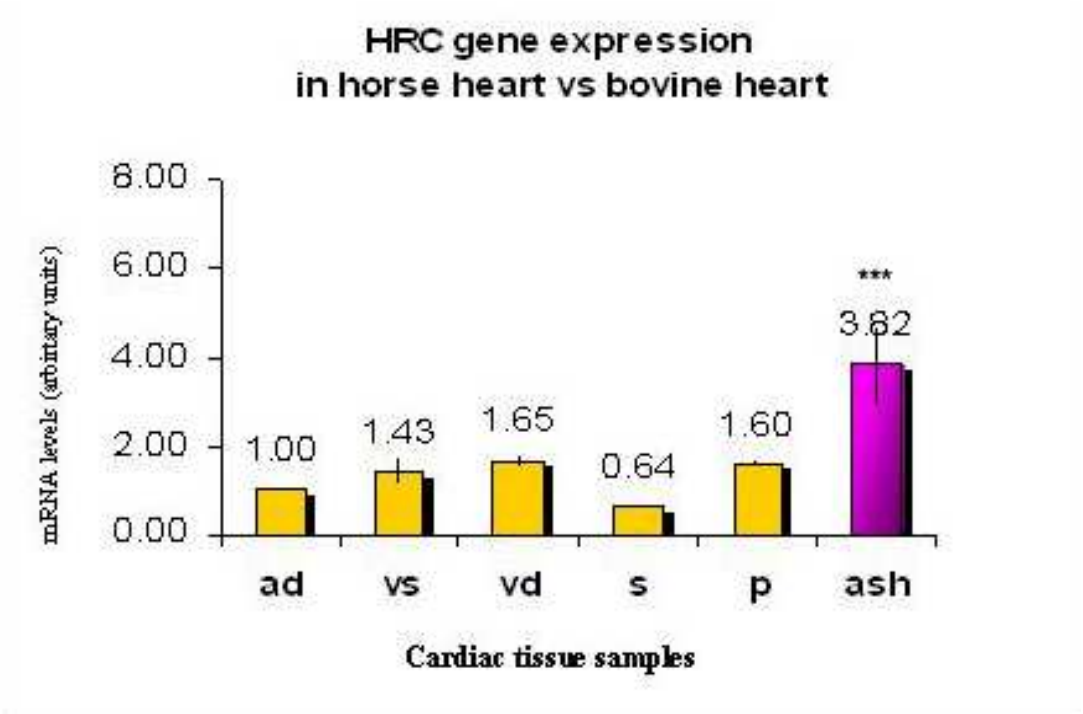

Fig.3 Comparative analysis of HRC gene expression in bovine respect to horse cardiac tissue. The HRC mRNA level results significatively lower in bovine cardiac tissue then in horse heart. As well as horse cardiac HRC is expressed in a ventricular part of the heart with ratio 3:1 versus atria, bovine heart doesn't show that relation difference between various parts of the heart. Values are shown as arbitrary units ± standard error obtained from six separate experiments and three experiments in case of skeletal muscle. (***P<0.001 *vs* bovine heart tissue samples).

Immunofluorescent localization of HRC and key proteins involved in Ca^{2+} release and Ca^{2+} uptake in equine ventricular tissue

After having ascertained HRC expression in horse heart at mRNA level, HRC has been study at protein level. Immunofluorescence experiments on longitudinal cryosections from left ventricle have been carried out to study the cellular localization of HRC in horse heart. Left ventricle longitudinal cryosections were also used to reinvestigate the immunolocalization of the key proteins SERCA2, PLN and RyR2 involved in Ca^{2+} release and Ca^{2+} uptake from cardiac SR. Expression of Ca^{2+} handling proteins has not been detected before in horse tissue. Commercially available antibodies raised against RyR2 and SERCA2 proteins expressed in small laboratory animals, resulted cross-reactive with the same proteins expressed in horse species. Immunolabelling of longitudinal sections with antibodies to SERCA2 and its regulatory protein phospholamban yielded a periodic cross-striated pattern, consistent with the localization of these proteins in the longitudinal

sarcoplasmic reticulum network (Fig.4). Recently it has been reported that SERCA2 could be a novel interacting partner of HRC in human cardiac tissue (Arvanitis DA et al. 2007). Confocal microscopy has been employed to analyze the pattern of immunostaining of cardiac ventricle with respect to sarcomeres, using polyclonal antibodies raised against rabbit purified HRC compared to monoclonal commercially available antibodies to RyR2. RyR2, the Ca^{2+} release channel, in cardiac muscle is largely localized to the junctional face of SR terminal cisternae that apposes the T tubules. In rat ventricular cells, RyR2 channels are grouped in clusters. The immunofluorescent pattern with RyR2 and HRC antibodies in equine left ventricular sections shows an extensive similarities with a punctuate appearance of immunofluorescent foci regularly aligned (Fig.5). These experiments support the hypothesis that RyR2 and HRC can be colocalized at junctional face SR membrane, as in rabbit skeletal muscle.

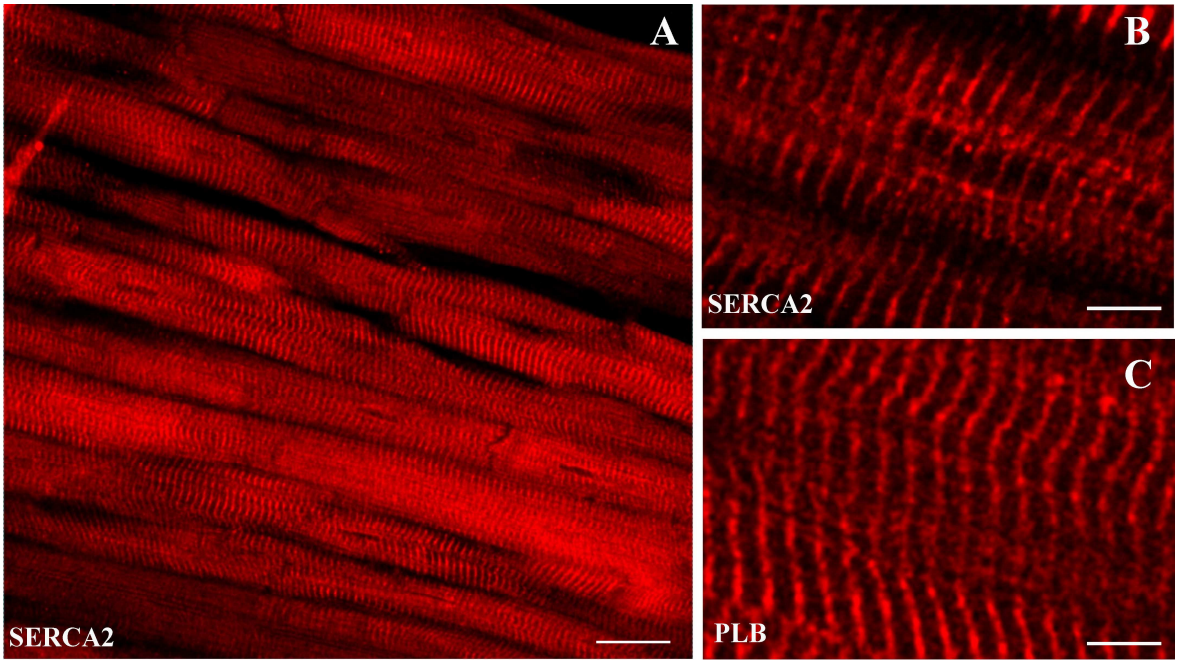

Fig.4 Confocal microscopy of horse left ventricular longitudinal cryostat sections. Sections were immunolabelled with monoclonal antibodies to SERCA2 and PLB and then with secondary antibody conjugated with TRITC (1:100 dilution). Longitudinal sections of the left ventricular of the horse heart show regular striated pattern of SR ATPase 2 and phospholamban localization. Scale bars 25 μm for A; 5 μm for B and C.

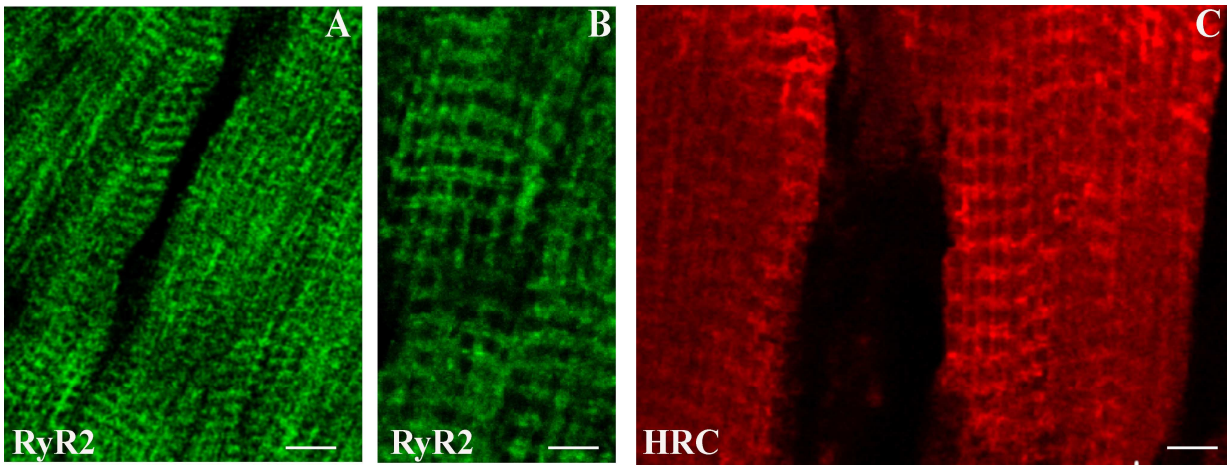

Fig.5 Comparative immunofluorescence localization of HRC and RyR2 in horse left ventricular cryostat sections. Longitudinal sections were labeled with monoclonal anti-RyR2 antibodies (1:100) and with polyclonal custom made guinea pig anti-HRC antibodies (1:100) followed by FITC- and TRITC-conjugated secondary antibodies respectively. Confocal microscopy shows regularly punctuate fluorescent foci with both antibodies. Scale bar for RyR2 5 μm (A) and 2.5 μm (B) for HRC 2.5 μm (C).

Horse heart HRC protein stains blue with the cationic dye Stains-All and appears to have less electrophoretic mobility vs rabbit and rat HRC proteins

To further study properties of HRC at protein level and to investigate subcellular localization of this protein, electrophoretic gel analysis were performed on membrane fractions extracted from horse cardiac muscle. Cardiac muscle homogenization and isopycnic sucrose-density centrifugation (Saito A et al. 1984) yielded four well-characterized membrane fractions called R1, R2, R3 and R4. R1 is prevalently enriched in T-tubule membranes; R2 consists of vesicles from longitudinal sarcoplasmic reticulum; R3 is composed principally of junctional terminal cisternae with a cross contamination of longitudinal SR; R4 consists of well-purified junctional terminal cisternae vesicles.

It is well known that the cationic dye Stains-All is used to identify acidic, Ca^{2+} binding proteins due to their differential staining: these proteins, such as calsequestrin and HRC stain dark blue, whereas all the other proteins stain purple. Moreover, it as has been already reported that HRC isoforms with different molecular masses are expressed in different animal species. In muscle fractions isolated from rabbit, the blue stained HRC protein band

migrates with an apparent molecular weight of 170 kDa. A unique isoform is expressed in both fast-twitch, slow-twitch and cardiac muscles of rabbit (Sacchetto R et al. 1999). In fractions isolated from rat, HRC protein exhibits an apparent molecular weight of 155 kDa (Malysheva AN et al. 2001).

To investigate properties and localization of horse HRC protein, same aliquots of fractions from R1 to R4 were separated on SDS-polyacrylamide gel and stained with Stains All. By comparison, R4 membrane fractions from rabbit skeletal and cardiac muscles, from rat skeletal muscles and the HRC protein purified from rabbit skeletal muscle, were loaded into the same gradient electrophoretic gel.

Figure 6 shows proteins membrane fractions separated on SDS gel and stained with Stains all. A blue staining band with molecular weight in the range of 116 to 200 kDa was observed in all fractions analyzed. HRC protein blue band can be identified at 170 kDa in fractions from rabbit muscle and as purified protein used as positive control. In fraction from rat skeletal muscle, HRC blue protein band migrates slightly below, as expected. In fractions from horse heart, a blue band with an apparent molecular mass of 145 kDa, can be easily identify. The blue band increases from fraction R1 to fraction R4, in which the band is more represented. The presence of blue band in R1 fraction, where the band is very faint. is probably due to the cross contamination of this fraction with membrane deriving from sarcoplasmic reticulum. These data, taken together, suggest that horse HRC exhibits a molecular mass different from that of mammalian species described until now.

With the aim to confirm that the blue band with a slower mobility found in horse fractions is HRC, the same fractions after being separated by SDS electrophoretic gel, were blotted onto nitrocellulose and probed with antibodies against HRC. Figure 7 shows Western blot analysis of horse heart fractions from R1 to R4 using polyclonal anti HRC antibody. A band with the same mobility of the blue band is recognized by anti HRC antibodies in fractions from horse heart and this band seems more abundant in the terminal cisternae fraction (R4) of horse heart, confirming its functional association to junctional sarcoplasmic reticulum membranes.

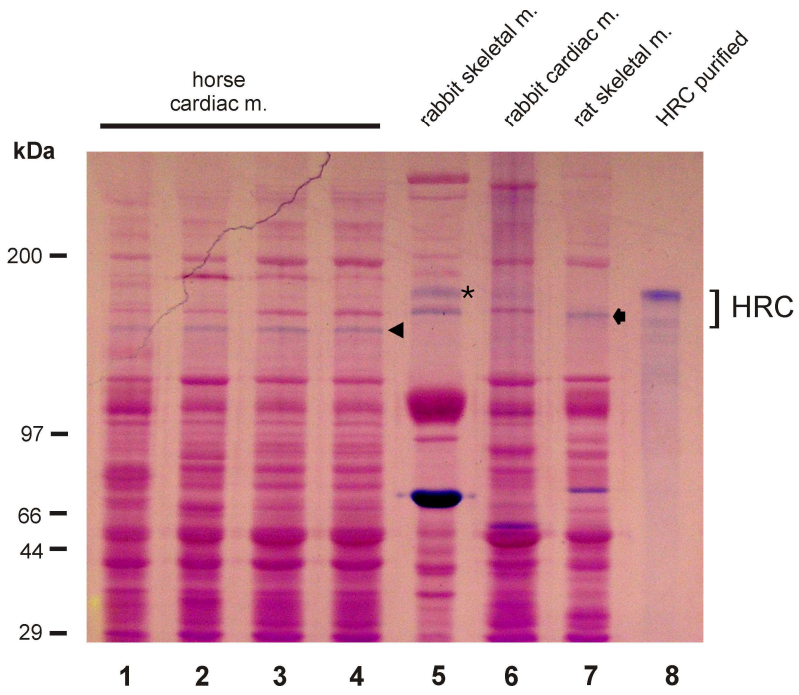

Fig. 6 Characterization and comparison of HRC from cardiac horse muscle (lanes from 1 to 4), rabbit cardiac (6) and skeletal (5) muscles and rat skeletal muscle (7). Purified rabbit skeletal HRC was loaded as a positive control (lane 8). Proteins loading was 100 µg/lane for horse cardiac muscle, 50 µg for rabbit skeletal and 100 µg for rabbit cardiac muscles and 60 µg for rat muscle and 1.5 µg of purified rabbit skeletal HRC. Lanes: 1-4 are fractions from horse cardiac muscle (1-trasverse tubule, 2- longitudinal SR, 3-L+CT, 4-terminal cisternae), 5 and 6 are terminal cisternae membrane fraction isolated from rabbit cardiac muscle, while 7 is from rat skeletal muscle. Total membrane fraction protein was resolved by gradient SDS-PAGE and stained with Stains-All. Molecular mass markers are indicated on the left.

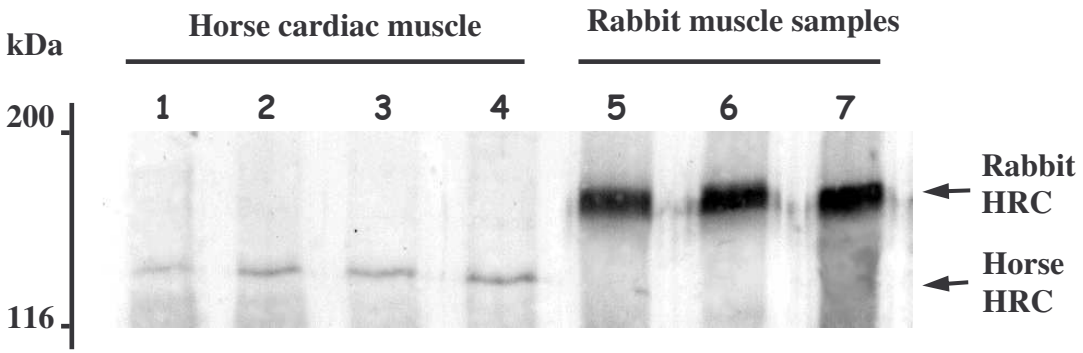

Fig.7 Western blot analysis of membrane fractions obtained from horse cardiac muscle was carried out using polyclonal antibody anti-rabbit HRC. Rabbit muscle samples, skeletal (5) and cardiac (6) muscle were used as positive control. Purified rabbit skeletal muscle HRC (7) was also loaded. Total quantity of proteins loading for a line was 120 µg for horse cardiac muscle, 50 µg for rabbit skeletal and 100 µg for rabbit cardiac muscles and 0.5 µg of purified rabbit skeletal HRC. Lanes: 1-4 are fractions from horse cardiac muscle isolated through centrifuge in isopycnic sucrose-density gradient (1-trasverse tubule, 2- longitudinal SR, 3-L+CT, 4-terminal cisternae), 5 and 6 are

terminal cisternae membrane fraction isolated from rabbit cardiac muscle, while 7 is a purified on sepharose column rabbit HRC. The positions of individual proteins, marked with specific anti-HRC antibody are indicated on the right. It is possible to notice how HRC quantity is achieved from 1 to 4 lanes with increasing the terminal cisternae component in membrane fraction obtained from horse heart.

Technical aspects of the adult equine ventricular cardiac myocytes isolation

Only a few laboratories work on successfully isolated and cultured cardiac myocytes. To obtain viable cells from adult mammal heart the perfusion system is usually used. After the heart of rabbit, rat or mouse is excised it may be perfused retrogradly in Langendorff mode through the aorta tied onto the cannula, and thus through the coronary arteries, which supply the muscle of the ventricles (Mitcheson JS et al. 1996). The basic principle of this method used for the isolation of cardiomyocytes is the heart tissue exposition to a dissociating medium, which is low in Ca^{2+} concentration and contains proteolytic enzymes. Initially the heart is perfused with solution without Ca^{2+} in order to dissociate Ca^{2+} – dependent desmosome structures in the intercalated discs, then a low concentration of Ca^{2+} is added to the proteolytic enzymes containing solution to minimize injury from Ca^{2+} paradox (see below) and to allow full activation of enzymes that cleave the connections of the individual cells with the extracellular matrix network. Enzyme applying may be harmful for the cells thus the perfusion time need to be minimal while the concentration of enzyme must be effective for dissociate the cells. Thus finding particular enzyme batches or combination of enzymes, which dissociate myocytes without causing permanent damage, is critical. When the enzyme starts to digest the heart, fluid leaving the heart becomes more viscous and is collected in the chamber surrounding the heart and recirculated. At the end of the enzyme digestion the heart becomes flaccid. After the heart is cut off the cannula and the vessels are dissected, various parts of it are chopped into the appropriate flasks and put on slowly shaker to mechanically dissociate single rod-shaped cells.

Techniques for the isolation of equine cardiomyocytes have been difficult to establish, due to a number of reasons including **(a)** Traditional method seems to be inappropriate for the horse heart considering its huge measure; it will be need litres of the solution to make it possible. This fact makes me refuse from traditional Langendorff perfusion method and try with immersion of small tissue chunks directly in dissociating medium. **(b)** Adult cells are strongly physically connected by intercalated discs and extracellular matrix, and therefore

are very difficult to cleave without injuring the cells. Enzymatic dissociation of tissue should processed fairy rapidly but enzyme does not reach any chunks cell in the same manner, injuring cardiomyocytes situated on the surface and remaining undigested the central zone. **(c)** Before and during the isolation procedures the equine heart is subjected to prolonged ischemic condition (oxygen deficiency up to 60 min), the time from the moment of animal sacrification to proceeding with single myocytes isolation protocol in the laboratory. To minimize this time is critical to have viable cells after dissociation. During ischemic condition the activity of sarcolemmal ion pumps is reduced. For this reason cardiomyocytes can take up Na^+ during the isolation procedure when the Ca^{2+} concentration is low. After isolation, when the Ca^{2+} concentration is again elevated to normal millimolar concentration, a rapid Na^+/Ca^{2+} exchange across the sarcolemma can lead to intracellular Ca^{2+} overload causing the hypercontracture and deterioration of the cells due to activation of protease and dysfunction of mitochondria that results in irreversible loss of mechanical and electrical activity of the cardiac myocytes. This phenomenon was named “calcium paradox” (Zimmerman ANE & Hulsmann WC, 1966; Zimmerman ANE et al. 1967) and has been confirmed later by other authors.

In line with observations described above I firstly tried to minimize the time of ischemic condition and excessive hypercontraction that occurs as a result of massive blood outflow during ventricle mincing. The minced pieces were briefly washed with the solution and for transferring the heart pieces toward laboratory (15-20 min) it was initially proposed 2,3-butanedione monoxime (BDM) (10-20 mM) that is commonly used to reversibly abolish the cells contraction by inhibition of the myofibrillar ATPase during cardiac culture cells preparation. The latter method did not give me successful results thus I used the cardioplegic (*plegia* means paralysis in Latin) solution, which is widely used in clinic practice of human cardiology for the heart transplantation and protection during cardiac surgery. Cardioplegic solution contains high concentration of potassium (15 mM), which is designed to arrest the heart rapidly in diastole. The proposed mechanism for potassium cardioplegia is that an excess of extracellular potassium ions abolishes the transmembrane gradient of potassium and inhibit repolarization, reversibly devoid the heart of electrical and mechanical activity and providing reliable protection against ischemia/reperfusion injury to recover normal metabolic mechanisms present within the cell. This solution is administrated most frequently under hypothermic conditions because hypothermia reduces the oxygen demands of the myocardium. Using hypothermic hyperkalemic cardioplegic

solution gave an expected protective effects to obtain a reversibly relaxed cells during transfer of tissue pieces to the laboratory and with following cells isolation. Chemical cardioplegia was reintroduced by Gay and Elbert in 1973 which demonstrated that potassium solution could arrest a canine heart for 60 minutes without cellular damage, but debate continues regarding the ideal chemical composition of the cardioplegic solution: its pH, its osmolarity, and also the relative merits of additives such as membrane-stabilizing agents. Another ion concentration considered is magnesium, which is recognized to compete with Ca^{2+} at the calcium channels level and to suppresse the inflow of Ca^{2+} into cells and inhibiting Ca^{2+} overload (Iseri LT & French JH, 1984). Cardioprotective effect depends on the relative combination of magnesium and calcium concentrations as reported by Takemoto (1992). What for the concentration of magnesium in cardioplegic solution for equine heart was increased up to 16 mM while Ca^{2+} concentration was 0.6 mM. It is really difficult consider an effective concentration of free extracellular calcium in this case due to Ca^{2+} release during the tissue mincing. Mannitol and adenosine, known to have cardioprotective properties, were proposed as additional components enable to improve the protection of the equine heart tissue from metabolic and functional damages caused by global ischemia and reperfusion of isolated cells. Mannitol prevents of free radical production during preservation and reperfusion of ischemic tissue and its control of osmotic pressure is beneficial. Also taurine and Na-pyruvate were added to the transport solution as metabolic substrates.

In spite of the fact to obtain good results using described formula of cardioplegic solution for equine cardiac tissue transport more work is needed to improve this formula in order to evaluate preservation in long term of the fresh isolated cardiomyocytes. However, from my study one aspect is clear: something may be some protein makes equine cardiac cell particularly resilient to global ischemia. We hypothesed here that HRC overexpression in horse heart could provide a protection against global ischemia and following reperfusion-induced cardiac injury.

Morphology and structural features of fresh isolated viable equine ventricular cardiac myocytes: T-tubule and contraction

Viable equine myocytes were rod-shape, had clearly defined sarcomeric striation and no granulation in cytoplasm and represented a quiescent state (no spontaneous contractile waves) at physiological concentrations of extracellular Ca^{2+} (1-2 mM). Functionally, the

viable myocytes exhibited a contraction during stimulation at 1 Hz (25 mV) at room temperature.

Fig. 8A shows a phase contrast image of rod-shaped morphology and striation of fresh isolated single cardiomyocytes.

The technique I used relies on the ability of enzyme solution to degrade the intracellular and collagen matrixes that hold the myocytes in myocardium without heart perfusion. However that method gives a major number of injured cells but this was the unique possibility to separate cardiomyocytes and isolate them singly from such a huge heart mass as equine. Here it is very important to separate effectively intact cells from damaged ones for a future electrophysiological study.

Cardiac myocyte is a highly specialized cell which primary function is contractile. Efficiency of excitation-contraction coupling in adult ventricular myocyte is enhanced by T-tubules, which leads the action potential into the centre of the cell, thus functionally contributed to contraction.

In order to control the amount and quality of T-tubules after isolation I performed cell-loading experiments with di-4-ANEPPS. Fresh isolated cell on Fig.9 does not present the detubulated area remaining after cells isolation.

The functional significance of the T-tubule has been closely studied, because immunohistochemical studies have shown a concentration of ion channels and transporters there (Scriven DR et al. 2000, Frank JS et al. 1992).

To delineate the T-tubules system on fixed cells I also used the immunohistochemistry technique to label Na^{+}- Ca^{2+} exchanger (NCX) that localize in an apparent high density in transverse tubules on Fig.10. The exchanger is the dominant mechanism of Ca^{2+} efflux from cardiac myocytes, thus its role in excitation-contraction coupling is significant.

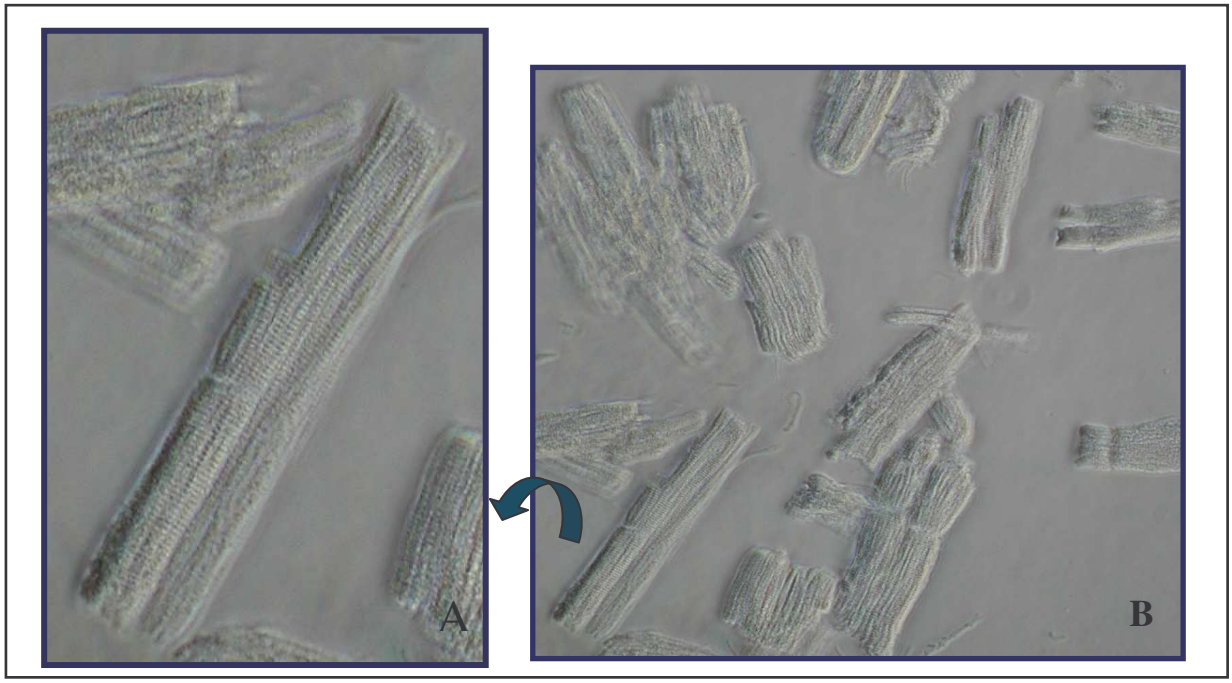

Fig.8 Phase contrast micrographs of horse cardiac myocytes after isolation (Day 0): resolution 20X (B) and zoomed cell (A). Cultured cells are rod-shape with clear cross-striations and without granulation in cytoplasm.

Fig.3.1 Phase contrast micrograph of horse cardiac myocytes after 10 days in culture without serum, resolution 20X. The cells attached on laminin coated glass is indicated by arrows has striations and has no rounded ends.

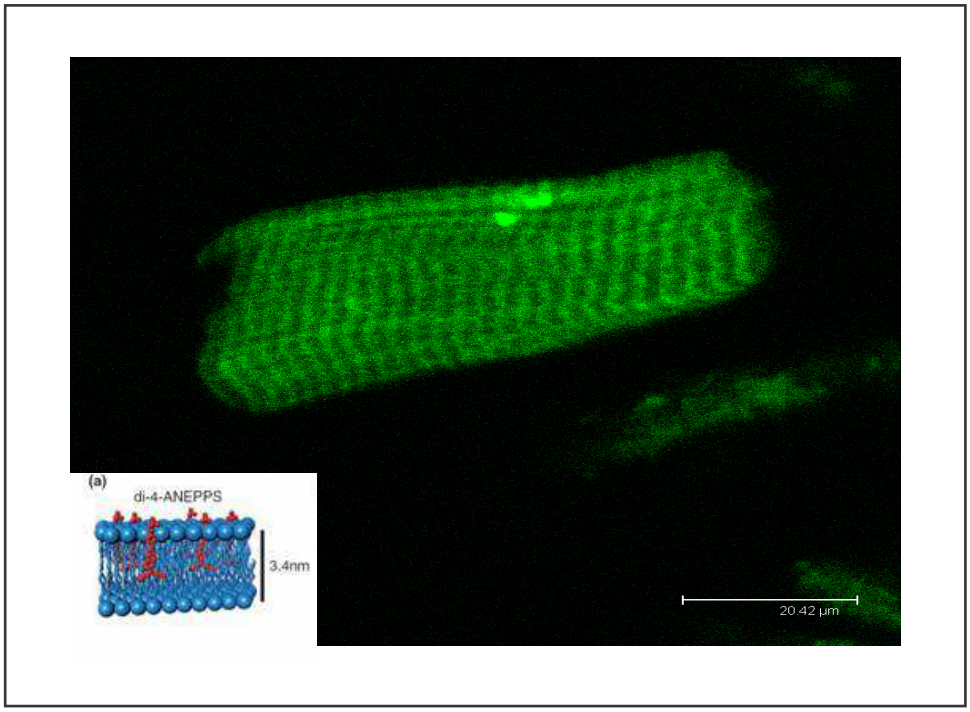

Fig.9 Confocal image of the fresh isolated ventricular cardiomyocyte loaded with fluorescent membrane dye di-4-ANEPPS to show intact T-tubule system. Bar is 20.42 µm. The introduction of molecules of di-4-ANEPPS into cardiac cell membrane is shown on an additive image (a).

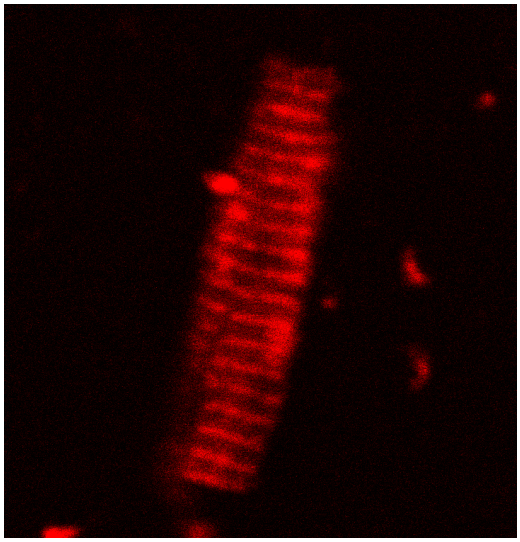

Fig.10 Confocal imaging of fixed with 4% paraformaldehyde cardiac myocyte stained with polyclonal anti NCX antibody (1:100) followed by Red Texas-conjugated secondary antibody. Another method to investigate T-tubule organization in isolated cells.

Sarcomeric structure of isolated equine ventricular cardiomyocytes

The second step was to confirm the integrity of sarcomeric structure of cardiomyocytes after enzymatic isolation. Many cytoskeletal components are responsible for sarcomeric arrangement. Here we considered following important components of cardiac cytoskeleton: α-actinin, plectin and vinculin. Sarcomeric structures were revealed using anti α-actinin antibodies on isolated equine ventricular muocytes. Cells have a regular cross-striated pattern. All three cytoskeletal components are associated with Z-line of horse ventricular myocytes (Fig.11). In particular α-actinin binding to thin filaments forms Z-disk thus maintaining sarcomeric structure.

Cytoskeleton has an important role in the organization of mitochondria into functional complexes with sarcoplasmic reticulum (SR) and sarcomeres, i.e. into intracellular energetic units.

Appaix and co-workers (2003) show that proteolytic treatment with trypsin results in the collapse of the cytoskeleton and disorganization of the regular arrangement of mitochondria within the cells. In particular plectin disappears completely after trypsin treatment. It seems that plectin is one of the components of the cardiac cell cytoskeleton that fix mitochondria, sarcoplasmic reticulum and one sarcomere into functional complexes where endogenous ADP is channelled by organized metabolic networks to mitochondria (Dzeja et al. 1998, 1999) in order to precisely regulate the free energy conversion rates with respect to workload, thus explaining the important phenomenon of the metabolic stability of the heart (Saks et al. 1995).

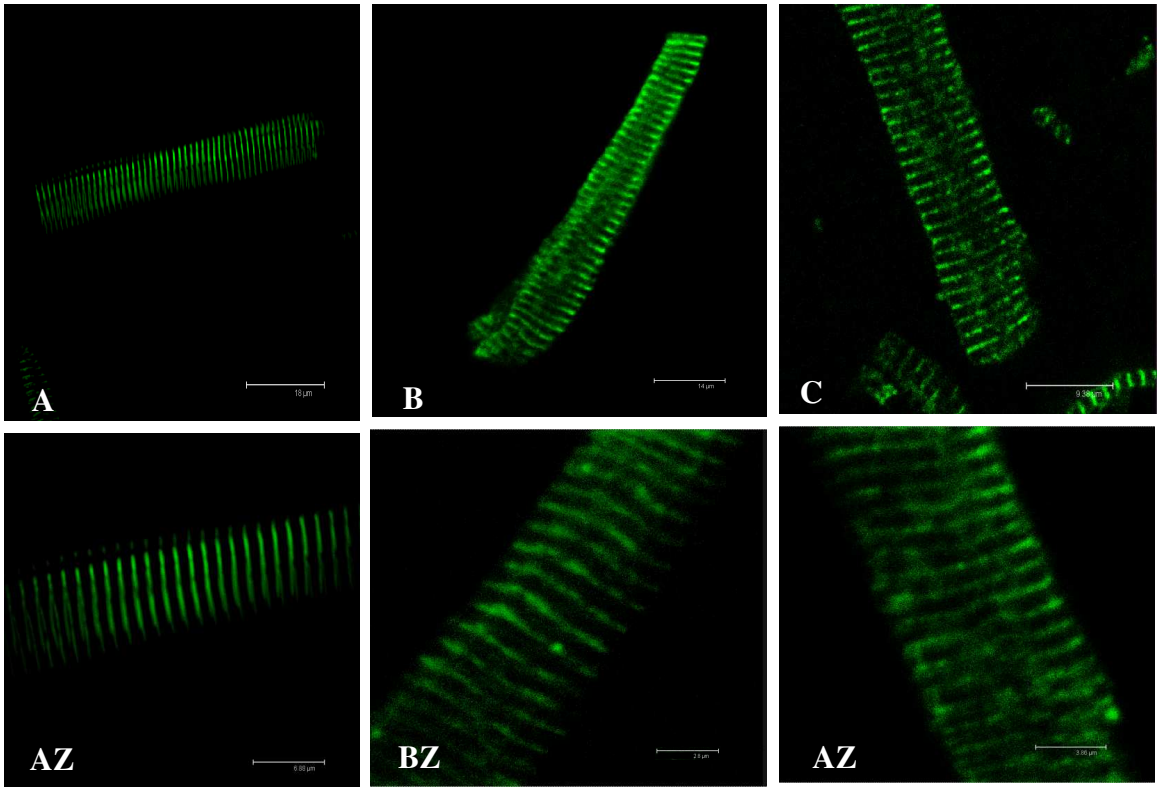

Fig.11 Confocal imaging immunofluorescence of left ventricular horse cardyomyocytes staining with sarcomeric α-actinin (A, AZ), cytoskeletal network proteins plectin (B, BZ) and vinculin (C, CZ) respectively followed by FITC-conjugated polyclonal antibody. Here Z indicates zoomed image.

Myostatin is expressed in horse heart

Myostatin, a TGF-β superfamily member, an endogenous negative regulator of skeletal mass in mammals were detected also in a minor quantity in mammalian animals as sheep and bovine heart. It were suggested by authors that this protein could play another role in heart than in skeletal

One couple of horse specific primers that amplifier 135 bases PCR product of heart myostatin gene were designed to detect myostatin gene expression in horse heart. Six parts of horse heart were monitored: both left and right ventricles and atria, intraventricular septum and papillary muscle from left ventricle sampled from six horses. A simple PCR reaction with a pair of gene-specific primers followed by an agarose gel would generate comprehensive expression profile of myostatin cloned gene from horse heart showed on Fig.12.

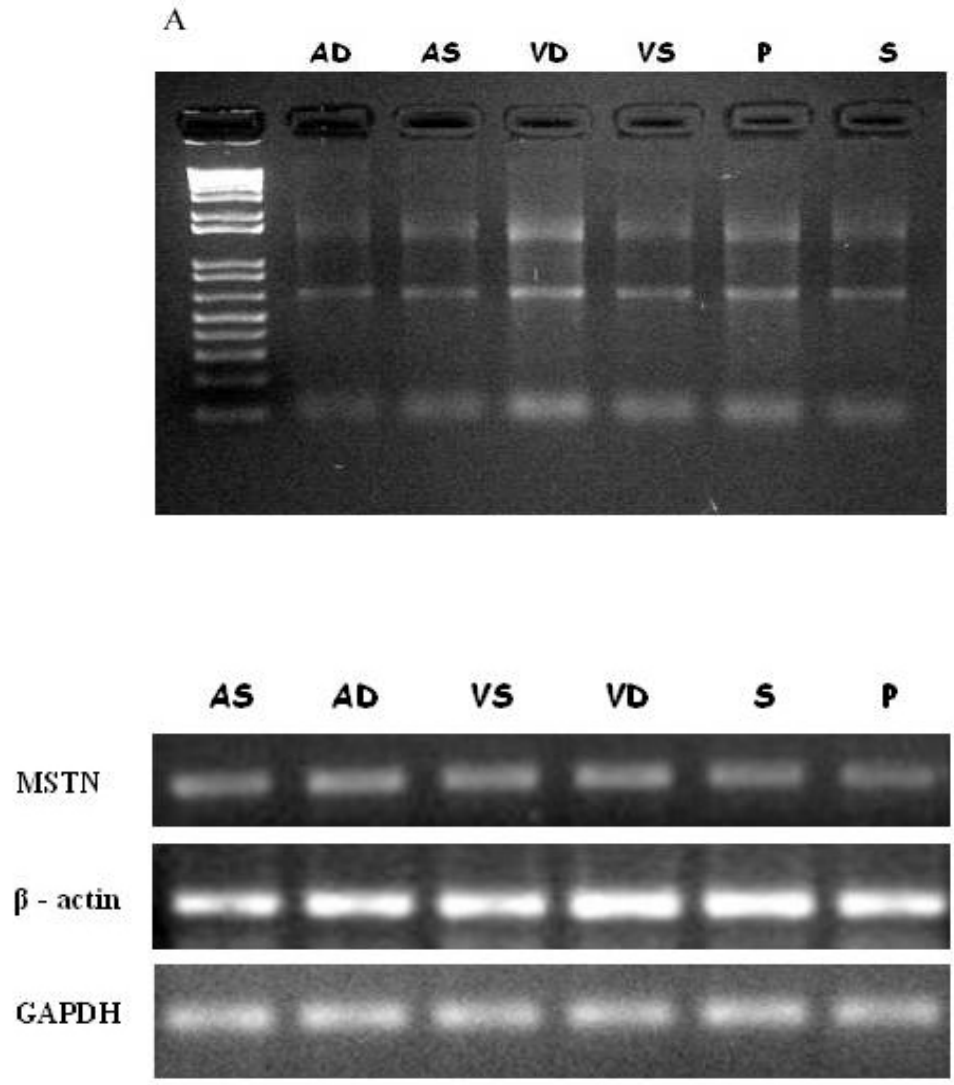

Fig.12 Qualitative PT-PCR analysis of myostatin mRNA expression profiles of horse heart. Representative agarose gel electrophoresis of PCR product of 135 bp obtained from RT-PCR using total RNA (A) isolated from various anatomical parts of the horse heart. Two housekeeping gene, β-actin (180 bp product) and GAPDH (101 bp product), were used as the internal control and were proposed to be Real-time analysis control.

Myostatin is upregulated in right atrium and left ventricle of horse heart

In order to investigate myostatin mRNA expression we used the same pair of specific primers used in simple PCR reaction. Histogram graphic of Real-time PCR reaction

analysis displayed on fig.13 revealed the visible upregulation of myostatin in right atrium and left ventricle respect of other anatomical parts of horse's heart. But the data resulted significatively different ($p<0.05$) only between left ventricle *versus* left atrium and right atrium. Therefore myostatin is upregulated in left ventricle. Although it should possible to approximate this data to have an idea about myostatin expression in horse heart but more experiments is needed, in particular it is important to standardize the experiments by measuring precisely animal body weight/heart weight ratio, taking into account animal derivation (sport carrier) and age. Because myostatin dates is quite variable inside of horse's group. In any case we suggest that noted here myostatin upregulation in left ventricle could be a result of major force that need to develop this muscle for blood pumping in aorta. But another version of myostatin role was not excluded.

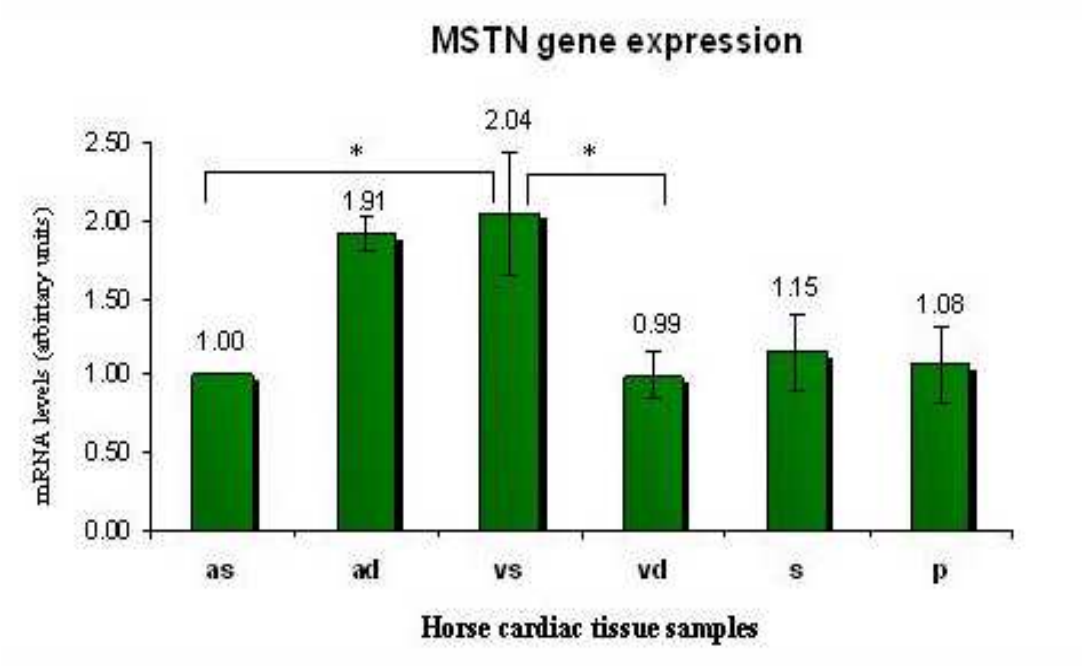

Fig.13 Real time quantitative analisys of myostatin RNA expression in anatomical part of the horse heart. Myostatin is upregulated in right atrium and left ventricle in horse heart. Values are shown as arbitrary units ± standard error obtained from six separate experiments and three experiments in case of skeletal muscle. (* $P<0.05$).

DISCUSSION

The ECC process within cardiomyocytes is known as the pathway by which depolarization of cardiac muscle cell membrane is coupled to contraction. The sarcoplasmic reticulum plays a critical role in ECC by regulating the concentration and distribution of intracellular calcium. This specialized membranes network that surrounds the myofibrils in cardiac and striated muscles, serves as the major intracellular calcium storage compartment of exchangeable calcium, and the calcium handling properties of SR mediate contraction.
The ECC process begins with an action potential. One important feature of horse cardiac tissue, is the duration of action potential and the low resting heart rate. In horse cardiomyocytes, the duration of action potential has been found considerably higher than that found in other mammalian species such as human, pig, dog, rabbit and guinea pig, although a similarity in cellular dimensions.
The special heart features of this important species of veterinarian interest have been studied by the groups of Finley MR (2002) and Loughrey CM (2004). The conclusion of the study of the first group, which investigated by patch-clamp analysis the characteristics of the various potassium channels, confirms that the cardiac repolarization, due to outward potassium currents, in the horse resembles that of humans more than that of other species, rodents in particular. The molecular basis of repolarization that were discussed in that case are important for action potential prolongation under the drugs administration and so have clinical implications for veterinary practice. Nevertheless these data does not seem enough to explain and to understand the extraordinary capacity of equine species cardiomyocytes to resist to calcium overload without developing high arrhythmogenic activity during physiological experiments that was noticed by Loughrey et al.
In a comparative study with rabbit, Loughrey and coworkers first reported the properties of Ca^{2+} release and uptake of SR in horse ventricular cardiomyocytes. They have found that the threshold of resting Ca^{2+} required to initiate spontaneous Ca^{2+} waves is higher in horse than in rabbit cardiomyocytes. This implies that a much higher elevation of cytoplasmic Ca^{2+} concentration is required, even if the resulting Ca^{2+} waves propagate in a similar fashion to other species. The resulting Ca^{2+} waves are diminished of four times in frequency but increased of about two times in amplitude, when compared to that of rabbit ventricular cardiomyocytes. Moreover horse waves have a three time longer duration compared with the rabbit and intracellular Ca^{2+} concentration remains elevated for

prolonged time. The comparative investigation of SERCA Ca^{2+} uptake rates in rabbit and equine myocardial homogenates gave no significant difference between the two species, while the rate of rise of Ca^{2+} during the wave in the rabbit was significantly greater than the horse. Authors have postulated that in equine species, the Ca^{2+} waves special features could be due to an higher Ca^{2+} loading capacity of SR, that could be related to an altered quantity/function of SR calcium binding proteins (Lougry CM et al. 2004).
The HRC is an SR Ca^{2+} binding protein, originally identified by Hofmann and co-workers in 1989. Since the HRC protein binds Ca^{2+} with high capacity and low affinity in vitro (Picello E et al. 1992), it has been defined as a good candidate in playing a role in SR Ca^{2+} handling. The protein is associated exclusively to the SR membrane of skeletal and cardiac muscles of mammals such as rabbit and human. The association with SR membranes is mediated by the interaction with triadin. The HRC-triadin interaction is Ca^{2+} dependent, suggesting for HRC a role in SR Ca^{2+} homeostasis (Sacchetto R et al. 1999, 2001, Lee H et al. 2001).
The importance of studying Ca^{2+} waves resulted pertinent in a species that shows a prolonged action potential duration and low resting heart rate as horse. The greater period of time held at more positive potentials during the prolonged action potential would be the cause of a greater influx of Ca^{2+} via Na/Ca exchanger (outward mode). This would lead to an elevation of intracellular Ca^{2+} concentration, higher SR Ca^{2+} content and production of spontaneous Ca^{2+} waves. These events increase the probability of arrhythmogenic inward currents, which are incompatible with normal heart functions. In small laboratory mammals, experimentally induced prolonged depolarization and consequent elevation in intracellular Ca^{2+} concentration increase the probability of triggered arrhythmias activating transient inward currents (Lougrey CM et al. 2004). Moreover, prolonged action potential duration has been described (Pogwizd SM & Bers DR, 2004) in animal models of ventricular hypertrophy and heart failure. In equine cardiomyocytes, although the intracellular Ca^{2+} concentrations to activate contraction cycle has been resulted more elevated than other mammals, the possibility for arrhythmogenic activity was not increased in this species. Recent studies which imply the use of genetically engineered mice overexpressing HRC in the heart (Gregory KN et al. 2006) and cultured rat myocytes overexpessing HRC (Fan G et al. 2004), have indicated that HRC is an important regulator of SR Ca^{2+} cycling and cardiac functions.

Experimenting with equine ventricular cells isolation I was confronted with difficulties of reperfusion after the period of global ischemia prolonged up to 1 hour. The investigations support a crucial role for SR Ca overload in contributions of apoptosis and necrosis to ischemia/reperfusion injury (Orrenius S et al. 2003). It is reported that increased Ca influx causes apoptosis by inducing SR Ca overload in adult feline cardiomyocytes (Chen X et al. 2005).

However no clearly apoptotic cells, included elongated with ruffled membranes, disorganized sarcomers or extensive blebbing with DNA extruded into vesicles were extremely abundant after the isolation procedure. Either necrotic amorphous rounded or square cells with large blebs were sequestered in mass.

A recently finding demonstrated that cardiac-specific overexpression of HRC in transgenic mouse model protects against ischemia/reperfusion injury by inhibition of apoptotic cell death (Zhou X et al. 2007). After 40 minutes of no-flow global ischemia in transgenic hearts authors observed the lowering of SR Ca-uptake rate in comparison to wild type hearts that could contribute also to detected alteration of anti-apoptotic protein expression following they suggested to simultaneous protection against apoptosis.

For all these reasons I spent my PhD period to study the expression and distribution of HRC in equine ventricular and atrial cardiomyocytes. Since SR is the main organelle involved in Ca^{2+} transients in both cardiac and skeletal muscle cells, here I have also analyzed by immunofluorescent techniques the localization of the molecular components regulating the Ca^{2+} release and reuptake into the lumen of SR. Commercially available antibodies against SR proteins markers (RyR2, SERCA2 and its regulatory protein PLB), resulted cross-reactive with horse cardiac SR proteins revealing a cross-striated pattern, in accordance with the sarcomeric localization of these markers and confirming high similarities between species. HRC expression was identify for the first time in equine cardiac tissue, by PCR analysis and then confirmed by Western blotting with specific anti HRC antibodies. Real Time PCR was carried out to asses possible transcriptional changes of HRC gene in different anatomical portions of equine heart. Data showed that HRC mRNA is mainly expressed in ventricles. Moreover, by comparison with another species of veterinarian interest, such as cattle, Real Time PCR data showed that the enhanced expression of HRC seems restricted to equine species. The dissimilar HRC mRNA expression in atria and ventricles may be due to the intrinsic features of heart parts, that could be emphasize by the special equine action potential duration. It is known that

ventricles represent the most of the muscle heart mass giving with their thickness the consistency to total heart. Moreover, they contract more forcefully than atrial chambers and because they are predominantly responsible for forcing blood out of the heart. Consistent with a role in calcium handling, overexpression of HRC in cultured neonatal rat cardiomyocytes results in an increase in SR calcium storage capacity and in depolarization-induced Ca^{2+} release (Kim E et al. 2003). Similarly, adult rat cardiomyocytes overexpressing HRC also display an increase in Ca^{2+} storage capacity (Fan GC et al. 2004). These studies altogether suggest a primary role for HRC in Ca^{2+} storage, consistent with the high capacity and low affinity Ca^{2+} binding properties, and a possible implication of this protein in the decreased possibility for arrhythmogenic activity in this species. Previous studies have indicated that HRC only comprises about 1% of total SR protein content in skeletal muscle (Damiani E et al. 1997). On account of the special features exhibited by horse cardiac tissue, taken together my data showing the overexpression of HRC in ventricular chambers, could strengthen the hypothesis of HRC as a candidate regulator of SR Ca^{2+} cycling during ECC. Although overexpression of HRC could result in an increase in Ca^{2+} storage capacity, the low abundance of HRC suggests that this protein more likely play a role in Ca^{2+} handling in vivo. In transgenic mice generation experiments authors pointed out that there was a threshold level of HRC abundance in cardiac SR: increases above this level result in alteration of cardiac myocyte function and heart phenotypic alterations which cannot be accommodated.
In my work, I provide the COOH terminal sequence the HRC in horse cardiac tissue. Although partial, the sequence analysis revealed a high homology with human, rabbit and cow HRC, respectively. This sequence corresponds to the COOH terminal, which is implicated in the Ca^{2+} mediated binding to triadin in rabbit (Sacchetto R et al. 1999, 2001) and human (Arvanitis DA et al. 2007) skeletal muscles. The HRC sequence in these species is substantially different with only the 41.7% of homology. In contrast to the rest of HRC sequence, the cysteine-rich domain is highly conserved (about 90%) between human, rabbit cow. This high homology was found also in HRC horse sequence. Taken together these results strengthen the hypothesis that HRC, through Ca^{2+} dependent interaction with triadin, has a role in fine-tuning of SR Ca^{2+} release and uptake.

Myostatin (MSTN) is an endogenous negative regulator of skeletal muscle mass in many animals including vertebrates and invertebrates (Patruno M et al. 2008). Among mammals,

several cattle breeds, such as Belgian blue, exhibit an increased muscle mass and therefore have been called double-muscled. This phenotype has been correlated with mutations identified at the *mstn* locus. The mutation consists in an 11 base pair deletion in the third exon in the Belgian blue breed (Kambadur) and this deletion induces a frame-shift resulting in the occurrence of a stop codon leading to the synthesis of a truncated myostatin protein with no physiological activity due to the lack of the last 102 carboxy-terminal amino acids. The MSTN knockout mouse, where the MSTN expression is genetically blocked, displays a considerable increase in skeletal muscle mass with both hypertrophy and hyperplasia. Although MSTN was initially postulated to be expressed exclusively in the skeletal muscle and to a much lower extent in fat tissue, low levels of MSTN have been detected in the myocardial tissue of sheep, fish and cattle (Sharma M et al. 1999, Ostbye TK et al 2001; Gregory DJ et al. 2004). In human, MSTN is expressed in muscle but not in heart (Hoenig MR, 2008)

The special features of horse heart helped me to study the MSTN expression at the mRNA level in the different anatomical portions of the heart of this large size animal. Using RT-PCR and Real Time PCR experiments, I found that MSTN gene is expressed in the horse heart. To our knowledge, the expression of MSTN in horse tissue has never been described.

Recently, it has been reported that MSTN overexpression in transgenic mice was associated with decreased cardiac and left ventricular mass and that MSTN inhibits cardiomyocytes proliferation without affecting apoptosis (Artaza JN et al. 2007). In addition MSTN is upregulated dramatically in the hearts of AKT (serine-threonine kinase) knockout mice, a genetic model of cardiac hypertrophy (Morissette MR et al. 2006). In case of the horse, understanding of the MSTN pathway could have an important approach into veterinary clinical practice used during horse training when athletic hypertrophy is a common phenomenon. The ability of myostatin to affect both hyperplastic and hypertrophic growth, depending on the physiological status of the cardiomyocytes, might be partly related to the transcriptional pathway activation by mstn itself. Along this line an intriguing hypothesis was discussed by Gaussin V & Depre C (2005), which proposes myostatin as a chalone molecule (compensatory mechanism) of the insulin-like growth factor-I pathway in the cardiac muscle. IGF-I promotes cardiac growth, improves cardiac contractility, cardiac output, stroke volume, and ejection fraction. The upregulation of MSTN gene expression detected in left ventricular of horse heart could be an interesting

data in favor to this hypothesis since the left ventricular chamber has a primary role in heart adaptation increased blood volume *(stroke volume)* to be injected during exhaustive sport exercise and therefore incrementing the final cardiac output. In this context Matsakas et al. (2007) found a great increase of MSTN mRNA content in cardiac muscle of chronic trained rats but the heart compartment was not specified.

However, many studies have to be performed in the field of MSTN expression in cardiac tissue. Whether MSTN expression in horse heart may be related to the special features of cardiac tissue of this species remains to be elucidated. More experiments are therefore requested to confirm this hypothesis.

REFERENCES

Anderson JP, Dodou E, Heidt AB, De Val SJ, Jaehnig EJ, Greene SB, Olson EN and Black BL. 2004. HRC is a direct transcriptional target of MEF2 during cardiac, skeletal, and arterial smooth muscle development in vivo. Mol Cell Biol. 24: 3757-3768.

Appaix F, Guerrero K, Rampal D, Izikki M, Kaambre T, Sikk P, Brdiczka D, Riva-Lavieille C, Olivares J, Longuet M, Antonsson B, Saks VA. 2003. Possibile role of cytoskeleton in intracellular arrangement and regulation of mitochondria. Exp Physiol 88: 175-90

Artaza JN, Reisz-Porszasz S, Dow JS, Kloner RA, Tsao J, Bhasin S, Gonzalez-Cadavid NF. 2007. Alterations in myostatin expression are associated with changes in cardiac left ventricular mass but not ejection fraction in the mouse. J Endocrinol 194:63-76

Arvanitis DA, Sanoudou D, Kolokathis F, Vafiadaki E, Papalouka V, Kontrogianni-Konstantopoulos A, theodorakis GN, Paraskevaidis I, Adamopoulos S, Dorn II GW, Kremasthinos Th.D, Kranias EG. 2008. The Ser96Ala variant in histidine-rich calcium-binding protein is associated with life-threatening ventricular arrhythmias in idiopathic dilated cardiomyopathy. Eur Heart J 29: 2514-25

Arvanitis DA, Vafiadaki E, Fan GC, Mitton BA, Gregory KN, Del Monte F, Kontrogianni-Konstantopoulos A, Sanoudou D, Kranias EG. 2007. Histidine-rich Ca-binding protein interacts with sarcoplasmic reticulum Ca-ATPase. Am J Physiol Heart Circ Physiol 293:H1581–H1589.

Ayettey AS and Navaratnam V. 1978. The T-tubule system in the specialized and general myocardium of the rat. J Anat 127: 125-140

Beard NA, Laver DR, Dulhunty AF. 2004. Calsequestrin and the calcium release channel of skeletal and cardiac muscle. Prog Biophys Mol Biol 85:33-69

Berridge MJ. 2002. The endoplasmic reticulum: a multifunctional signaling organelle. Cell Calcium 32:235-249

Bers DM. 2000. Calcium fluxes involved in control of cardiac myocyte contraction. Circ Res 87:275-81

Bers DM. 2001. Excitation-contraction coupling and cardiac contractile force. Klumer Academic Publishers, Dordrecht.

Bers DM. 2002. Cardiac excitation-contraction coupling. Nature 415:198-205

Bortolami R, Callegari E, Beghelli V. Anatomia e fisiologia degli animali domestici. Edagricole. 2006

Braunwald E.1997. Heart Disease. 5th edn. Philadelphia: W.B. Saunders.

Brutsaert DL. 1989. The endocardium. Ann Rev Physiol 51:263-273

Budras KD, Sack WO and Röck S. Anatomy of the horse. An illustrated text. Schlütersche, Honnover and Mosby-Wolfe, London 1994. Edn 2

Bustin SA. 2000. Absolute quantification of mRNA using real-time reverse transcription polymerase chain reaction assays. Journal of Molecular Endocrinology 25:169–193

Campball PN and Sargent JR. 1967. Techniques in protein biosynthesis. 299-311

Campbell KP, MacLennan DH, Jorgensen AO, Mintzer MC. 1983. Purification and characterization of calsequestrin from canine cardiac sarcoplasmic reticulum and identification of the 53,000 Dalton glycoprotein. J Biol Chem 258:1197– 1204

Chen X, Zhang X, Kubo H, Harris DM, Mills GD, Moyer J, et al. 2005. Ca2+ influx-induced sarcoplasmic reticulum Ca overload causes mitochondrial-dependent apoptosis in ventricular myocytes. Circ Res 97:1009–17

Chen-Izu Y, McCulle SL, Ward CW, Soeller C, Allen BM, Rabang C, Cannell MB, Balke CW and Izu LT. 2006. Three-dimensional distribution of ryanodine receptor clusters in cardiac myocytes. Biophys J 91:1-13

Cohn RD, Liang HY, Shetty R, Abraham T and Wanger KR. 2007. Myostatin does not regulate cardiac hypertrophy or fibrosis. Neuromuscular Disorders 17: 290–296

Damiani E, Tobaldin G, Bortoloso E and Margreth A. 1997. Functional behaviour of the ryanodine receptor/Ca2+-release channel in vesiculated derivatives of the junctional membrane of terminal cisternae of rabbit fast muscle sarcoplasmic reticulum. Cell Calcium 22: 129±151

Derman KD and Noakes TD. 1994. Comparative aspects of exercise physiology. In the Athletic Horse pp.13-27

Dyce KM, Sack WO, Wensing CJG. Textbook of veterinary anatomy. Antonio Delfino Editore. 2006. Edn 3

Dzeja PP, Vitkevicius KT, Redfield MM, Burnett JC, Terzik A. 1999. Adenylate-kinase catalyzed phosphotransfer in the myocardium: increased contribution in heart failure. Circ Res 84:1137–1143.

Dzeja PP, Zeleznikar RJ and Goldberg ND.1998. Adenylate kinase: kinetic behaviour in intact cells indicates it is integral to multiple cellular processes. Mol Cell Biochem 184: 169–182

Eldar M, Pras E, Lahat H. 2003. A missense mutation in the CASQ2 gene is associated with autosomal-recessive catecholamine-induced polymorphic ventricular tachycardia. Trends Cardiovasc Med 13:148–151

Fan GC, Gregory KN, Zhao W, Park WJ, and Kranias EG. 2004. Regulation of myocardial function by histidine-rich, calcium-binding protein. Am J Physiol Heart Circ Physiol. 287:H1705–H1711

Fan GC, Yuan Q, Zhao W, Chu G, Kranias EG. 2007. Junctin is a prominent regulator of contractility in cardiomyocytes. Biochem Biophis Res Commun 352: 617-622.

Finley MR, Li Y, Hua F, Lillich J, Mitchell KE, Ganta S, Gilmour RF Jr, and Freeman LC. 2002. Expression and coassociation of ERG1, KCNQ1, and KCNE1 potassium channel proteins in horse heart. Am J Physiol Heart Circ Physiol 283: H126–H138

Frank JS, Mottino G, Reid D, Molday RS, Philipson KD. 1992. Distribution of the Na^+/Ca^{2+} exchanger protein in mammalian cardiac myocytes: an immunofluorescence and imunocolloidal gold-labeling study. The Journal of Cell Biology 117:2, 337-45

Franzini-Armstrong C, Kenney L, Varriano-Marston E. 1987. The structure of calsequestrin in triads of vertebrate skeletal muscle: a deep-etch study. J Cell Biol 105:45–56

Franzini-Armstrong C, Protasi F and Ramesh V. 1999. Shape, size, and distribution of Ca^{2+} release units and couplons in skeletal and cardiac muscles. Biophys J 77:1528-1539

Franzini-Armstrong C, Protasi F and Tijskens P. 2005. The assembly of calcium release units in cardiac muscle. Ann NY Acad Sci 1047:76-85

Fryer MW, Stephenson DG. 1996. Total and sarcoplasmic reticulum calcium contents of skinned fibres from rat and skeletal muscle. J Physiol 493:357-370

Gaussin V and Depre C. 2005. Myostatin, the cardiac chalone of insulin-like growth factor-1. Cardiovascular Research 68: 347–349

Gay WA and Elbert PA.1973. Functional, metabolic, and morphologic effects of potassium/induced cardiologia. Surgery 74(2):284-90

Gorelik J, Gu Y, Spohr HA, Shevchuk AI, Lab MJ, Harding SE, et al. 2002. Ion channels in small cells and subcellular structures can be studied with a smart patch-clamp system. Biophys J 83:3296-303

Grant RP. 1965. Notes on the muscular architecture of the heart. Circulation 32:301-8

Gregory KN, Ginsburg KS, Bodi I, Hahn H, Marreez YM, Song Q, Padmanabhan PA, Mitton BA, Waggoner JR, Del Monte F, Park WJ, Li GW, Bers DM, Kranias EG. 2006. Histidine-rich Ca2+-binding protein: a regulator of sarcoplasmic reticulum calcium sequestration and cardiac function. J Mol Cell Cardiol 40:653-665

Gunn HM. 1989. Heart weight and running ability. Journal of Anatomy 167:225-233

Györke I, Hester N, Jones LR, Györke S. 2003. The role of calsequestrin, triadin, and junctin in conferring cardiac ryanodine receptor responsiveness to luminal calcium. Biophys J 84: 2082 (abstract)

Gyorke I, Hester N, Jones LR, Gyorke S. 2004. The role of calsequestrin, triadin, and junctin in conferring cardiac ryanodine receptor responsiveness to luminal calcium. Biophys J 86:2121–2128

Hoenig MR. 2008. Hypothesis: myostatin is a mediator of cardiac cachexia. Int J Cardiol 124(2):131-133

Hofmann S, Brown MS, Lee E, Pathak RK, Anderson RG, and Goldstein J. 1989. Purification of a sarcoplasmic reticulum protein that binds Ca21 and plasma lipoproteins. J Biol Chem 264: 8260–8270

Hofmann S, Goldstein J, Orth K, Moomaw CR, Slaughter C and Brown M. 1989. Molecular cloning of a histidine-rich Ca2+-binding protein of sarcoplasmic reticulum that contains highly conserved repeated elements. J. Biol. Chem. 264: 18083– 18090

Hofmann S, Topham M, Hsieh C-L, and Francke U. 1991. cDNA and genomic cloning of HRC, a human sarcoplasmic reticulum protein, and localization of the gene to human chromosome 19 and mouse chromosome 7. Genomics 9: 656–669

Hong CS, Cho MC, Kwak YG, Song CH, Lee YH, Lim JS, Kwon YK, Chae SW, Kim DH. 2002. Cardiac remodeling and atrial fibrillation in transgenic mice overexpressing junctin, FASEB J 16:1310– 1312

Houle TD, Ram ML, Cala SE. 2004.Calsequestrin mutant D307H exhibits depressed binding to its protein targets and a depressed response to calcium. Cardiovasc Res 64:227–233.

Ikemoto N, Antoniu B, Kang JJ, Meszaros LG, Ronjat M. 1991. Intravesicular calcium transient during calcium release from sarcoplasmatic reticulum. Biochemistry 30:5230-5237

Ikemoto N, Bhatnagar GM, Nagy B, Gergely J. 1972. Interaction of divalent cations with the 55,000-dalton protein component of the sarcoplasmic reticulum.mStudies of fluorescence and circular dichroism. J Biol Chem 247:7835-37

Iseri LT, French JH. 1984. Magnesium: neture's physiologic calcium blocker. Am Heart J 108:188-193

Jones LR, Suzuki YJ, Wang W, Kobayashi YM, Ramesh V, Franzini-Armstrong C, Cleemann L and Morad M. 1998. Regulation of Ca21 signaling in transgenic mouse cardiac myocytes overexpressing calsequestrin. J Clin Invest 101:1385–1393

Jones LR, Zhang L, Sanborn K, Jorgensen AO, and Kelley J. 1995. Purification, primary structure, and immunological characterization of the 26-kDa calsequestrin binding protein (junctin) from cardiac junctional sarcoplasmic reticulum. J Biol Chem 270:30787–30796.

Jones PP, Bazzazi H, Kargacin GJ and Colyer J. 2006. Inhibition of cAMPdependent protein kinase under conditions occurring in the cardiac dyad during a Ca2+ transient. Biophys J 91: 433-443

Jorgensen AO and Campbell KP. 1984. Evidence for the presence of calsequestrin in two structurally different regions of myocardial sarcoplasmic reticulum. J Cell Biol 98(4):1597-602

Jorgensen AO, Broderick R, Somlyo AP, Somlyo AV. 1988. Two structurally distinct calcium storage sites in rat cardiac sarcoplasmic reticulum: an electron microprobe analysis study. Circ Res 63(6): 1060-1069

Jorgensen AO, McLeod AG, Campbell KP, Denney GH. 1984. Evidence for the presence of calsequestrin in both peripherial and interior regions of sheep Purkinje fibers. Circ Res 55(2):267-70

Jorgensen AO, Shen AC, Arnold W, McPherson PS and Campbell KP. 1993. The Ca2+-release channel/ryanodine receptor is localized in junctional and corbular sarcoplasmic reticulum in cardiac muscle. J Cell Biol 120: 969-980

Jorgensen AO, Shen AC, Campbell KP. 1985. Ultrastructural localization of calsequestrin in adult rat atrial and ventricular muscle cells. J Cell Biol 101(1): 257-68

Jorgensen AO, Shen AC, Daly P, MacLennan DH. 1982. Localization of Ca2+ + Mg2+ - ATPase of the sarcoplasmic reticulum in adult rat papillary muscle. J Cell Biol 93(3): 883-92

Katz AM. Physiology of the heart. Lippincott Williams & Wilkins 2006. Edn 4

Kim E, Shin DW, Hong CS, Jeong D, Kim do H, Park WJ. 2003. Increased Ca2+ storage capacity in the sarcoplasmic reticulum by overexpression of HRC (histidine-rich Ca2+ binding protein). Biochem Biophys Res Commun 300:192-196

Kirchhefer U, Hanske G, Jones LR, Justus I, Kaestner L, Lipp P et al. 2006. Overexpression of junctin causes adaptive changes in cardiac myocyte Ca(2+) signaling. Cell Calcium 39:131–142

Kirchhefer U, Neumann J, Baba HA, Begrow F, Kobayashi YM, Reinke U et al. 2001. Cardiac hypertrophy and impaired relaxation in transgenic mice overexpressing triadin 1. J Biol Chem 276:4142–4149.

Kirchhefer U, Neumann J, Bers DM, Buchwalow IB, Fabritz L, Hanske G et al. 2003. Impatred relaxation in transgenic mice overexpressing junctin. Cardiovasc Res 59:369–379

Kubalova Z, Györke I, Terentyeva R, Viatchenko-Karpinski S, Terentyev D, Williams SC, Györke S. 2004. Modulation of cytosolic and intra-sarcoplasmic reticulum calcium waves by calsequestrin in rat cardiac myocytes. J Physiol 561(Pt 2):515-24

Laemmli UK.1970. Cleavage of structural proteins during the assembly of the head of bacteriophage T4. Nature 277:680-685

Lahat H, Pras E, Olender T, Avidan N, Ben-Asher E, Man O et al. 2001. A missense mutation in a highly conserved region of CASQ2 is associated with autosomal recessive catecholamine-induced polymorphic ventricular tachycardia in Bedouin families from Israel. Am J Hum Genet 69:1378–1384

Lee HG, Kang H, Kim DH and Park WJ. 2001 Interaction of HRC (histidine-rich Ca21-binding protein) and triadin in the lumen of sarcoplasmic reticulum. J Biol Chem 276:39533–39538

Lee SJ, Reed LA, Davies MV, et al. 2005. Regulation of muscle growth by multiple ligands signaling through activin type II receptors. Proc Natl Acad Sci USA 102:18117–22

Livak KJ and Schmittgen TD. 2001. Analysis of relative gene expression data using real-time quantitative PCR and the 2^{-DDCt}. Method 25:402–408

Lo HM, Lin FY, Lin JL, Hsu KL, Chiang FT, Tseng CD and Tseng YZ. 1999. Impaired cardiac performance relating to delayed left atrial activation after atrial compartment operation for chronic atrial fibrillation. Pacing Clin Electrophysiol 22: 379-381

Loughrey CM, Smith GL, MacEachern KE. 2004. Comparison of Ca2+ release and uptake characteristics of the sarcoplasmic reticulum in isolated horse and rabbit cardiomyocytes. Am J Physiol Heart Circ Physiol 287(3):H1149-59

Lowry OH, Rosebrough NJ, Farr AL and Randall RJ. 1951. Protein measurement with the Folin phenol reagent. J Biol Chem 265:10118-10124

Luss I, Boknik P, Jones LR, Kirchhefer U, Knapp J, Linck B, Luss H, Meissner A, Muller FU, Schmitz W et al.1999. Expression of cardiac calcium regulatory proteins in atrium vs ventricle in different species. J Mol Cell Cardiol 31:1299-1314.

Mackenzie L, Bootman MD, Berridge MJ and Lipp P. 2001. Predetermined recruitment of calcium release sites underlies excitation-contraction coupling in rat atrial myocytes. J Physiol 530: 417-429

Mackenzie L, Roderick HL, Berridge MJ, Conway SJ and Bootman MD. 2004. The spatial pattern of atrial cardiomyocyte calcium signalling modulates contraction. J Cell Sci 117: 6327-6337

MacLellan WR, Brand T, Schneider MD. 1993. Transforming growth factor-β in cardiac ontogeny and adaption. Circ Res 73:783–791

MacLennan DH and Kranias EG. 2003. Phospholamban: a crucial regulator of cardiac contractility. Nat Rev Mol Cell Biol 4:566-577

Malysheva AN, Storey KB, Lopina OD, Rubtsov AM. 2001. Ca-ATPase activity and protein composition of sarcoplasmic reticulum membranes isolated from skeletal muscles of typical hibernator, the ground squirrel Spermophilus undulatus. Biosci Rep 21(6): 831-8

Marx SO, Reiken S, Hisamatsu Y, Jayaraman T, Burkhoff D, Rosemblit N et al. 2000. PKA phosphorylation dissociates FKBP12.6 from the calcium release channel (ryanodine receptor): defective regulation in failing hearts. Cell 101:365–376

Matsakas A, Bozzo C, Cacciani N, Caliaro F, Reggiani C, Mascarello F and Patruno M. 2006. Effect of swimming on myostatin expression in white and red gastrocnemius muscle and in cardiac muscle of rat. Exp Physiol 91:983–994

McKeever KH, Hinchcliff KW, Reed SM, Robertson JT. 1993. Role of decreased plasma volume in hematocrit alterations during incremental treadmill exercise in horses. Am J Physiol 265:R404-408

McKoy G, Bicknell KA, Patel K and Brooks G. 2007. Developmental expression of myostatin in cardiomyocytes and its effect on fetal and neonatal rat cardiomyocyte proliferation. Cardiovascular Research 74: 304–312

McPherron AC, Lawler AM, Lee SJ. 1997. Regulation of skeletal muscle mass in mice by a new TGF-beta superfamily member. Nature 387: 83–90

Meissner G. 2004. Molecular regulation of cardiac ryanodine receptor ion channel. Cell. Calcium 35:621-628

Mitchell RD, Simmerman HK, Jones LR. 1988. Ca2þ binding effects on protein conformation and protein interactions of canine cardiac calsequestrin. J Biol Chem 263:1376–1381

Mitcheson JS, Hancox J, Levi AJ. 1996. Action potentials, ion channel currents and transverse tubule density in adult rabbit ventricular myocytes maintained for 6 days in cell culture. Pflug Arch 431:814-827

Morissette MR, Cook SA, Foo S, et al. 2006. Myostatin regulates cardiomyocyte growth through modulation of Akt signaling. Circ Res 99:15–24

Orrenius S, Zhivotovsky B, Nicotera P. 2003. Regulation of cell death: the calcium-apoptosis link. Nat Rev Mol Cell Biol 4:552–65

Ostbye TK, Galloway TF, Nielsen C, Gabestad I, Bardal T, Anderson O. 2001. European Journal of Biochemistry 268: 5249-5257

Park H, Wu S, Dunker AK, Kang C. 2003. Polymerization of calsequestrin. Implications for Ca2+ regulation. J Biol Chem 278:16176–16182.

Patruno M, Caliaro F, Maccatrozzo L, Sacchetto R, Martinello T, Toniolo L, Reggiani C, Mascarello F. 2008. Myostatin shows a specific expression pattern in pig skeletal and extraocular muscles durino pre- and post-natal growth. Differentiation 76(2):168-181

Patruno M, Maccatrozzo L, Funkenstein B and Radaelli G. 2006. Cloning and expression of insulin-like growth factor I and II in the Shi drum (Umbrina cirrosa). Comp Biochem Physiol B 144:137–151

Peskoff A and Langer GA. 1998. Calcium concentration and movement in the ventricular cardiac cell during an excitation-contraction cycle. Biophys J 74: 153-174

Picello E, Damiani E, and Margreth A. 1992. Low-affinity Ca21-binding sites versus Zn2+-binding sites in histidine-rich Ca2+-binding protein of skeletal muscle sarcoplasmic reticulum. Biochem Biophys Res Commun 186: 659–667

Pogwizd SM and Bers DM. 2004. Cellular basis of triggered arrhythmias in heart failure. Trends Cardivasc Med 14:61-66

Poole DC and Erikson HH. 2003. Heart and vessels: function during exercise and response to traning. Equine Sports Medicine and Surgery.

Postma AV, Denjoy I, Hoorntje TM, Lupoglazoff JM, Da Costa A, Sebillon P et al. 2002. Absence of calsequestrin 2 causes severe forms of catecholaminergic polymorphic ventricular tachycardia. Circ Res 91:e21–e26

Realini C, Rechsteiner M. 1995. A proteosome activator subunit binds calcium. J Biol Chem 270 (50): 29664–29667

Realini C, Rogers SW and Rechsteiner M. 1994. KEKE motifs. Proposed roles in protein-protein association and presentation of peptides by MHC class I receptors. FEBS Lett 348: 109–113

Ridgeway AG, Petropulos H, Siu A, Ball JK, and Skerjanc I. 1999. Cloning, tissue distribution, subcellular localization and overexpression of murine histidine-rich Ca2+ binding protein. FEBS Lett 456: 399–402

Sacchetto R, Damiani E, Turcato F, Nori A, Margreth A. 2001. Ca(2+)-dependent interaction of triadin with histidine-rich Ca(2+)-binding protein carboxyl-terminal region. Biochem Biophys Res Commun 289(5):1125-34

Sacchetto R, Turcato F, Damiani E, and Margreth A. 1999. Interaction of triadin with histidine-rich Ca21-binding protein at the triadic junction in skeletal muscle fibers. J Muscle Res Cell Motil 20: 403–415

Saito A, Seiler S, Chu A, and Fleischer S. 1984. Preparation and morphology of sarcoplasmic reticulum terminal cisternae from rabbit skeletal muscle. J Cell Biol 99**,** 875–885

Saks VA, Kuznetsov AV, Khuchua ZA, Vasilyeva EV, Belikova JO, Kesvatera T and Tiivel T.1995. Control of cellular respiration in vivo by mitochondrial outer membrane and by creatine kinase. A new speculative hypothesis: possible involvement of mitochondrial-cytoskeleton interactions. J Mol Cell Cardiol 27:625–645

Sathish V, Xu A, Karmazyn M, Sims SM and Narayanan N. 2006. Mechanistic basis of the differences in Ca^{2+} - handling properties of sarcoplasmic reticulum in right and left ventricles of normal rat myocardium. Am J Physiol Heart Circ Physiol 291: H88-H96

Sato Y, Ferguson DG, Sako H, Dorn GW 2nd, Kadambi VJ, Yatani A et al. 1998. Cardiac specific overexpression of mouse cardiac calsequestrin is associated with depressed cardiovascular function and hypertrophy in transgenic mice. J Biol Chem 273:28470-28477

Scott BT, Simmerman HK, Collins JH, Nadal-Ginard B, Jones LR. 1988. Complete amino acid sequence of canine cardiac calsequestrin deduced by cDNA cloning. J Biol Chem 263:8958–8964

Scriven DR, Dan P, Moore ED. 2000. Distribution of proteins implicated in excitation-contraction coupling in rat ventricular myocytes. Biophys J 79:2682-91

Sequence detection systems chemistry guide. Applied Biosystem, 2003

Sham JSK, Cleemann L, Morad M. 1995. Functional coupling of Ca2+ channels and ryanodine receptors in cardiac myocytes. Proc Natl Acad Sci USA 92:121–125

Sharma M, Kambadur R, Matthews KG, SomersWG, Devlin GP, Conaglen JV, Fowke PJ and Bass JJ. 1999. Myostatin, a transforming growth factor-beta superfamily member, is expressed in heart muscle and is upregulated in cardiomyocytes after infarct.J Cell Physiol 180(1):1-9

Shyu KG, Ko WH, Yang WS,Wang BW and Kuan P. 2005. Insulin-like growth factor-I mediates stretch-induced upregulation of myostatin expression in neonatal rat cardiomyocytes. Cardiovasc Res 68: 405–414

Takemoto N, Kuroda H, Mori T.1992. The reciprocal protective effects of magnesium and calcium in hyperkalemic cardioplegic solutions on ischemic myocardium. Basic Res Cardiol 87:559-569

Takeshima H, Nishimura S, Matsumoto T, Ishida H, Kangawa K, Minamino N, et al. 1989. Primary structure and expression from complementary DNA of skeletal muscle ryanodine receptor. Nature 339:439-445

Tanaami T, Ishida H, Seguchi H, Hirota Y, Kadono T, Genka C, Nakazawa H and Barry WH. Difference in propagation of Ca^{2+} release in atrial and ventricular myocytes. JJP 2005; 55: 81-91.

Terentyev D, Cala SE, Houle TD, Viatchenko-Karpinski S, Györke I, Terentyeva R et al. 2005. Triadin overexpression stimulates excitationcontraction coupling and increases predisposition to cellular arrhythmia in cardiac myocytes. Circ Res 96:651–658

Terentyev D, Viatchenko-Karpinski S, Györke I, Volpe P, Williams SC, Györke S. 2003. Calsequestrin determines the functional size and stability of cardiac intracellular calcium stores: Mechanism for hereditary arrhythmia. Proc Natl Acad Sci USA 100:11759–11764.

Thomas M, Langley B, Berry C, Sharma M, Kirk S, Bass J & Kambadur R. 2000. Myostatin, a negative regulator of muscle growth, functions by inhibiting myoblast proliferation. J Biol Chem 275: 40235–40243

Towbin H, Staehelin T and Gordon J.1979. Electrophoretic transfer of protein from polyacrilamide gels to nitrocellulose sheets: procedure and some applications. Proc Natl Acad Sci USA 76:4350-4354

Viatchenko-Karpinski S, Terentyev D, Gyorke I, Terentyeva R, Volpe P, Priori SG et al. 2004. Abnormal calcium signaling and sudden cardiac death associated with mutation of calsequestrin. Circ Res 94:471–477

Wang S, Trumble WR, Liao H, Wesson CR, Dunker AK, Kang CH. 1998. Crystal structure of calsequestrin from rabbit skeletal muscle sarcoplasmic reticulum. Nat Struct Biol 5:476–483

Workman AJ, Kane AK, Rankin AC. 2001. The contribution of ionic currents to changes in refractoriness of human atrial associated with chronic atrial fibrillation. Cardiovascular research 52:226-235

Yamasaki Y, Furuya Y, Araki K, Matsuura K, Kobayashi M and Ogata T. 1997. Ultra-high-resolution scanning electron microscopy of the sarcoplasmic reticulum of the rat atrial myocardial cells. Anat Rec 248: 70-75

Young LE. 2003. Equine athletes, the equine athlete's heart and racing success. Experimental physiology 88(5):659-663

Zhang L, Kelley J, Schmeisser G, Kobayashi YM, Jones LR. 1997. Complex formation between junctin, triadin, calsequestrin, and the ryanodine receptor. Proteins of the cardiac junctional sarcoplasmic reticulum membrane. J Biol Chem 272:23389–23397

Zhou X, Fan GC, Ren X, Waggoner JR, Gregory KN, Chen G, et al. 2007. Overexpression of histidine-rich Ca-binding protein protects against ischemia/reperfusion-induced cardiac injury. Cardiovasc Res 75:487–97.

Zimmerman ANE, Daems W, Hulsmann WC, Snijder J, Wisse E, Durrer D. 1967. Morphological changes of heart muscle caused by successive perfusion with calcium-free and calcium-containing solutions (calcium paradox). Cardiovasc Res 1:201-209

Zimmerman ANE, Hulsmann WC. 1966. Paradoxical influence of calcium ions on the permeability of the cell membranes of the isolated rat heart. Nature 211:646-647